Electronic Structure of Diatomic Molecules Composed of a First-Row Transition Metal and Main-Group Element (H−F)

James F. Harrison

Department of Chemistry and Center for Fundamental Materials Research, Michigan State University, East Lansing, Michigan 48824

Received May 5, 1999

Contents

I. Introduction

Understanding the nature of the transition-metal (TM)−main-group-element bond is important in many areas of science, such as organometallic chemistry,[1,2] surface science,[3] catalysis,[4] high-temperature chemistry,[5,6] and astrophysics.[7,8] For example, the oxides are of interest to astrophysics as the constituents of cool stars and to surface science as zero-order models for the oxidation of a transition-metal surface.[9] These systems are electronically complex and very difficult to treat theoretically. Indeed, while the use of quantum chemistry to obtain useful and reliable information about small organic molecules is now routine,[11] a very different situation arises in the theoretical description of molecules containing a transition element. This is due to several factors, but the most important is that the extent of electron correlation required for even qualitatively correct results is significantly raised relative to molecules containing only main-group elements.

The correlation between the electronic states of a molecule and the states of its constituent atoms has been an important concept in chemistry and physics for many years. For example, we know that if a molecule is composed of atoms that have large energy differences between their various electronic states, the molecule will be characterized by electronic states that are widely spaced, or granular. In the context of the preeminent orbital theory, the Hartree−Fock (HF) theory, this means that the molecular orbitals of molecules formed from these atoms will be widely spaced in energy, and the HF configuration will dominate the wave function around equilibrium. This is, of course, the reason the HF theory has achieved its unique role as both an interpretive and predictive tool in the chemistry of the first- and second-row, main-group elements. While the situation becomes somewhat flawed as one moves away from equilibrium structures, the conceptual simplicity and interpretability of the orbital picture can be preserved by constructing self-consistent wave functions in which the HF configuration is augmented by one or more configurations. This multiconfiguration, self-consistent field (MCSCF) approach is capable, in principle, of providing a uniform description of the evolution

10.1021/cr980411m CCC: $35.00
Published on Web 01/08/2000

James F. Harrison was born in Philadelphia, PA, in 1940. He studied chemistry at the Drexel Institute of Technology, earning a B.S. in 1962. He received a Ph.D. from Princeton in 1966 working with Professor Leland Allen and then spent two years as a postdoctoral associate with Professor Harrison Shull at Indiana University. He has been on the faculty of Michigan State University since 1969 and is presently Professor of Chemistry. His research interests include the use of ab initio theory to understand the electronic structure of atoms, molecules, and solids.

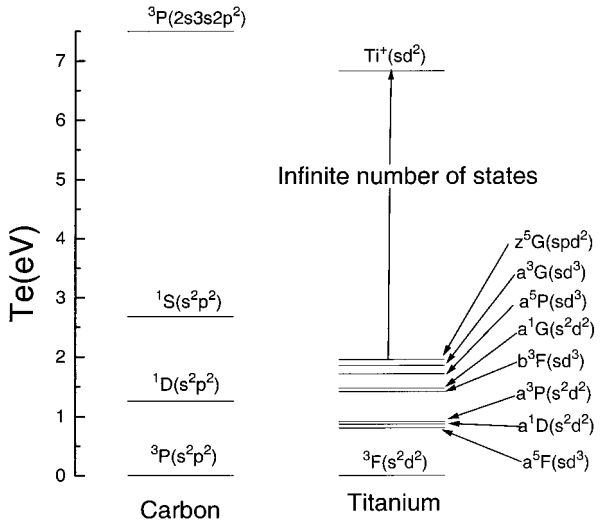

Figure 1. Experimental energy levels of C and Ti.

of the electronic structure of small systems from separated atoms to the assembled molecule. If one has isolated the structure-sensitive component of the electronic correlation in the basic orbital description (SCF or MCSCF), one has a qualitatively (perhaps quantitatively) correct, physically suggestive description of the system. One may improve the function by perturbation theory or, more traditionally, using configuration interaction as one's needs require. This agreeable state of affairs does not seem to be obtained, at least as directly, in the case of molecules containing an element of the first transition series.

To illustrate the differences between a transition element and a main-group element, we compare, in Figure 1, the experimentally determined[10] low-lying energy levels of C and Ti. Note that the first three states of the carbon atom derive from the $2s^22p^2$ configuration, and the two excited states are 1.26 and 2.68 eV above the ground state. The next configuration is $2s2p^3$, and the resulting ^5S state is at 4.18 eV. The lowest energy configuration in which an electron is excited from an orbital that is occupied in the ground state is the $2s2p^23s$, which is 7.5 eV above the ground state. In titanium, the situation is very different, in that the first excited state is obtained from an electronic configuration of $3d^34s^1$, which is different from the ground $3d^24s^2$ configuration, and a third configuration $3d^24s4p$ is only 1.96 eV above the ground state. Indeed, while carbon has four electronic states within 7.5 eV of the ground state, Ti has an infinite number (its ionization energy is 6.83 eV)! An additional complexity is that the size of the 3d orbitals in the configurations $4s^23d^N$, $4s3d^{N+1}$, and $3d^{N+2}$ is significantly different, while the size of the 2s and 2p orbitals in the s^2p^N, sp^{N+1}, and p^{N+2} configurations of a main-group atom are similar. We show, in Table 1, the average value of r for the orbitals in the lowest term of the neutral transition-metal atoms.[12] Note that $\langle r\rangle_{4s}$, for the $4s^23d^N$ configuration, decreases monotonically from Sc (3.98 a_0) to Cu (3.00 a_0), while $\langle r\rangle_{3d}$, in these configurations, drops from 1.675 a_0 in Sc to 0.918 a_0 in Cu. Additionally, the 3d orbitals in the $4s3d^{N+1}$ and $3d^{N+2}$ are significantly larger than those in the $4s^23d^N$ configuration. This is because the excitation of a 4s electron to a 3d orbital transfers charge toward the nucleus and deshields the resulting 3d shell, which then expands. This effect is not present, to any significant degree, in the main-group elements. The computational consequences of this are that orbitals constructed in the HF or MCSCF model tend to be biased toward the configuration selected, and this bias may be difficult to remove in subsequent correlation calculations.

Table 1. Radial Expectation Values (a_0)

	$\langle r\rangle_{3d}$[a]			$\langle r\rangle_{4s}$[b]
atom	$4s^23d^N$	$4s3d^{N+1}$	$3d^{N+2}$	$4s^23d^N$
Sc	1.68	2.07	2.64	3.98
Ti	1.46	1.73	2.10	3.80
V	1.32	1.52	1.78	3.65
Cr	1.22	1.37	1.61	3.52
Mn	1.13	1.28	1.47	3.40
Fe	1.07	1.19	1.35	3.29
Co	1.02	1.11	1.25	3.18
Ni	0.97	1.05	1.17	3.09
Cu	0.92	0.99	-	3.00

[a] Hay, ref 16. [b] Calculated using Wachters 4s orbitals, ref 63.

Absent electron correlation, the energy separation between the terms of the low-lying s^2d^N, sd^{N+1}, and d^{N+2} configurations of the neutral transition-metal atoms are seriously flawed (vide infra). At the Hartree−Fock level, the $s^2d^N \rightarrow d^{N+2}$ excitation is in error by 0.46 eV at Sc and by an incredible 4.33 eV at Ni. This error is a consequence of the large correlation energy associated with the 3d electrons. In a molecular calculation, this atomic misalignment affects the relative mixture of the TM s, p, and d orbitals in the bond and, therefore, the spectroscopic properties including the bond distance, bond energy vibrational frequency, and dipole moment. Studies, over the past 20 years by several groups,[13] have shown that theoretical studies can provide usefully accurate descriptions of transition-metal-containing systems, provided one constructs a molecular wave function that takes into account the correlation energy neces-

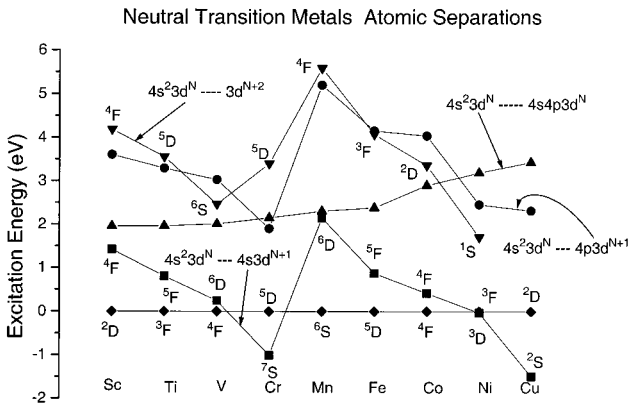

Figure 2. Atomic separations in the neutral transition metals.

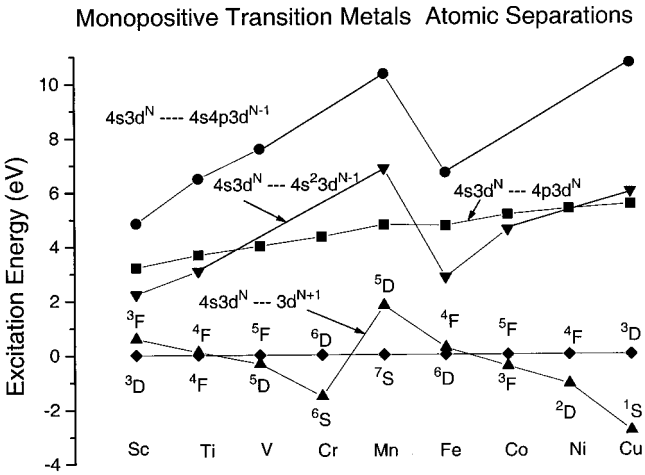

Figure 3. Atomic separations in the monopositive transition metals.

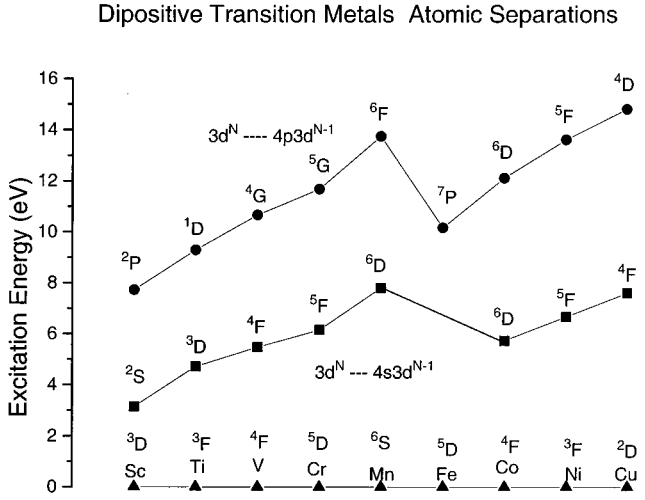

Figure 4. Atomic separations in the dipositive transition metals.

sary to properly order the in situ atomic (or ionic) states of the transition-metal atom and that also accounts for the molecular correlation associated with bond formation.

In this review, we will describe the current understanding of the bonding in the ground and low-lying electronic states of diatomics consisting of a first-row transition element (Sc−Cu) and a first-row main-group element (H−F). We will also discuss the mono and dications of these systems and the change in the bonding with the molecular charge.

II. Transition-Metal Atoms and Ions: General Concepts

A. Preliminaries

To appreciate the problems in accurately describing transition-metal (TM) diatomics, it is useful to consider the electronic structure of the constituent TM atom. Figure 2 shows the experimental[10] separations of the lowest states of the configurations $4s^23d^N$, $4s^13d^{N+1}$, $4p3d^{N+1}$, $4s^14p^13d^N$, and $3d^{N+2}$ for the first transition row. The $4s^23d^N-4s^13d^{N+1}$ separations can be understood qualitatively, in terms of two competing effects: first, the increased stabilization of the 3d orbital, relative to the 4s orbital, as one goes from Sc to Cu and, second, the preference for high-spin d shells. The first effect is obtained as a result of the increasing nuclear charge, while the second is a consequence of the large gain in exchange energy due to the increasing number of compact 3d orbitals, as one goes from Sc to Cu. For the elements Sc−Cr, both effects differentially stabilize the $4s3d^{N+1}$ configuration, relative to $4s^23d^N$. The $4s^23d^5$ configuration of Mn is favored over the $4s3d^6$, because the loss in exchange energy[14] that is obtained in coupling the sixth 3d electron into the high-spin $3d^5$ configuration is much larger than the differential gain that is obtained from occupying the increasingly stable 3d orbital. For the elements Mn−Cu, the $4s^13d^{N+1}-4s^2-3d^N$ separation again decreases monotonically due to the increasing differential stabilization of 3d relative to 4s. Note that, in the elements Sc−Cr, the $4s^13d^{N+1}$ configuration has a higher spin than the $4s^23d^N$ configuration, while, in the elements Mn−Cu, both configurations have the same number of unpaired electrons. The relative energy of the $3d^{N+2}$ configuration decreases in going from Sc−V, increases abruptly at Cr and Mn, due to exchange energy loss, and then drops monotonically from Mn to Ni. The $4s^23d^N-4s^14p^13d^N$ energy separation increases monotonically from Sc (1.96 eV) to Cu (3.43 eV). From these data, we expect a covalent bond to a neutral TM to involve primarily the $4s^23d^N$, $4s3d^{N+1}$, and $4s4p3d^N$ configurations.

In Figure 3, we show the relative energies of the same configurations for the monopositive elements. Once again, the 4s and 3d orbitals are expected to dominate the bonding of these ions to a first-row element. Note, in particular, the $4s3d^N-3d^{N+1}$ energy separation is significantly reduced, relative to the neutrals, reflecting the increased differential stability of the 3d electrons. The $4s^23d^{N-1}$ and $4p3d^N$ configurations are between 1.5 and 7 eV above the $4s3d^N$ and are likely to be important in the low-lying states of $M-X^+$ only for the early members of the series. The relative energies of the $3d^N$ and $4s3d^{N-1}$ configurations of the dipositive ions are shown in Figure 4. Clearly, for these ions, d electrons will dominate the bonding.

B. Differential Correlation Effects

The generic reason for the failure of the Hartree−Fock model, in treating transition-metal atoms, is the differential in the electron correlation between states that arise from different configurations—in particular, different numbers of occupied d electrons. Over the past 20 years, the structure of this differential correlation has come into focus. Starting with the seminal work of Froese-Fischer[15] and Hay[16] and then more globally with the work of several groups—most notably Guse, Ostlund, and Blyholder;[17] Botch, Dunning, and Harrison;[18] Bauschlicher, Walch, and Partridge;[19] Martin;[20] and Raghavachari and Trucks[21]—it has been established that the differential correlation energy associated with states arising from s^2d^N, sd^{N+1}, and d^{N+2} configurations may be partitioned into three components: valence−valence, valence−core, and core−core. There are also differential relativistic effects,[22] and these will be discussed later.

The valence−valence contribution has three components. (a) The first component is the near degeneracy of the 4s, 4p orbitals with the resulting importance of $4s^2 \rightarrow 4p^2$ configurations in the wave function in direct analogy with the main-group elements. This near-degeneracy effect lowers the $4s^2$-$3d^N$ states. (b) The second component is the 3d−3d correlation that affects all states containing two or more d electrons and scales with the number of 3d electron pairs within a given configuration. It turns out that the magnitude of the d−d correlation energy in the three configurations, $4s^23d^N$, $4s3d^{N+1}$, and $3d^{N+2}$, increases faster than the number of 3d pairs; so, given $4s^23d^N$ and $4s3d^{N+1}$ configurations with the same number of 3d electrons, the $4s3d^{N+1}$ will have more 3d−3d correlation energy. Incorporating both the radial and angular contributions to this correlation effect in the wave function requires a flexible d basis and several, preferably three, uncontracted f functions. (c) The third component is the 4s−3d correlation that increases with the number of 4s and 3d electrons and will, thus, be largest for the $4s^23d^N$ configuration. Excitations of the type $4s3d \rightarrow 4p4f$ are necessary to account for this correlation.

The most significant contributions to the valence−core interaction involve simultaneous single excitations of (3s,3p) and (3d,4s) electrons into the virtual space. This effect will be largest for the state with the most d electrons and will require excitations that involve, say, $(3p3d) \rightarrow (nd4f)$, and it will decrease the $s^2d^N \rightarrow sd^{N+1}$ excitation energy. The existence of a differential core−core effect means, unfortunately, that the 3s,3p electrons are "semi-core-like" and participate in (a) near-degeneracy-like correlations with the 3d electrons for which excitations of the type $3p^2 \rightarrow 3d^2$ are called for and (b) dynamic correlations requiring excitations such as $3p^2 \rightarrow 4f^2$. This differential core−core effect is largest for Sc and decreases rapidly as the 3d shell fills. The (3s,3p,3d) near degeneracy favors the $4s^23d^N$ states, while the dynamic correlation of the 4s,3d with the 3s,3p electrons will favor the $4s^13d^{N+1}$ and $3d^{N+2}$ states. A particularly lucid representation of these differential effects is obtained by writing the correlation energy contribution to the difference $\Delta E = E(sd^{N+1}) - E(s^2d^N)$ as

$$\Delta E = \Delta\epsilon(4s^2) + \Delta\epsilon(3d^2) + \Delta\epsilon(4s,3d) + \Delta\epsilon(3d-\text{core}) + \Delta\epsilon(4s-\text{core}) + \Delta\epsilon(\text{core}-\text{core})$$

and plotting the individual contributions as a function of transition element.[23] These data have been extracted from the work of Guse et al.[17] and are plotted in Figure 5. Guse et al. use a small basis set and the second-order Møller−Plesset perturbation theory (MP2) method to add correlation, and while the values of the correlation corrections are not as accurate as one could obtain from more recent calculations, the qualitative behavior of the various correlation effects is expected to be correct.

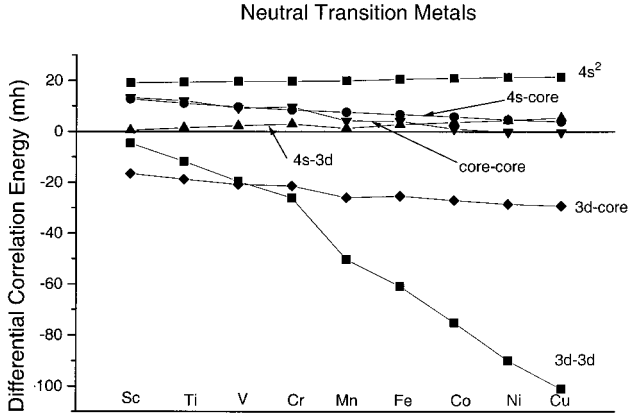

Figure 5. Differential correlation energy in the neutral transition.

Note the $4s^2$ correlation is constant across the table, reflecting the continuous availability of the empty 4p orbital. The 4s−core correlation decreases smoothly, reflecting the increasing occupancy of the 3d shell and, thus, the decreasing opportunity for 4s3p−4p3d excitations. The core−core decreases as one goes from Sc to Cr because of the decreasing opportunity for $3p^2-3d^2$ excitations. It then drops to its Mn value, as $3p^2-3d4d$ effects take over, and this channel vanishes when the d shell is full. The 4s−3d interaction increases slightly as the number of 3d electrons increases. Both the 3d−core and 3d−3d correlations favor the "d-rich" state, and the differential increases linearly with N, although with very different slopes. All differential effects, except those involving 4s electrons, have the characteristic discontinuity between Cr and Mn. Because of limitations in the basis and the reference to the spin-unrestricted Hartree−Fock (UHF) rather than the spin-restricted Hartree−Fock (RHF), the absolute value of the various contributions shown in Figure 5 are not directly comparable to those that may be extracted from more recent calculations. However, the trends are clear and show that the competing effects of the core−valence and core−core correlation will cancel *to some degree*.

C. Relativistic Effects and Comparison with Experiment

Most atomic and molecular electronic-structure calculations neglect scalar relativistic effects, and one must account for this when comparing with experi-

ment. Our limited experience with these effects suggests that they are insensitive to the level of calculation and that relativistic corrections to the various states of the transition elements can be obtained using the Cowan−Griffin[28] procedure. Martin and Hay[22] have calculated the relativistic correction for the transition-metal states of interest. To compare with experiment, we can either augment the results of the nonrelativistic calculations with the relativistic corrections, or we may remove them from the experimental data and generate a set of nonrelativistic, "experimental" data. We have chosen this latter approach (vide infra).

III. Computational Methods

Computational methods commonly used in transition-metal−main-group calculations have been reviewed by several workers,[24−27] and we will comment on the more prominent methods for completeness.

Most calculations, to date, use the Schrödinger equation in the Born−Oppenheimer approximation and neglect relativistic effects, especially those arising from LS coupling. Comparing with experiments requires that one average over the J values in a given atomic term and over Ω for diatomics. Scalar relativistic effects[28,29] (Darwin and mass-velocity terms) are usually taken into account perturbatively. There have been, however, a few relativistic calculations performed variationally, using the "no-pair" Hamiltonian.[30]

The nonrelativistic wave function is a linear combination of determinants often constrained to be an eigenfunction of $\hat{S}^2$ and $\hat{L}_z$. The elements of these determinants are spin−orbitals, the spatial part being a linear combination of basis functions, usually Gaussians. The method used to determine the particular linear combination of Gaussian basis functions, the molecular orbitals, depends on the characteristics of the system and how electron correlation will be included. When the molecular state is accurately described by a single electronic configuration, the molecular orbitals can be determined, using the spin-unrestricted Hartree−Fock (UHF) or the spin-restricted Hartree−Fock (RHF or HF) methods.[31] The UHF method results in a single determinant that is not a spin eigenfunction, and this is sometimes a problem. Subsequent electron correlation is recovered, using a configuration-interaction[31] method (CI) like SDCI, that allows all single and double excitations from this single configuration. In the literature and in this review, this is sometimes called CISD. This CI method is not size extensive, and one may attempt to correct for this and the absence of higher excitations, using the Davidson[32] correction (SDCI+Q). Alternatively, there are single-configuration based methods that are size extensive such as the coupled-pair functional (CPF) of Ahlrichs et al.,[33] the closely related modified CPF (MCPF) method of Chong and Langhoff,[34] and the coupled-cluster singles and doubles approach of Cizek,[35] including a perturbational estimate of triple excitations (CCSD(T)). When the coupled-cluster calculations use UHF or RHF orbitals, they are often designated UCCSD(T) or RCCSD(T).[36−39] Another popular single-reference based method is Möller−Plesset (MP)[40,42] perturbation theory carried out to second order (MP2), third order (MP3), etc.

Because of the large number of isoenergetic d orbitals and the possible near degeneracies in transition elements, it is often necessary to describe the system with a linear combination of configurations and to generate the molecular orbitals using a multiconfiguration SCF (MCSCF)[43−45] approach. Two special MCSCF methods are the complete active space SCF or CASSCF method of Roos et al.[46−48] and the GVB technique of Goddard.[49] CI calculations in which the configuration list is generated by allowing single and double excitations from the MCSCF or CASSCF reference space are called multireference CI (MRCI) and second-order CI (SOCI), respectively. Frequently, the SOCI configuration list is too large to be practical, and one selects a subset of reference configurations from the CASSCF list, based on the weight with which the configuration contributes to the CASSCF wave function. Single and double excitations from the selected list generate a MRCI function. Occasionally, one will see MCSCF+1+2 instead of MRCI. A popular and useful variant of these CI techniques is the internal contraction (ic) method of Werner and Knowles,[50] often designated with the prefix "ic" affixed to the CI method, as icMRCI. Instead of using a CI approach to add correlation to the MCSCF or CASSCF wave function, one can use perturbation theory in the spirit of Møller and Plesset, and this is referred to generically as multireference MP (MRMP2, for example).[52−54] Roos et al. have developed this method for CASSCF reference spaces and call it CASPT2.[55]

When one is interested in the electronic spectroscopy of TM-containing diatomics, one does not want to bias the correlation calculation of the low-lying excited states by the selection of the molecular orbital basis. Two approaches have been found useful. The first one uses molecular orbitals optimized for each state of interest and adds correlation as warranted. This is very effective, as long as the states of interest have different symmetries and one can afford to do the calculations on each state. In the second approach, one generates the orbitals by minimizing the average energy of the states of interest, using the MCSCF/CASSCF method, and uses one set of orbitals for all states in the subsequent CI calculation. This latter method is economical and has been found to be effective in describing closely lying states, especially those with the same symmetry. Orbitals generated in this manner are referred to as state averaged.[56,57]

Many calculations on TM-containing molecules replace the inner-shell electrons ($1s^22s^22p^6$ and, occasionally, $3s^23p^6$) by a relativistic effective core potential[58,59] in order to include scalar relativistic effects in a transparent fashion and to reduce the number of electrons in the calculation.

The basis sets used to expand the molecular orbitals in these calculations have to be adequate on two levels. First, they must be sufficiently flexible to accurately represent the solution to the SCF problem, and, second, they must contain functions with angu-

Table 2. Neutral Atom $s^2d^N \rightarrow sd^{N+1}$ Excitation Energies (eV)

atom	exp[a]	exp(NR)[b]	HF[b]	CISD[c]	CISD (3s3p)[c]	QCISD(T)[d]	MCPF[e]	DFT[f]	MP4[d]	GMP2 (3s3p)[g]
Sc	1.437	1.31	1.00	1.66 (1.75)	1.30 (1.48)	1.49	1.63	0.64	1.46	-
Ti	0.806	0.67	0.54	0.94 (1.02)	0.67 (0.81)	0.81	0.95	0.11	0.77	0.93
V	0.245	0.08	0.12	0.36 (0.46)	0.12 (0.27)	0.21	0.34	−0.38	0.12	?
Cr	−1.003	−1.21	−1.27	−1.09 (−0.95)	−1.20 (−1.04)	−1.10	−1.08	−1.55	−1.24	−1.10
Mn	2.144	1.94	3.33	2.77 (2.86)	-	2.24	2.58	1.04	1.98	-
Fe	0.875	0.61	1.80	1.19 (1.25)	1.09 (1.13)	0.86	1.17	−0.12	0.37	+1.25
Co	0.417	0.12	1.53	-	-	0.33	0.70	−0.45	−0.49	-
Ni	−0.029	−0.39	1.27	−0.01 (−0.02)	−0.04 (−0.10)	−0.18	−0.24	−0.75	−1.46	+0.20
Cu	−1.490	−1.92	−0.37	−1.37 (−1.33)	−1.35 (−1.33)	−1.85	−1.46	−2.05	−3.63	-

[a] Moore, ref 10. [b] Martin and Hay, ref 22. [c] Bauschlicher, Walch, and Partridge, ref 19; results with Davidson's correction are in parentheses. [d] Raghavachari and Trucks, ref 21. [e] Bauschlicher, Langhoff, Partridge, and Barnes, ref 105B. [f] Russo, Martin, and Hay, ref 104. [g] Murphy and Messmer, ref 102.

lar momentum necessary to accurately account for electron correlation. There are many basis sets for first-row, main-group elements that satisfy these criteria, most notably the correlation consistent basis sets developed by Dunning et al.[60−62] The most popular TM basis set has been the 14s9p5d set of Wachters,[63] augmented with two optimized p functions to describe the 4p orbital. Additionally, because the Wachters set is optimized for the $4s^23d^N$ configuration, it must be supplemented by a diffuse d function[16] to better represent the expanded 3d orbital in the $4s3d^{N+1}$ configuration. Radial d−d correlation[18] is accounted for by a flexible contraction of the d functions, and angular correlation and polarization effects require functions of f and g symmetry. Very large primitive sets have been developed by Partridge,[64] Widmark et al.,[65,66] Pierloot et al.,[67] and Bauschlicher,[68] among others. The primitive Partridge-Bauschlicher[68] set, for example, is 20s15p10d6f4g and is typically contracted (using the atomic natural orbital ideas of Almlöf and Taylor,[69] and the generalized contraction ideas of Raffenetti[70]) to 7s6p4d3f2g for valence-correlation calculations. This contraction eliminates the error associated with segmented contractions[71] and reduces the basis set superposition error. It also simplifies the interpretation of the wave function, since the contracted functions may often be thought of as atomic orbitals.

Density-functional theory (DFT) calculations[72−76] on TM atoms and diatomics are becoming increasingly popular. There are several variants of DFT in use, and they are characterized by the local exchange and correlation functionals used as well as any gradient corrections to those that may be used. The review by Zeigler[74] is recommended. The most promising version for TM systems seems to be the hybrid method developed by Becke[77,78] and called B3LYP, which includes a mixture of a traditional Hartree−Fock-like exchange energy, the Slater exchange functional,[76] with gradient corrections due to Becke, and the correlation potential of Vosko, Wilk, and Nusair, with gradient corrections due to Lee, Yang, and Parr. Becke fixed the ratio of these terms by optimizing the performance of DFT relative to a set

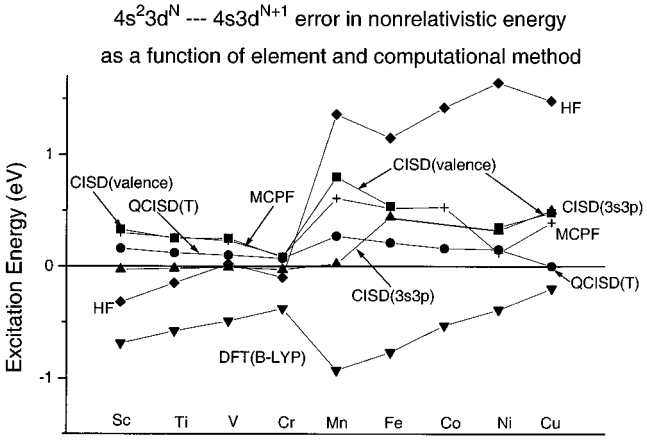

Figure 6. Error in the neutral atom $4s^23d^N-4s3d^{N+1}$ separation as a function of element and computational method.

of main-group molecules. There have been several comparisons between the "traditional" correlation methods described above and DFT methods (vide infra). The advantage of DFT methods is their speed, relative to traditional correlation techniques, and the much-reduced basis set requirements. The main disadvantage is the absence of a well-defined path for improving the accuracy of the results. The method is very promising.

IV. Transition-Metal Atom Calculations

There have been many calculations on the TM atoms,[16−21,79−105] and we compare, in Table 2, the $s^2d^N \rightarrow sd^{N+1}$ energy separation calculated with various nonrelativistic theoretical methods, while Figure 6 compares the errors in these calculations. While there is some unevenness in the quality of the basis set in going from one method to another (and even within the CISD columns), several conclusions may be drawn. The SCF results for the elements Ti−Cr are in relatively good agreement with experiment, because the errors from the neglected $4s^2$ near-degeneracy effect and the 3d−3d correlation cancel. Comparing the CISD and CISD (3s3p), which include

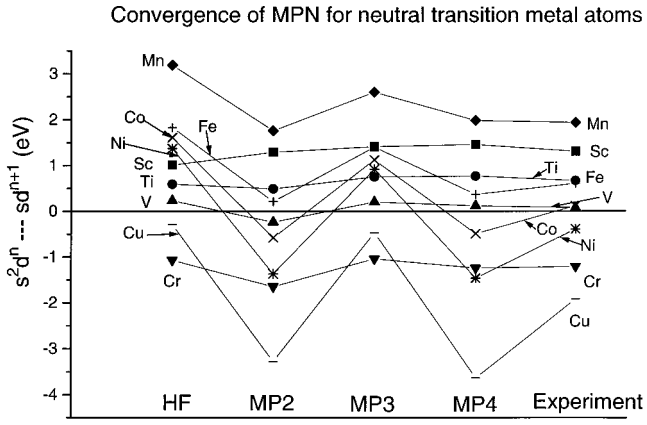

Figure 7. Convergence of MPN for neutral transition-metal atoms.

the core−core and core−valence effects, we see that 3s3p correlation is important for Sc−Cr but not for Mn−Cu, where both methods have comparable errors. This is consistent with the reduced opportunity for $3p^2 \rightarrow 3d^2$ excitations as the d shell fills. The QCISD(T) calculations of Raghavachari and Trucks[21] treat the entire transition series uniformly with a mean error of 0.14 eV. These same authors also investigated the behavior of Møller−Plesset perturbation theory through fourth order. The results in Table 2 suggest that MP4 performs well for Sc−Mn but fails dramatically for Fe−Cu. Figure 7 shows the convergence properties of this perturbation theory, and the large oscillations for Fe−Cu show that the series is far from converged at MP4. This is clearly due to the poor representation of d−d correlation effects involved in the doubly occupied 3d orbitals that are obtained as a result of the single-configuration reference determinant used in the MP calculation. Raghavachari and Trucks;[21] Rohlfing and Martin;[93] and Salter, Adamowicz, and Bartlett[95] have noted that the $s^1d^9 \rightarrow d^{10}$ excitation energy in Ni is in error by 4.99 eV, and, at the MP4 level, the ^1S-(d^{10}) state is predicted to be the ground state. This remarkable deficiency in the single-configuration reference MP perturbation theory has been addressed by Murphy and Messmer[102] as well as Andersson and Roos.[101] These authors explored the characteristics of a multireference-configuration perturbation theory for Ti, Cr, Fe, and Ni[102] and Ni.[101] Murphy and Messmer call their method generalized MP2 or GMP2 and, in their transition-metal calculations, used a large spd basis but only one tight f function to correlate the 3s3p shell. Their reference space includes the $4s^2$ near-degeneracy configurations as well as 3d−3d′ radial correlation configurations and their results are promising. We will discuss the Andersson and Roos results later. The DFT results of Russo, Martin, and Hay[104] are comparable to the CISD+Q results and much better than the SCF for the doubly occupied d configurations (Mn−Cu). These DFT calculations use a restricted open-shell formalism with a Becke gradient-corrected exchange functional and the correlation function of Lee, Yang, and Parr (B-LYP). DFT calculations on Fe by Ricca and Bauschlicher,[105a] using the B3LYP hybrid functional, yield 0.30 eV for the $^5D(3d^64s^2) \rightarrow {}^5F(3d^74s^1)$ excitation. Although this is in error by 0.35 eV, it is less than half of the 0.77 eV error in the B-LYP calculation and suggests that B3LYP-DFT calculations could be competitive with QCISD(T). The MCPF results of Bauschlicher, Langhoff, Partridge, and Barnes[105b] are, on average, somewhat more accurate than the CISD results. The benchmark calculations by Bauschlicher[97] on the Fe $^5D(4s^23d^6) \rightarrow {}^5F(4s^13d^7)$ excitation energy illustrate how difficult a problem this is. The nonrelativistic experimental energy is 0.62 eV, and the SCF result is 1.80 eV, in error by a factor of 3. A full (valence) CI in a limited basis results in 1.20, while a valence SDCI in a very large basis reduces the excitation energy to 0.98 eV, too large by 0.32 eV. Finally, a SDCI that correlates the 3s3p, as well as the valence electrons, reduces the excitation energy to 0.82 eV, which is still in error by 0.2 eV. While there is a small error due to lack of basis set completeness, most of the error is due to the lack of higher excitation in the CI. It is interesting that the excitation energy of 0.82 eV is in better agreement with the experimental result (uncorrected for relativity) of 0.875 eV. Relativity and higher excitations tend to cancel for this energy difference.

Another example that illustrates the difficulty in calculating both the $s^2d^N \rightarrow sd^{N+1}$ and $sd^{N+1} \rightarrow d^{N+2}$ excitation energy is the nickel atom, which has been studied by several groups.[18,19,21,84,92,93,95,96,98,101,102,104] The SCF result is especially bad for both transitions in Ni, with errors of − 1.60 eV ($s^2d^8 \rightarrow sd^9$) and 4.20 eV ($s^2d^8 \rightarrow d^{10}$), and the best valence SDCI is still in error by − 0.34 eV ($s^2d^8 \rightarrow sd^9$) and 0.64 eV ($s^2d^8 \rightarrow d^{10}$). A MRCI calculation that includes radial d correlations via $d \rightarrow d'$ excitations in the reference space reduces the two errors to −0.23 eV ($s^2d^8 \rightarrow sd^9$) and + 0.14 eV ($s^2d^8 \rightarrow d^{10}$), a remarkable improvement in the latter transition. The QCISD(T) calculations of Raghavachari and Trucks[21] (which include 3s3p correlation) are in error by − 0.18 eV and + 0.17 eV, respectively. The valence CASPT2 results of Andersson and Roos[101] also include the $d \rightarrow d'$ excitation in the reference space and have comparable errors, − 0.18 eV and + 0.16. When they correlate the 3s3p electrons as well, the errors are reduced to − 0.08 and 0.03 eV. These are so close to the nonrelativistic estimates that slight changes in the relativistic corrections could result in even better agreement. As of this writing, these CASPT2 calculations are the most accurate available for Ni and are very promising as a computationally viable alternative to MRCI studies of TM-containing molecules.

V. Transition-Metal Ion Calculations

The correlation effects in the positive ions are expected to be similar in nature to those in the neutrals. The most significant change is the absence of a $4s^2$ pair and the associated near-degeneracy effect. As can be seen, from Figure 3, the 3d orbitals are stabilized relative to the 4s more than in the neutrals, and the d^{N+1} configuration is the lowest for five of the nine elements. An incomplete accounting for the excess dd correlation in the d^{N+1} configuration will artificially lower the sd^N. We compare the $sd^N \rightarrow d^{N+1}$ excitation energies calculated with the HF,[22] MCPF,[149] and two variants of DFT[104,113] to experi-

Table 3. Positive Ions $sd^N \rightarrow d^{N+1}$ Excitation Energies (eV)

atom	exp[a]	exp(NR)[a]	HF[a]	MCPF[b]	DFT (BLYP)[c]	LDA+B+P[d]
Sc^+	+0.60	+0.44	+0.94	+0.73	+0.18	+0.47
Ti^+	+0.10	−0.07	+0.45	+0.16	−0.20	−0.33
V^+	−0.33	−0.55	+0.15	−0.34	−0.56	−0.97
Cr^+	−1.52	−1.78	−1.15	−1.71	−1.66	−1.80
Mn^+	+1.81	+1.54	+3.48	+2.09	+1.07	+1.25
Fe^+	+0.25	−0.07	+1.67	+0.40	−0.35	+0.05
Co^+	−0.43	−0.80	+1.13	−0.33	−0.90	−0.85
Ni^+	−1.08	−1.48	+0.63	−1.01	−1.44	−1.75
Cu^+	−2.81	−3.36	−1.28	−3.05	−2.93	−3.02
average absolute error (Sc^+−Cr^+)			0.61	0.22	0.13	0.19
average absolute error (Mn^+−Cu^+)			1.97	0.47	0.23	0.19

[a] Martin and Hay, ref 22. [b] Pettersson, Bauschlicher, Langhoff, and Partridge, ref 150. [c] Russo, Martin, and Hay, ref 104. [d] Ziegler and Li, ref 113.

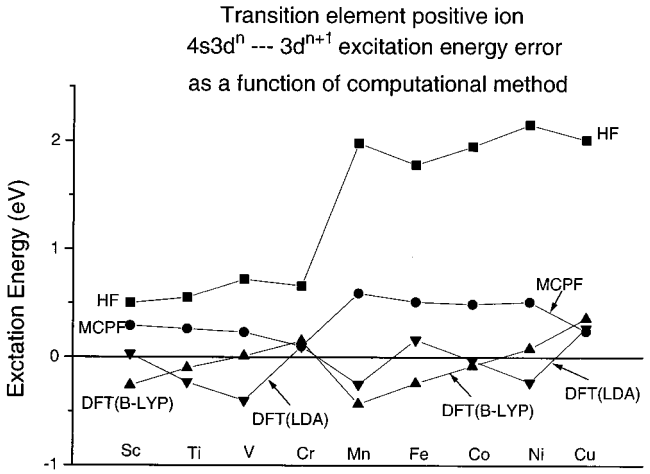

Figure 8. Error in the positive con $4s3d^N$−$3d^{N+1}$ separation as a function of computational method.

ment, in Table 3. The errors (method − nonrelativistic experiment) are shown in Figure 8. As expected, the HF method artificially lowers the sd^N relative to d^{N+1}, especially when the d orbitals begin to be doubly occupied. The MCPF method reduces the error considerably but is still in error by 0.22 eV for Sc^+−Cr^+ and 0.47 eV for Mn^+−Cu^+. The DFT methods are much more accurate, having mean errors of 0.13 and 0.23 (BLYP) and 0.19 and 0.19 (BP) eV.

VI. Transition-Metal Hydrides

A. Introduction

The model of the bonding in TM hydrides that has emerged from the published ab initio studies has two rather distinct historical components. Self-consistent field calculations done prior to the 1977 work of Hay[16] (on the role diffuse d orbitals play in the s^2d^N and sd^{N+1} splitting in the first transition series) may suffer from a poor basis, and each should be reexamined in the light of the Hay results. The second aspect is the recognition of the structure of the differential in the s^2d^N and sd^{N+1} correlation energy in the first transition series. As noted earlier, calculations that do not consider the proper description of the in situ TM at the MCSCF or MRCI level will not properly mix the atomic asymptotes in the molecular wave function. How this manifests itself will depend on the calculation and the properties of interest. For example, the early work[116] on ScH failed to correlate the Sc $4s^2$ pair (near-degeneracy effect) and, thus, predicted the ground state to be $^3\Delta$. When the proper correlation is included,[117] the $^1\Sigma^+$ becomes the ground state. There have been several studies that have focused on trends in the series[106−114] and studies on specific molecules: ScH,[115−120] TiH,[119,121−124] VH,[119,121,125] CrH,[126] MnH,[127−129] FeH,[130−135] CoH,[136] NiH,[137−143] and CuH.[143−147] There are studies of the trends in the positive hydrides,[148−150] as well as specific molecules: ScH^+,[148] TiH^+,[151] CrH^+,[152] FeH^+,[153,154] and CoH^+.[155] There is one study of the dipositive hydrides.[156] The published ab initio results for the ground states of the hydrides are summarized in Tables 4−6, and these calculations will be discussed in what follows. There have been several recent reviews of the hydrides that deal with the experimental situation, (Armentrout and Sunderlin[157]) and theoretical aspects (Langhoff and Bauschlicher[158,159]).

B. General Considerations

When a H atom approaches a first-row transition element, it can bond with the $4s^23d^N$ and $4s3d^{N+1}$ configuration. When it bonds to the $4s^23d^N$ configuration, there are two options. First, it could form a bond with the $3d_\sigma$ orbital or a hybridized $4s-3d_\sigma$ orbital. This keeps the $4s^2$ pair essentially intact and will result in a molecular state with one less unpaired electron than the atomic state. The relative energies and spatial extension of the 4s and 3d orbitals are comparable on the Sc side of the transition-metal series and diverge rapidly as the atomic number increases; detailed calculations show that 3d−4s hybridization is important only for ScH and TiH. Second, it could bond to an sp hybrid formed when the $4p4s3d^N$ configuration mixes with the $4s^23d^N$. We will represent the sp hybrid involved in the bond as $sz = 4s + 4p$, its companion as $\overline{sz} = 4s - 4p$, and a bond to the H atom involving this hybrid as $sz + 1s$. The resulting molecular state has one more unpaired electron than the atomic state of the TM. If H bonds to the $4s3d^{N+1}$ configuration, it forms a bond with the 4s electron, $4s + 1s$, resulting in a molecular-spin state with one fewer unpaired electron than the atom. When these bonding mechanisms are coupled with the atomic separations (Figure 2), we expect (1) bonds with $4s^23d^N$ character ($sz + 1s$) to be dominant for Sc and Mn, where the $4s^23d^N$ is well below the

Table 4. Computational Studies of ScH($X^1\Sigma^+$), TiH($X^4\Phi$), and VH($X^5\Delta$)

molecule	ref	R_e (Å)	ω_e cm^{-1}	μ (D)	D_e (eV)	comment
ScH($^1\Sigma^+$)	112	1.794	1587	1.374	2.27	MCPF (valence)
	112	1.776	1572	1.641	2.25	MCPF (3s3p)
	120	1.80	1621	1.49	2.21	MRD-CI (valence)
	120	1.80	-	1.32	2.33	MRD-CI (3s3p)
	114	1.730	1663	-	1.74	B3LYP (DZP)
	118	1.789	1524	-	1.99	MCSCF+1+2 (valence)
	117	1.78	-	-	-	MCSCF/CI (valence)
	115	1.77	1690	-	1.8	SCF ($^3\Delta$ is ground state)
	106	1.85	1203		1.41	OVC-pseudopotential ($^3\Delta$ is ground state)
	experiment[157]				2.08	D_0^0
TiH($^4\Phi$)	106	1.91	1331	-	1.7	OVC−valence correlation
	122	1.86	1510	-	1.6	SCF
	124	1.84	1498	1.90	1.97	MRD-CI (valence)
	124	1.84	-	-	2.00	MRD-CI (3s3p) (R_e assumed)
	107	1.83	1407	-	2.12	CASSCF/CI (valence)
	112	1.820	1548	2.185	2.06	MCPF (valence)
	112	1.781	1407	2.122	2.05	MCPF (3s3p)
	110	1.81	-	2.0	1.95	CI pseudopotential
	123	1.788	1572	2.32	2.054	full valence CI (14s11p6d4f)/[5s4p3d1f]
	114	1.744	1601	-	2.61	B3LYP(DZP)
	experiment			2.455[160]	2.09[161]	D_0^0
VH($^5\Delta$)	121	1.79	1550	-	-	SCF
	125	1.76	1585	-	1.87	OVC/CI
	106	1.75	1609	-	1.77	OVC/CI
	107	1.74	1590	-	2.30	CASSCF/CI (valence)
	112	1.719	1635	2.021	2.33	MCPF (valence)
	114	1.677	1614	-	2.77	B3LYP (DZP)
	experiment[162]				2.13	D_0^0

Table 5. Computational Studies of CrH($X^6\Sigma^+$), MnH($X^7\Sigma^+$), FeH($X^4\Delta$), and CoH($X^3\Phi$)

molecule	ref	R_e (Å)	ω_e cm^{-1}	μ (D)	D_e (eV)	comment
CrH($^6\Sigma^+$)	106	1.71	1570	-	2.0	OVC
	107	1.70	1465	-	2.10	CASSCF/CI
	112	1.694	1647	3.807	2.13	MCPF (valence)
	126	1.690	1592	3.864	2.11	SOCI
	114	1.654	1637	-	2.34	B3LYP(DZP)
	experiment	1.6557[164]	1581[164]	-	1.93[163]	D_0^0
MnH($^7\Sigma^+$)	127	1.789	1549	1.6	1.57	HF
	128	1.8			1.5	GVB
	106	1.84	1432	-	1.9	OVC
	107	1.77	1639	-	1.71	CASSCF/CI
	112	1.753	1530	1.239	1.67	MCPF (valence)
	129	1.750	1518	1.21[a]	-	MRCI+Q
	114	1.723	1586	-	1.08	B3LYP(DZP)
	experiment	1.731[164]	1548[164]		1.37 ± 0.2[165]	
FeH($^4\Delta$)	130	1.60	2535	-	2.4	HF (calculated to be 14 700 cm^{-1} above $^6\Delta$)
	131	1.53	1910	-	-	HF (calculated to be 23 430 cm^{-1} above $^6\Delta$)
	107	1.72	1560	-	1.95	CASSCF/CI
	132	1.60	1710	-	-	CASSCF/CI
	112	1.573	1915	2.90	1.67	MCPF (valence)
	133	1.578	1846	-	-	MCPF (3s3p)
	134	1.578	1701	-	1.54	HF-CI relativistic pseudopotnetial
	135	1.588	1672	-	2.05 ± 0.08	MRCI+Q
	114	1.561	1829	-	1.76	B3LYP(DZP)
	experiment	1.589[170]	1827[157]		1.60[166]	D_0^0
CoH($^3\Phi$)	106	1.58	1998	-	2.2	OVC (valence)
	112	1.532	1842	2.743	1.94	MCPF (valence)
	136	1.49	2026	-	-	MRD-CI (valence) relativity included
	114	1.510	1868	-	1.88	B3LYP(DZP)
	experiment	1.52[157]	1925[157]		1.98[167]	D_0^0

[a] Estimated from Figure 3.

$4s3d^{N+1}$; (2) bonds with $4s3d^{N+1}$ character (4s + 1s) for Cr and Cu, where $4s3d^{N+1}$ is well below $4s^23d^N$; and (3) bonds with mixed character, where the configurations are close in energy. One measure of the character of the bond is the d-electron population of the molecule. For example, if the bond in TiH is primarily sz + 1s arising from the $4s^23d^2$ configuration, one would expect a 3d population of ~2. However, if the bond was primarily 4s + 1s arising from the $4s^13d^3$ configuration, one would expect a 3d population of ~3. A bond with a mixed character should have a 3d population between 2 and 3. Table 7 shows the 3d population calculated by Chong et al.,[112] using a flexible basis and the MCPF method.

Table 6. Computational Studies of NiH($^2\Delta$) and CuH($^1\Sigma^+$)

molecule	reference	R_e (Å)	ω_e cm^{-1}	μ (D)	D_e (eV)	comment
NiH($^2\Delta$)	168	1.45	1911	-	2.78	GVB
	106	1.55	1917	-	2.5	OVC
	137	1.50	~1640	-	-	SCF/CI (4e)
	139	1.470	1911	-	2.28	CI
	107	1.47	1982	-	2.79	CASSCF/CI
	112	1.485	1987	2.557	2.69	MCPF (valence)
	141	1.46	1997	2.32	-	MRCI (investigates relativistic effects)
	142	1.464	1949	2.522 (2.4)		ACPF (3d−3d′)/relativistic μ
	143	1.439		2.43	2.89	CASPT2 (valence) dd′; relativistic correction
	143	1.440	2082	2.32	2.91	CASPT2 (3s3p) dd′; relativistic correction
	114	1.509	2008	-	2.61	B3LYP(DZP)
	experiment	1.475[164]	1007[157]	2.4 ± 0.1[169]	1.54[167]	D_0^0
CuH($^1\Sigma^+$)	106	1.50	1836	-	2.7	OVC
	144	1.454	2089	-	2.79	MP4 (SDTQ)
	145	1.49	1834	-	2.64	valence CI pseudopotential
	112	1.509	1852	2.951	2.63	MCPF
	146	1.458	?	-	2.52	CIPSI relativistic pseudopotential
	147	1.47	1952	2.66		MRD-CI relativistic no-pair equation
	114	1.460	1901	-	2.75	B3LYP(DZP)
	143	1.458	?	2.73	2.67	CASPT2 (valence) d → d′ relativistic correction
	143	1.457	1936	2.70	2.66	CASPT2 (3s3p) d → d′ relativistic correction
	experiment	1.463[164]	1941[164]		1.63[167]	

Table 7. Experimental D_0^0 with Experimental and Calculated R_e's and Calculated d Populations for the Neutral and Monopositive Hydrides

	neutrals				positive ions			
	state	D_0^{0a} (eV)	R_e (Å)	d_{pop}[b]	state	D_0^0 (eV)[f]	R_e (Å)[g]	d_{pop}[g]
ScH	$^1\Sigma^+$	2.08	1.776[b]	0.84	$^2\Delta$	2.40	1.830	1.29
TiH	$^4\Phi$	2.09	1.781[b]	2.30	$^3\Phi$	2.31	1.740	2.34
VH	$^5\Delta$	2.13	1.719[b]	3.40	$^4\Delta$	2.05	1.661	3.37
CrH	$^6\Sigma^+$	1.93	1.6557[c]	4.83	$^5\Sigma^+$	1.37	1.604	4.45
MnH	$^7\Sigma^+$	1.37	1.731[c]	5.05	$^6\Sigma^+$	2.06	1.652	5.10
FeH	$^4\Delta$	1.60	1.589[d]	6.52	$^5\Delta$	2.12	1.603	6.19
CoH	$^3\Phi$	1.98	1.52[e]	7.60	$^4\Phi$	1.98	1.547	7.22
NiH	$^2\Delta$	2.54	1.475[c]	8.65	$^3\Delta$	1.67	1.487	8.26
CuH	$^1\Sigma^+$	2.63	1.463[c]	9.80	$^2\Sigma^+$	0.92	1.445	9.45

[a] Experimental references in Tables 6−8. [b] MCPF values from ref 112. [c] Experimental values from ref 164. [d] Experimental value from ref 170. [e] Experimental value from ref 157. [f] Experimental values from ref 157. [g] MCPF values from ref 149.

The population of 2.30 for TiH does, indeed, suggest a bond of mixed character. Note the d population in ScH is less than 1, reflecting the 3d + 1s bond and subsequent charge transfer that is obtained from the $4s^23d^1$ configuration. As Walch and Bauschlicher have noted, a d-bonded ground state is unique to ScH because, (1) as one moves from Sc to Cu, the $\langle r\rangle_{4s}$ and $\langle r\rangle_{3d}$ both contract, but the ratio $\langle r\rangle_{4s}/\langle r\rangle_{3d}$ increases monotonically from 2.364 to 3.239, favoring bonding to the hybridized $4s^2$ pair; and (2) there is only one d electron in Sc, and, therefore, no dd exchange-energy loss is incurred when it is coupled into a singlet spin function with the H 1s orbital. The exchange-energy loss increases with the number of high-spin electrons and is largest at the center of the row.

Bonding in the monopositive ions involves the $4s^1$-$3d^N$, $4s^23d^{N-1}$, $4s4p3d^{N-1}$, and $3d^{N+1}$ configurations, and their relative importance depends on their relative energy, as given in Figure 3. Accordingly, we expect the bonding to be dominated by the $4s3d^N$ and $3d^{N+1}$ configurations. As with the neutrals, the d population of the wave function is a measure of the relative mixture of these two configurations. The published ab initio results for the ground states of the monopositive hydride are summarized in Tables 8 and 9; the d populations for the ground state, as calculated by Pettersson et al.,[149] are shown in Table 7. These data suggest that, regardless of the relative energy of the $4s^13d^N$ and $3d^{N+1}$ configuration, we can think of the bonding as being primarily 4s + 1s with some admixture of $3d_\sigma$ + 1s. This makes sense because, even when the $3d^{N+1}$ configuration is below the $4s3d^N$, forming a 3d + 1s bond will result in an exchange-energy loss[14,171] that will raise the in situ $3d^{N+1}$ state above the $4s3d^N$, thus favoring a bond that is primarily 4s + 1s. Bonding in the dipositive hydrides is exclusively via the $3d^N$ configuration, and recent calculations[156] show that the 3d population in the ground state of MH^{2+} is essentially N and that the bonding is electrostatic.

The challenge to a theoretical description of a TM hydride is 2-fold. First, the basis set used must be able to describe both the radial and angular correlation of the d's and the $4s^2$ correlation. Second, the method of calculation must include enough correlation to properly order the in-situ atomic configurations of the TM. The basis set required to do this is reasonably well understood—a flexible d contraction and several f functions with carefully chosen exponents—and, at least for the low-lying electronic states, presents no problem. How to add correlation is another matter, and the method chosen depends on the molecule and the computational goals.

C. Ground-State Properties

1. Bond Characteristics and Ground-State Symmetry

The ground state of Sc is a $^2D(s^2d^1)$ and gives rise to singlet and triplet molecular states of Σ^+, Π, and Δ symmetries. If H forms a bond with the $3d_\sigma$ electron, the valence configuration is

$$4s^2\,(3d_\sigma + 1s)^2$$

Table 8. Transition-Metal Hydride Cations D_0^0 (eV)

	ScH^+	TiH^+	VH^+	CrH^+	MnH^+	FeH^+	CoH^+	NiH^+	CuH^+
GVB[a]	2.39	2.34	1.89	1.05	1.72	2.03	1.89	1.55	0.91
MCPF[b]	2.34 (2.43)	2.21 (2.31)	2.04 (2.11)	1.21 (1.20)	1.77 (1.89)	2.13 (2.27)	1.76 (1.93)	1.58 (1.78)	0.69 (0.80)
LDA+B+P[c]	2.61	2.43	2.26	1.68	2.27	2.52	2.38	2.09	1.48
B3LYP[d]	2.60	2.80	2.21	1.67	2.25	2.64	2.46	1.99	1.29
various	1.93[e]	2.02[f]	-	0.99[g]	-	1.81[h]	2.05[i]	-	-
experiment[j]	2.40 ± 0.10	2.31 ± 0.11	2.05 ± 0.06	1.37 ± 0.09	2.06 ± 0.15	2.12 ± 0.06	1.98 ± 0.06	1.67 ± 0.08	0.92 ± 0.13

[a] References 148 and 150. [b] Reference 149 (the results in parentheses include relativistic and further correlation corrections). [c] Reference 113. [d] Reference 114. [e] Reference 118. [f] Reference 151. [g] Reference 152. [h] Reference 153. [i] Reference 155. [j] Reference 157.

Table 9. Transition-Metal Hydride Cations: Bond Lengths (Å)

	ScH^+	TiH^+	VH^+	CrH^+	MnH^+	FeH^+	CoH^+	NiH^+	CuH^+
GVB[a]	1.810	1.730	1.662	1.602	1.702	1.653	1.606	1.561	1.513
MCPF[b]	1.830	1.740	1.661	1.604	1.652	1.603	1.547	1.487	1.445
LDA+B+P[c]	1.795	1.689	1.646	1.589	1.573	1.556	1.533	1.473	1.494
B3LYP[d]	1.766	1.700	1.648	1.594	1.600	1.561	1.541	1.466	1.478
various	1.856[e]	1.755[f]	-	1.63[g]	-	1.619[h]	1.53[i]		

[a] References 148 and 150. [b] Reference 149. [c] Reference 113. [d] Reference 114. [e] Reference 118. [f] Reference 151. [g] Reference 152. [h] Reference 153. [i] Reference 155.

and the resulting state is $^1\Sigma^+$. If the $4s^2$ pair hybridizes and forms a sp hybrid pointing toward H, $sz = 4s + 4p$, and one pointing away from H, $\overline{sz} = 4s - 4p$, one can form a $sz + 1s$ bond with the configuration

$$\overline{sz}\ 3d_i\ (sz + 1s)^2$$

with the states $^{1,3}\Sigma^+$, $^{1,3}\Pi$, and $^{1,3}\Delta$.

The $d_\sigma + 1s$ bonded state is stabilized by interacting with the $sz + 1s$ bonded state and is the ground state, as shown by Walch and Bauschlicher.[117] The $^3\Delta$ is the HF ground state, but, in the correlated calculations, is ~0.3 eV higher. The ground state of Ti is $^3F(s^2d^2)$ with a $^5F(sd^3)$ 0.7 eV higher. Unlike Sc, Ti does not form a d bond with H, for two reasons. First, the Ti d is more contracted than in Sc, and, second, the d electrons in these two configurations are high spin and would have to uncouple and add in some singlet character to form a bond. This results in an exchange-energy loss that makes the process less likely. As the ^3F ground-state approaches H, the d electrons remain high spin and the $4s^2$ pair hybridize, resulting in the valence-electron configuration

$$\overline{sz}\ 3d^2\ (sz + 1s)^2$$

which results in $^{2,4}\Phi$, $^{2,4}\Delta$, $^{2,4}\Pi$, and $^{2,4}\Sigma^-$ states, with the $3d^2$ always high spin and the $\overline{sz}$ coupled into a doublet or quartet. Which of these is the ground state? In the Ti atom, each of the states associated with the $^3F(4s^23d^2)$ term has the orbital composition shown in Table 10. The $4s^2$ pair is doubly occupied and does not affect the d couplings. If the d electrons are to remain high spin and if we minimize electron repulsion by minimizing the $3d_\sigma$ occupancy, then we would predict that the ^3F term would form molecular states in the order $^4\Phi \sim {}^4\Sigma^- < {}^4\Pi < {}^4\Delta$. One anticipates that $^4\Phi < {}^4\Sigma^-$ because the electron repulsion associated with the $\pi_\pm\delta_\mp$ configuration is less than the $\pi_+\pi_-$ and $\delta_+\delta_-$ configurations. This is the order calculated by Anglada et al.,[124] using a highly correlated MRD-CI technique. The $^5F(sd^3)$ state of Ti could also form a bond to H, using the 4s orbital resulting in the valence configuration

$$d^3\ (4s + 1s)^2$$

Table 10. Composition of the $^3F(d^2)$ and $^3P(d^2)$ Terms, Using Real Orbitals in $C_{\infty v}$ Symmetry

State	Orbital Structure
$^3\Sigma^-\ (^3F)$	$\frac{1}{\sqrt{5}}\lvert\delta_+\delta_-\rangle - \sqrt{\frac{4}{5}}\lvert\pi_x\pi_y\rangle$
$^3\Pi_x\ (^3F)$	$\sqrt{\frac{2}{5}}\lvert\sigma\pi_x\rangle - \sqrt{\frac{3}{5}}\left\lvert\frac{\pi_x\delta_+ + \pi_y\delta_-}{\sqrt{2}}\right\rangle$
$^3\Pi_y\ (^3F)$	$-\sqrt{\frac{2}{5}}\lvert\sigma\pi_y\rangle + \sqrt{\frac{3}{5}}\left\lvert\frac{\pi_x\delta_- - \pi_y\delta_+}{\sqrt{2}}\right\rangle$
$^3\Delta_+\ (^3F)$	$\lvert\sigma\delta_+\rangle$
$^3\Delta_-\ (^3F)$	$\lvert\sigma\delta_-\rangle$
$^3\Phi_x\ (^3F)$	$\frac{1}{\sqrt{2}}\lvert\pi_x\delta_+ - \pi_y\delta_-\rangle$
$^3\Phi_y\ (^3F)$	$\frac{1}{\sqrt{2}}\lvert\pi_x\delta_- + \pi_y\delta_+\rangle$
$^3\Sigma^-\ (^3P)$	$\sqrt{\frac{4}{5}}\lvert\delta_+\delta_-\rangle + \sqrt{\frac{1}{5}}\lvert\pi_x\pi_y\rangle$
$^3\Pi_x\ (^3P)$	$\sqrt{\frac{3}{5}}\lvert\sigma\pi_x\rangle + \sqrt{\frac{2}{5}}\left\lvert\frac{\pi_x\delta_+ + \pi_y\delta_-}{\sqrt{2}}\right\rangle$
$^3\Pi_y\ (^3P)$	$\sqrt{\frac{3}{5}}\lvert\sigma\pi_y\rangle + \sqrt{\frac{2}{5}}\left\lvert\frac{\pi_x\delta_- - \pi_y\delta_+}{\sqrt{2}}\right\rangle$

Table 11. Composition of the $^4F(d^3)$ and $^4P(d^3)$ Terms, Using Real Orbitals in $C_{\infty v}$ Symmetry

State	Orbital Structure
$^4\Sigma^-$ (^{4}F)	$\left\|\sigma\left(\sqrt{\frac{4}{5}}\|\delta_+\delta_-\rangle+\sqrt{\frac{1}{5}}\pi_x\pi_y\right)\right\rangle$
$^4\Pi_x$ (^{4}F)	$\sqrt{\frac{2}{5}}\|\pi_y\delta_+\delta_-\rangle-\sqrt{\frac{3}{5}}\left\|\sigma\left(\frac{\delta_+\pi_x+\delta_-\pi_y}{\sqrt{2}}\right)\right\rangle$
$^4\Pi_y$ (^{4}F)	$-\sqrt{\frac{2}{5}}\|\pi_x\delta_+\delta_-\rangle+\sqrt{\frac{3}{5}}\left\|\sigma\left(\frac{\delta_+\pi_y-\delta_-\pi_x}{\sqrt{2}}\right)\right\rangle$
$^4\Delta_-$ (^{4}F)	$\|\pi_x\pi_y\delta_+\rangle$
$^4\Delta_+$ (^{4}F)	$\|\pi_x\pi_y\delta_-\rangle$
$^4\Phi_x$ (^{4}F)	$\frac{1}{\sqrt{2}}\|\sigma(\delta_+\pi_x-\delta_-\pi_y)\rangle$
$^4\Phi_y$ (^{4}F)	$\frac{1}{\sqrt{2}}\|\sigma(\delta_+\pi_y-\delta_-\pi_x)\rangle$
$^4\Sigma^-$ (^{4}P)	$\left\|\sigma\left(\sqrt{\frac{1}{5}}\|\delta_+\delta_-\rangle-\sqrt{\frac{4}{5}}\|\pi_x\pi_y\rangle\right)\right\rangle$
$^4\Pi_x$ (^{4}P)	$\sqrt{\frac{3}{5}}\|\pi_y\delta_+\delta_-\rangle+\sqrt{\frac{2}{5}}\left\|\sigma\left(\frac{\delta_+\pi_x+\delta_-\pi_y}{\sqrt{2}}\right)\right\rangle$
$^4\Pi_y$ (^{4}P)	$\sqrt{\frac{3}{5}}\|\pi_x\delta_+\delta_-\rangle+\sqrt{\frac{2}{5}}\left\|\sigma\left(\frac{\delta_+\pi_y-\delta_-\pi_x}{\sqrt{2}}\right)\right\rangle$

From Table 11, we anticipate the molecular states

$$^4\Delta < {}^4\Pi < {}^4\Phi < {}^4\Sigma^-$$

and the observed states will be a mixture of the s^2d^2 and s^1d^3 asymptotes. To the extent that the 3d atomic couplings are preserved in the molecule, the$^4\Sigma^-$ and $^4\Pi$ states are intrinsically multiconfigurational and will be poorly represented by a single-determinant HF wave function. This is illustrated by the HF calculation of Scott and Richards,[122] which predicts the order

$$^4\Phi < {}^4\Delta < {}^4\Pi < {}^4\Sigma^-$$

Walch and Bauschlicher[107] have discussed the role of atomic couplings in determining the ground state of the TM hydrides from a slightly different perspective. Moving on to VH, one has vanadium with a ^{4}F-(s^2d^3) ground state and a low-lying $^6\Delta$ (sd^4) only 0.4 eV higher. A bond to the s^2d^3 configuration would result in a VH valence configuration

$$\overline{sz}\, d^3\, (sz + 1s)^2$$

which would give rise to triplets and quintets of Φ, Δ, Π, and Σ^- symmetry. From Table 11, we see that the $^4\Delta$ ($\pi_x\pi_y\delta$) state has no d_σ orbital occupied, and we, therefore, expect a $^5\Delta$ ground state followed by $^5\Pi < {}^5\Phi < {}^5\Sigma^-$. On the other hand, the excited ^{6}D would give rise to $^5\Sigma^+ < {}^5\Pi < {}^5\Delta$. Calculations of Bruna and Anglada[119] predict $^5\Delta < {}^5\Pi < {}^5\Sigma^-$ with no mention of $^5\Phi$, while Henderson, Das, and Wahl[125] and Walch and Bauschlicher[107] report $^5\Delta < {}^5\Pi < {}^5\Sigma^- < {}^5\Phi$.

There are two additional low-lying atomic states of V that are important. The ^{6}D gives rise to the quintet molecular configurations

$$d^4\, (4s + 1s)^2$$

and the symmetries Σ^+, Π, and Δ.

This $^5\Delta$ looks like

$$d^1_\sigma\, d^1_{\pi_x}\, d^1_{\pi_y}\, d^1_\delta\, (4s + 1s)^2$$

which can interact with the $^5\Delta$ from the ^{4}F

$$\overline{sz}^1\, d^1_\pi d_{\delta_+} d_{\delta_-}\, (sz + 1s)^2$$

and stabilize it via $\overline{sz}$, d_σ hybridization. Likewise, the $^5\Pi$ from the ^{6}D looks like

$$d^1_\sigma\, d^1_\pi d_{\delta_+} d_{\delta_-}\, (4s + 1s)^2$$

which can interact with and stabilize the

$$\overline{sz}^1\, d^1_\pi d_{\delta_+} d_{\delta_-}\, (sz + 1s)^2$$

component of the $^5\Pi$ from the ^{4}F atom, also via $\overline{sz}$, d_σ hybridization. The low-lying $^4\Pi$ term of the s^2d^3 configuration gives rise to a molecular $^5\Sigma^-$ state that interacts with the $^5\Sigma^-$ from the V(^{4}F) term. These considerations suggest $^5\Delta < {}^5\Pi < {}^5\Sigma^- \sim < {}^5\Phi$, which is consistent with the calculations of Das;[106] Henderson, Das, and Wahl;[125] Walch and Bauschlicher;[107] and Bruna and Anglada.[119] For CrH, we anticipate that the ground $^7S(sd^5)$ state of Cr will result in a molecular configuration

$$d^5\, (4s + 1s)^2$$

and a $^6\Sigma^+$ state, as found by Dai and Balasubramanium.[126] For MnH, the ground state must come from the $^6\Sigma$ state of Mn, which is 2 eV below the excited ^{6}D. Accordingly, it is a $^7\Sigma^+$ state with a 4s + 1s bond. Note that the ground-state spin and spatial multiplicity of TiH and VH are the same, whether one forms a $\overline{sz}$ + 1s from the s^2d^N configuration or a 4s + 1s bond from the sd^{N+1} configuration. This is not the case for Fe, Co, and Ni. The ground ^{5}D of Fe can form a sz + 1s bond with the configuration

$$\overline{sz}\, d^6\, (sz + 1s)^2$$

which gives rise to quartets and sextets of Σ^+, Π, and Δ symmetries with the order $\Delta < \Pi < \Sigma^+$ for both the quartets and sextets. The lowest Δ has the configuration,

$$\overline{sz}^1 d^1_\sigma\, d^1_{\pi_x}\, d^1_{\pi_y}\, d^1_{\delta_+}\, d^2_{\delta_-}\, (sz + 1s)^2, \quad {}^4\Delta \text{ or } {}^6\Delta$$

Table 12. Composition of the $^4F(d^7)$ and $^4P(d^7)$ Terms, Using Real ($C_{\infty v}$ Symmetry) Orbitals

State	Orbital structure
$^4\Sigma^-(^4F)$	$\sqrt{\frac{4}{5}}\left\|\pi_x^2\pi_y^2\sigma\delta_+\delta_-\right\rangle+\sqrt{\frac{1}{5}}\left\|\delta_+^2\delta_-^2\sigma\pi_x\pi_y\right\rangle$
$^4\Pi_x(^4F)$	$\sqrt{\frac{2}{5}}\left\|\sigma^2\pi_x^2\pi_y\delta_+\delta_-\right\rangle-\sqrt{\frac{3}{5}}\left\{\frac{\left\|\delta_-^2\pi_y^2\sigma\delta_+\pi_x\right\rangle+\left\|\delta_+^2\pi_x^2\sigma\delta_-\pi_y\right\rangle}{\sqrt{2}}\right\}$
$^4\Pi_y(^4F)$	$-\sqrt{\frac{2}{5}}\left\|\sigma^2\pi_y^2\pi_x\delta_+\delta_-\right\rangle+\sqrt{\frac{3}{5}}\left\{\frac{\left\|\delta_-^2\pi_x^2\sigma\delta_+\pi_y\right\rangle-\left\|\delta_+^2\pi_y^2\sigma\delta_-\pi_x\right\rangle}{\sqrt{2}}\right\}$
$^4\Delta_-(^4F)$	$\left\|\sigma^2\delta_-^2\pi_x\pi_y\delta_+\right\rangle$
$^4\Delta_+(^4F)$	$\left\|\sigma^2\delta_+^2\pi_x\pi_y\delta_-\right\rangle$
$^4\Phi_x(^4F)$	$\frac{1}{\sqrt{2}}\left\{\left\|\delta_-^2\pi_y^2\sigma\delta_+\pi_x\right\rangle-\left\|\delta_+^2\pi_x^2\sigma\delta_-\pi_y\right\rangle\right\}$
$^4\Phi_y(^4F)$	$\frac{1}{\sqrt{2}}\left\{\left\|\delta_-^2\pi_x^2\sigma\delta_+\pi_y\right\rangle+\left\|\delta_+^2\pi_y^2\sigma\delta_-\pi_x\right\rangle\right\}$
$^4\Sigma^-(^4P)$	$\sqrt{\frac{1}{5}}\left\|\pi_x^2\pi_y^2\sigma\delta_+\delta_-\right\rangle+\sqrt{\frac{4}{5}}\left\|\delta_+^2\delta_-^2\sigma\pi_x\pi_y\right\rangle$
$^4\Pi_x(^4P)$	$\sqrt{\frac{3}{5}}\left\|\sigma^2\pi_x^2\pi_y\delta_+\delta_-\right\rangle+\sqrt{\frac{2}{5}}\left(\frac{\left\|\delta_-^2\pi_y^2\sigma\delta_+\pi_x\right\rangle+\left\|\delta_+^2\pi_x^2\sigma\delta_-\pi_y\right\rangle}{\sqrt{2}}\right)$
$^4\Pi_y(^4P)$	$\sqrt{\frac{3}{5}}\left\|\sigma^2\pi_y^2\pi_x\delta_+\delta_-\right\rangle+\sqrt{\frac{2}{5}}\left\{\frac{\left\|\delta_-^2\pi_x^2\sigma\delta_+\pi_y\right\rangle-\left\|\delta_+^2\pi_y^2\sigma\delta_-\pi_x\right\rangle}{\sqrt{2}}\right\}$

Table 13. Composition of the $^3F(d^8)$ and $^3P(d^8)$ Terms, Using Real ($C_{\infty v}$ Symmetry) Orbitals

State	Orbital structure
$^3\Sigma^-(^3F)$	$\sqrt{\frac{1}{5}}\left\|\sigma^2\pi_x^2\pi_y^2\delta_+\delta_-\right\rangle-\sqrt{\frac{4}{5}}\left\|\sigma^2\delta_+^2\delta_-^2\pi_x\pi_y\right\rangle$
$^3\Pi_x(^3F)$	$\sqrt{\frac{2}{5}}\left\|\delta_+^2\delta_-^2\pi_y^2\sigma\pi_x\right\rangle-\sqrt{\frac{3}{5}}\left(\frac{\left\|\sigma^2\delta_-^2\pi_y^2\pi_x\delta_+\right\rangle+\left\|\sigma^2\delta_+^2\pi_x^2\pi_y\delta_-\right\rangle}{\sqrt{2}}\right)$
$^3\Pi_y(^3F)$	$-\sqrt{\frac{2}{5}}\left\|\delta_+^2\delta_-^2\pi_x^2\sigma\pi_y\right\rangle+\sqrt{\frac{3}{5}}\left(\frac{\left\|\sigma^2\delta_+^2\pi_y^2\pi_x\delta_-\right\rangle-\left\|\sigma^2\delta_-^2\pi_x^2\pi_y\delta_+\right\rangle}{\sqrt{2}}\right)$
$^3\Delta_+(^3F)$	$\left\|\delta_-^2\pi_x^2\pi_y^2\sigma\delta_+\right\rangle$
$^3\Delta_-(^3F)$	$\left\|\delta_+^2\pi_x^2\pi_y^2\sigma\delta_-\right\rangle$
$^3\Phi_x(^3F)$	$\frac{1}{\sqrt{2}}\left(\left\|\sigma^2\pi_y^2\delta_-^2\pi_x\delta_+\right\rangle-\left\|\sigma^2\pi_x^2\delta_+^2\pi_y\delta_-\right\rangle\right)$
$^3\Phi_y(^3F)$	$\frac{1}{\sqrt{2}}\left(\left\|\sigma^2\pi_y^2\delta_+^2\pi_x\delta_-\right\rangle+\left\|\sigma^2\pi_x^2\delta_-^2\pi_y\delta_+\right\rangle\right)$
$^3\Sigma^-(^3P)$	$\sqrt{\frac{4}{5}}\left\|\sigma^2\pi_x^2\pi_y^2\delta_+\delta_-\right\rangle+\sqrt{\frac{1}{5}}\left\|\sigma^2\delta_+^2\pi_-^2\pi_x\pi_y\right\rangle$
$^3\Pi_x(^3P)$	$\sqrt{\frac{3}{5}}\left\|\delta_+^2\delta_-^2\pi_y^2\sigma\pi_x\right\rangle+\sqrt{\frac{2}{5}}\left(\frac{\left\|\sigma^2\delta_-^2\pi_y^2\pi_x\delta_+\right\rangle+\left\|\sigma^2\delta_+^2\pi_x^2\pi_y\delta_-\right\rangle}{\sqrt{2}}\right)$
$^3\Pi_y(^3P)$	$\sqrt{\frac{3}{5}}\left\|\delta_+^2\delta_-^2\pi_x^2\sigma\pi_y\right\rangle+\sqrt{\frac{2}{5}}\left(\frac{\left\|\sigma^2\delta_+^2\pi_y^2\pi_x\delta_-\right\rangle-\left\|\sigma^2\delta_+^2\pi_x^2\pi_y\delta_+\right\rangle}{\sqrt{2}}\right)$

with the five unpaired electrons all high spin for the $^6\Delta$ and the $\overline{sz}$ coupled into an open-shell quartet for the $^4\Delta$. The first excited state of Fe is $^5F(sd^7)$ and can form a (4s + 1s) bond and the states $^4\Phi$, $^4\Delta$, $^4\Pi$, $^4\Sigma^-$. From Table 12, we see that the $^4\Delta$ has the configuration

$$d_\sigma^2\, d_{\pi_x}^1\, d_{\pi_y}^1\, d_{\delta_+} d_{\delta-}^2\, (4s + 1s)^2$$

which can interact with the $^4\Delta$ with the sz + 1s bond configuration and thus lower it, relative to the $^6\Delta$. The same mechanism is available to the $^4\Pi$. The $^4\Delta$ is, indeed, the ground state of FeH, with the $^6\Delta$ only 0.25 eV higher. Calculations by Langhoff and Bauschlicher[135] and Sodupe, Lluch, Oliva, Illas, and Rubio[134] suggest

$$^4\Delta < {}^4\Pi < {}^6\Delta < {}^6\Pi < {}^6\Sigma^+ < {}^4\Sigma^+$$

an order that is consistent with this analysis. The ground state of Co is a $^4F(s^2d^7)$ with an excited $^4F(sd^8)$ 0.5 eV higher. The s^2d^7 state gives rise to triplets and quintets of Φ, Δ, Π, and Σ^-, with the order $\Phi < \Sigma^- < \Pi < \Delta$ and configuration

$$\overline{sz}\, d^7\, (sz + 1s)^2$$

The $^{3,5}\Phi$ looks like

$$\overline{sz}^1\, d_\sigma{}^1\, \pi_x^1\, \pi_y^2\, \delta_+\delta_-^2\, (sz + 1s)^2$$

The excited sd^8 forms triplets with a 4s + 1s bond and the symmetries Φ, Δ, Π, and Σ^- (Table 13). Each of these triplets will stabilize its companion from the s^2d^7 configuration and will differentially lower all of the triplets, relative to the quintets. Calculations by Freindorf, Marian, and Hess[136] predict that the four lowest states are

$$^3\Phi < {}^3\Sigma^- < {}^3\Pi < {}^3\Delta$$

and the next four are

$$^5\Phi < {}^5\Sigma^- < {}^5\Pi < {}^5\Delta$$

in remarkable agreement with the atomic-based order. The first two states of Ni, $^3D(s^1d^9)$ and $^3F(s^2d^8)$, are essentially degenerate, and predicting the ground state of the hydride is difficult. The ^3D will give rise (Table 13) to a 4s + 1s bond with configurations

$$d^9(4s + 1s)^2$$

and doublets in the order $^2\Sigma^+ < {}^2\Pi < {}^2\Delta$. The ^3F will give rise to a sz + 1s bond with doublets and quartets of Φ, Δ, Π, and Σ^- symmetry. Clearly, the $^2\Pi$ and $^2\Delta$ will be favored by configuration interaction and $^2\Sigma^+$ by the presence of a singly occupied d_σ orbital. The experimental and theoretical order is $^2\Delta(0.0) < {}^2\Sigma^+$ (0.27 eV) $< {}^2\Pi$ (0.32 eV), with the experimental energy separations in parentheses. The

Table 14. Comparison of Ground-State Properties of the Neutral Hydrides for MCPF and B3LYP Methods

		ScH	TiH	VH	CrH	MnH	FeH	CoH	NiH	CuH
R (Å)	MCPF[a]	1.776	1.781	1.719	1.694	1.753	1.573	1.532	1.485	1.509
	B3LYP[b]	1.730	1.744	1.677	1.654	1.723	1.561	1.510	1.509	1.460
	experiment[d]	-	-	-	1.6557	1.731	1.589	(1.54)	1.475	1.463
ω_e (cm^{-1})	MCPF[a]	1572	1407	1635	1647	1530	1915	1842	1987	1852
	B3LYP[b]	1663	1601	1614	1637	1586	1829	1868	2008	1901
	experiment[d]	-	-	-	1581	1548	1827	-	1927	1941
D_e (eV)	MCPF[a]	2.25	2.05	2.33	2.13	1.67	1.67	1.94	2.69	2.63
	B3LYP[b]	1.74	2.61	2.77	2.34	1.08	1.76	1.88	2.61	2.75
	experiment[c]	2.06 ± 0.09	2.17 ± 0.10	2.23 ± 0.10	2.03 ± 0.07	1.35 ± 0.19	1.70 ± 0.08	2.10 ± 0.14	2.66 ± 0.16	2.75 ± 0.18

[a] Chong et al., ref 112. [b] Barone and Adams, ref 114. [c] Armentrout and Sunderlin, ref 157. [d] Huber and Herzberg, ref 164.

ground state of CuH is dominated by the $^2S(sd^{10})$ state and is a $^1\Sigma^+$ with a 4s + 1s bond.

2. Spectroscopic Properties

Many of the calculations reported in Tables 4−6 were designed to investigate the adequacy of a particular theoretical method to properly account for the correlations required for a balanced description of the TM hydride chemical bond. Most of them have explored the basis set requirements and level of correlation in various configuration interaction models (SDCI, MRD-CI, MCSCF+1+2, MCPF, etc.). There have been a few perturbation-theory studies and two DFT studies. There are a few trends in the calculated and experimental data that we will use the MCPF[112] and a DFT[114] study to discuss. These are not the most accurate but are representative of the accuracy one may achieve with reasonable computational effort, and they have the advantage of being extendable to larger systems. In Table 14, we collect the bond lengths, bond energies, and vibrational frequencies calculated using the MCPF and the B3LYP-DFT methods and compare them with the available experimental quantities. The bond lengths are in reasonable agreement with both techniques, having an average error of 0.026 Å with the MCPF and 0.015 Å for the B3LYP-DFT. Both techniques account for the characteristic saw-tooth variation with TM; and, while the DFT usually underestimates R_e, the MCPF technique usually overestimates it. The situation with bond energies is not so clear. The MCPF and DFT have average errors of 0.13 eV and 0.25 eV, respectively. The MCPF calculation are uniformly accurate while the DFT has an average error of 0.38 for ScH−MnH and 0.08 for FeH−CuH. The harmonic vibrational frequencies have an average error of 60 cm^{-1} and 43 cm^{-1} for the MCPF and DFT, respectively.

D. Monopositive Hydrides

1. Bond Characteristics and Ground-State Symmetry

The ground state of Sc^+ is a $^3D(sd)$ with the $^3F(d^2)$ 0.60 eV higher. We expect the $^3D(sd)$ to form either a 4s + 1s or $3d_\sigma$ + 1s bond to H. The 4s + 1s bond gives rise to the states $^2\Delta < {}^2\Pi < {}^2\Sigma^+$, while the $3d_\sigma$ + 1s bond results in a $^2\Sigma$. Additionally, the $^3F(d^2)$ state results in $^2\Phi$, $^2\Delta$, $^2\Pi$, and $^2\Sigma^-$ states. The calculated order[118] is $^2\Delta$ (0.0 eV) < $^2\Pi$ (0.21 eV) < $^2\Sigma^+$ (0.26 eV), suggesting that the $3d_\sigma$ + 1s bond is not as dominant as it is in neutral ScH. However,

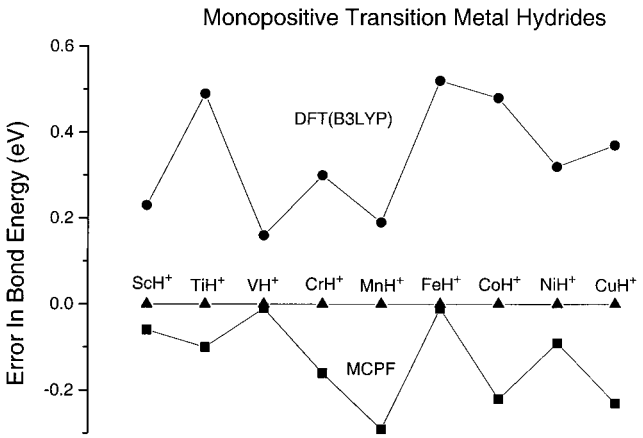

Figure 9. Comparison of the MCPF, B3LYP, and experimental bond energies for the positive hydrides.

the calculated bond lengths, $^2\Delta$ (1.822 Å), $^2\Pi$ (1.816 Å), and $^2\Sigma^+$ (1.776 Å), reflect the large $3d_\sigma$ + 1s character in the $^2\Sigma^+$ state. Indeed, the large d occupation (1.29) in the $^2\Delta$ and $^2\Pi$ states reflect the contribution of the $^3F(d^2)$ states.

The ground states of the remaining monopositive hydrides are all mixtures of 4s + 1s and $3d_\sigma$ + 1s bonds from the $4s3d^N$ and $3d^{N+1}$ configurations, and there is one fewer unpaired electron in the molecule than in the atomic ion. As the d orbital stabilizes, relative to the 4s, the $3d^{N+1}$ configuration increases in importance in going from TiH^+ to CrH^+, and this is reflected in the d population in Table 7. There is an abrupt change in the bonding in MnH^+ that is dominated by the 4s + 1s configuration, and then the $3d^{N+1}$ configuration increases in importance as one goes from FeH^+ to CuH^+.

2. Spectroscopic Properties

There are considerably fewer calculations on the positive hydrides, and, while the bond energies have been measured, there are no experimental data on bond lengths or vibrational frequencies. The experimental bond energies are compared with the available calculations in Table 8 and specifically with the MCPF and B3LYP calculations in Figure 9. Both computational techniques track the variation of the experimental bond energies, with the MCPF tending to underestimate and the B3LYP tending to overestimate the bond energy. As Armentrout and Kickel[172] have pointed out, this variation correlates nicely with the sd^N-d^{N+1} gap in the atomic ion. The bond in each of the hydrides is primarily 4s + 1s; and, when the ground state of the atomic ion is d^{N+1}, the promotion

energy required to access the sd^N state decreases the bond strength. Ohanessian and Goddard[150] have discussed this variation in terms of this promotion energy and exchange-energy loss.

E. Comparison of Neutral and Monopositive Hydrides

There are several interesting similarities and differences between the neutral and monopositive hydrides. Looking at Table 7 (excluding ScH, because of its unique $d_\sigma + 1s$ bond), we see that ionizing TiH−MnH results in a lower multiplicity ion, but ionizing FeH−CuH increases the multiplicity. In both cases, one is ionizing an electron with considerable sz character, which is, however, high-spin coupled to the d electrons in the early hydrides and low-spin coupled in the latter hydrides. Recall that the latter hydrides have low-spin, open-shell character because the lowest states from the sd^{N+1} configuration of the atom are also low-spin and differentially stabilize the low-spin coupling of the sz to the high-spin d^N configuration. Note that, once the sz electron is gone, the ion reverts to a 4s + 1s bond (except in CuH^+, where it must mix some $d_\sigma + 1s$), and the d population will drop to that of the atomic ion in the sd^N configuration plus a small increase due to $s-d_\sigma$ hybridization. The bond strengths of the neutral hydrides increases as one goes from MnH to CuH, due to the increasing availability of the sd^{N+1} state, while the bond strengths in the cationic hydrides decrease as one goes from FeH^+ to CuH^+, due to the decreasing availability of the sd^{N+1} state. The bond lengths for both the neutral and cationic hydrides decrease from TiH to CrH, increase at MnH, and then decrease from FeH to CuH. The bond lengths of the neutrals are greater than those of the cations for TiH, VH, and CrH and less for MnH−CuH.

F. Dipositive Hydrides

Recently, Harrison and Christopher[156] have published a detailed study of the early dipositive hydrides, using MCSCF and internally contracted MRCI techniques. All electronic states that correlate with the lowest term of the dipositive transition element and $H(^2S)$ have been studied as a function of internuclear separation. A theme in these calculations is whether the M^+ and H^+ asymptote is below M^{2+} and H and if the MH^{2+} molecule is thermodynamically stable. This is the case for Sc, where the $Sc^{2+}(^2D) + H(^2S)$ asymptote is below the $Sc^+(^3F) + H^+$ asymptote. The $^2D(d^1)$ state of Sc^{2+} forms singlets and triplets of Σ^+, Π, and Δ symmetries, and the only state with a singlet coupled Σ electron pair in the Σ system is the $^1\Sigma^+$, and it is bound by 1.35 eV. The other states are electrostatically bound with D_e's between 0.41 and 0.22 eV. The $Ti^{2+}(^3F)$ and $H(^2S)$ and $Ti^+(^4F) + H^+$ asymptotes are essentially degenerate, and, accordingly, TiH^{2+} is thermodynamically stable. The ^3F state of Ti^{2+} forms doublets and quartets of Σ^-, Π, Δ, and Φ symmetries, and the $^2\Delta$ is the ground state ($D_e = 0.86$ eV). This is consistent with the /M/ = 2 component of the ^3F, having an entire d_σ electron

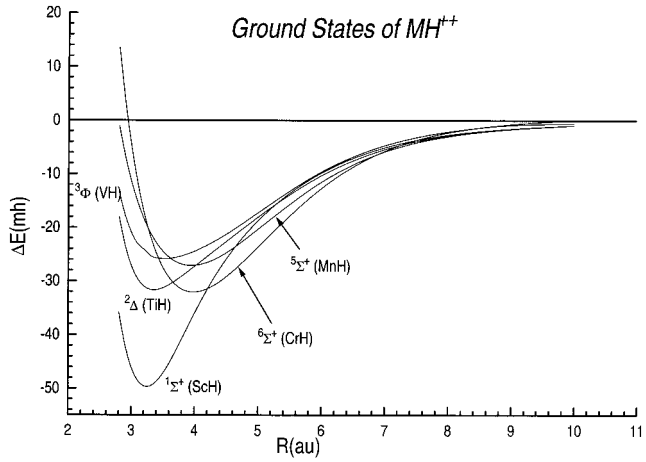

Figure 10. Potential energy curves for the ground state of MH^{++}.

Table 15. Calculated Spectroscopic Properties of MH^{++}[a]

molecule	state	R_e (Å)	ω_e (cm^{-1})	d_{pop}	D_e(eV)
ScH^{++}	$^1\Sigma^+$	1.718	1602	0.87	1.35
TiH^{++}	$^2\Delta$	1.777	1096	2.00	0.86
VH^{++}	$^3\Phi$	1.858	703	3.06	0.71
CrH^{++}	$^6\Sigma^+$	2.107	883	4.09	0.93
MnH^{++}	$^5\Sigma^+$	2.089	758	5.05	0.74

[a] From Harrison and Christopher, ref 156.

available to form a single bond with H. The small bond energy, relative to ScH^{2+}, reflects the exchange-energy loss that occurs when the d_σ and d_δ electrons are uncoupled during bond formation. The triplet states of VH^{2+} that correlate with the $^4F(V^{+2}) + H(^2S)$ asymptote are also thermodynamically stable, while the quintets are thermodynamically unstable but kinetically stable. The quartet states of CrH^{2+} are thermodynamically stable, while the sextet states are very long-lived, as will be the $^5\Sigma^+$ and $^7\Sigma^+$ states of MnH^{2+}. The bonding in the series ScH^{2+}, TiH^{2+}, and VH^{2+} is a mixture of a covalent bond between the metal $3d_\sigma$ and H 1s orbitals and an electrostatic component with both contributions decreasing as one goes from Sc to V. The covalent interaction decreases as the exchange-energy loss in the high-spin 3d system increases and essentially vanishes for CrH^{2+} and MnH^{2+}. These two molecules are bound primarily by the polarization of H by the metal cation. The potential energy curves for the ground states are shown in Figure 10 and the spectroscopic parameters in Table 15. The sequence of neutral, monopositive, and dipositive transition-metal hydrides is an interesting sequence in which to study the effects of successive ionization on the nature of the metal−hydrogen bond. Figure 11 compares the D_e's in this sequence and shows that the D_e's for the MH^{2+} sequence are all smaller than those of the neutral or monopositive hydrides and decrease more uniformly. This reflects the considerably simpler electronic structure of M^{+2}, relative to M and M^+. The bonding characteristics of M and M^+ are dominated by nuances in the relative positions of the s^2d^N and sd^{N+1} and d^{N+2} configurations, while M^{+2} is unencumbered by these options—the 4s orbitals are extremely high in energy and of no concern in the bonding. The

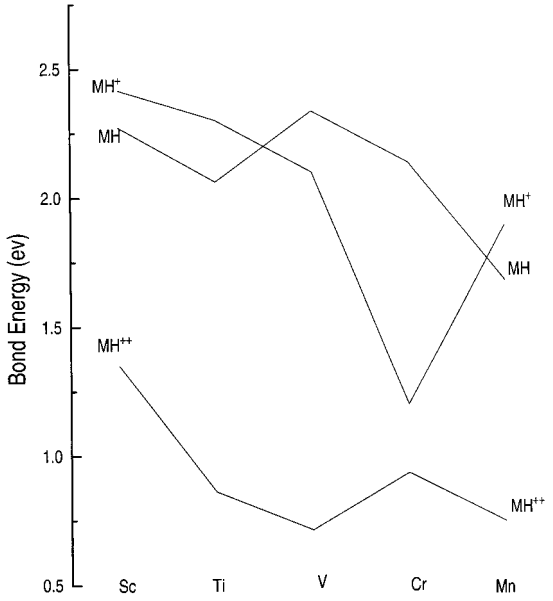

Figure 11. Dissociation energies of the neutral, mono-, and dipositive transition-metal hydrides.

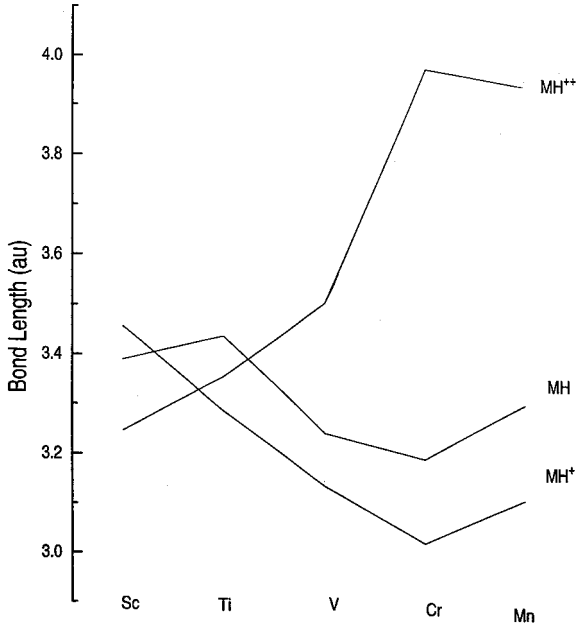

Figure 12. Bond lengths of the neutral, mono-, and dipositive transition-metal hydrides.

increasing compactness of the 3d orbitals in the remaining dipositive elements and the increasingly large exchange-energy loss required for bonding suggest that the remaining dipositive hydrides, FeH^{2+}, CoH^{2+}, NiH^{2+}, and CuH^{2+}, will all have D_e's that are comparable to CrH^{2+} and MnH^{2+}. Figure 12 compares the equilibrium bond length in MH^{2+} with MH and MH^+. While R_e in MH and MH^{2+} more or less decreases in going from Sc to Mn, it increases in MH^{2+}. There are no experimental data on MH^{2+}, and the variation of D_e and R_e with TM presents an interesting prediction.

G. Excited States of the Hydrides

The differences in the amount and type of electron correlation in the atoms ensures that the accurate

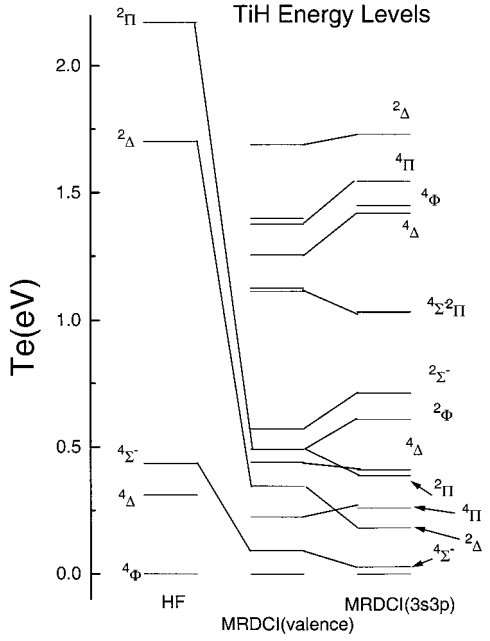

Figure 13. Effect of electron correlation on the low-lying states of TiH.

calculation of the excited states of the TM hydrides is challenging and requires large, single-particle basis sets and MRCI calculations with a carefully chosen reference space, and there have been a few such calculations. Most notably are the ScH and TiH MRD-CI studies of Anglada, Bruna, and Peyerimhoff;[120,124] the full second-order CI and multireference CI calculations on CrH by Dai and Balasubramanian;[126] the CASSCF/MRCI studies on MnH by Langhoff, Bauschlicher, and Rendell;[129] the relativistic pseudo-potential CI studies of Sodupe, Lluch, Oliva, Illas, and Rubio[134] on FeH; the MCSCF/MRCI calculations of Langhoff and Bauschlicher[135] on FeH; the variational relativistic CI study of CoH by Freindorf, Marian, and Hess;[136] the CASSCF/MRCI calculations on NiH by Blomberg, Siegbahn, and Roos;[139] and the variational relativistic CI study of CuH by Marian.[147] To illustrate the problem associated with these calculations, consider the effect of electron correlation on the low-lying states of TiH, as calculated by Anglada et al. Figure 13 shows a comparison of the HF results with MRD-CI calculations that correlate the valence (5) electrons and the 3s3p and valence (13) electrons. At the SCF level, the $^2\Delta$ and $^2\Pi$ are 1.65 and 2.35 eV above the $^4\Phi$, and the quartets are in the order $^4\Phi < {}^4\Delta < {}^4\Sigma^-$. Correlating the valence electrons drops the $^2\Delta$ and $^2\Pi$ to 0.35 and 0.5 eV above the $^4\Phi$ and inverts the order of the $^4\Delta$ and $^4\Sigma^-$. Additionally, more states are found as higher roots of the CI Hamiltonian. Correlating the 3s3p electrons results in further differential lowerings and brings the $^4\Sigma^-$ to within 0.07 eV of the $X^4\Phi$. The information content in these calculations is enormous. In addition to detailed potential energy curves, one has bond lengths, vibrational frequencies, transition moments, dipole moments, and charge distributions for all states.

VII. Transition-Metal Lithides

Very little is known about the TM lithides, and there are only four published experimental studies. Neubert and Zmbov[173] have estimated the dissociation energy of CuLi (1.96 ± 0.09 eV), using a Knudsen effusion technique combined with analysis of the vapor composition, while Van Zee et al.[174] have identified the ESR spectrum of CrLi ($^6\Sigma^+$) in an argon matrix at 4 K. Brock et al.[175] have reported the electronic spectrum of CuLi, using resonant one-color, two-photon ionization, and have determined the ground-state constants R_e, ω_e, and D_e as 2.26 Å, 466 cm^{-1}, and 1.95 eV. These authors argue that there is considerable ionic character in X $^1\Sigma^+$ CuLi. Russon, Rothschopf, and Morse[176] have also used resonant two-photon ionization spectroscopy to study CuLi and concur with the findings of Brock et al. They also estimate D_0 of $CuLi^+$ ($^2\Sigma^+$) as 0.97 ± 0.20 eV from the CuLi ionization energy of 6.37 ± 0.20 eV. These authors suggest that the bonding is primarily ionic. There have been four theoretical studies. The first, by Harrison,[177] discussed the structure of ScLi and was followed by Beckmann et al.,[178] in which they examined the electronic structure of ScLi, CuLi, and PdLi. Bauschlicher et al.[179] studied various metal dimers and trimers, including CuLi, using SDCI and CPF techniques. The most recent work is by Lawson and Harrison,[180] who used MRCI and ACPF techniques to study ScLi, TiLi, VLi, CrLi, and CuLi, as well as their positive ions. These authors have found that Li forms a weak bond to the s^2d^N configuration, primarily through sd_σ hybridization, and a much stronger bond to the sd^{N+1} configuration. In both Sc and Ti, the sd^{N+1} is above the s^2d^N configuration, and the resulting 4s + 2s bond is not strong enough to become the ground state. For these two elements, the ground state of the lithides are the $^3\Delta$ and $^4\phi$, respectively, which correlate with the ground s^2d^N configuration. At VLi, however, the proximity of the $^6D(sd^4)$ to the $^4F(s^2d^3)$ configuration allows the $^5\Delta$ from the d^4 $(4s + 2s)^2$ configuration to be the ground state by ~ 0.26 eV (relative to the $^4F(s^2d^3)$ state). The bonding in CrLi and CuLi is also dominated by a (4s + 2s) bond and results in a $^6\Sigma^+$ and $^1\Sigma^+$ ground state, respectively. The calculated potential curves are shown in Figures 14 and 15, and the theoretical results for CuLi are compared to experiment, in Table 16. The theoretical results all overestimate R_e and underestimate D_e, and it is of interest to know if it is primarily a basis set problem (inadequate representation of $Cu^-(s^2d^{10})$) or a differential effect involving sd^{10} and s^2d.[9]

VIII. Transition-Metal Borides

There are no experimental data nor theoretical studies of the neutral borides. For the positive ions, there is a series of high-level MRCI calculations with a large ANO basis by Kalemos and Mavridis[181−183] on ScB^+, TiB^+, VB^+, and CrB^+. These authors have constructed potential energy curves for the ground and many low-lying excited states and have determined R_e, ω_e, and D_e for each state and the charge distribution for selected states. The predicted ground state for each of these molecules is a high-spin state that is obtained from an intimate mixture of the sd^N and d^{N+1} TM asymptotes interacting with s^2p boron. The bonding in each molecule is due to three delo-

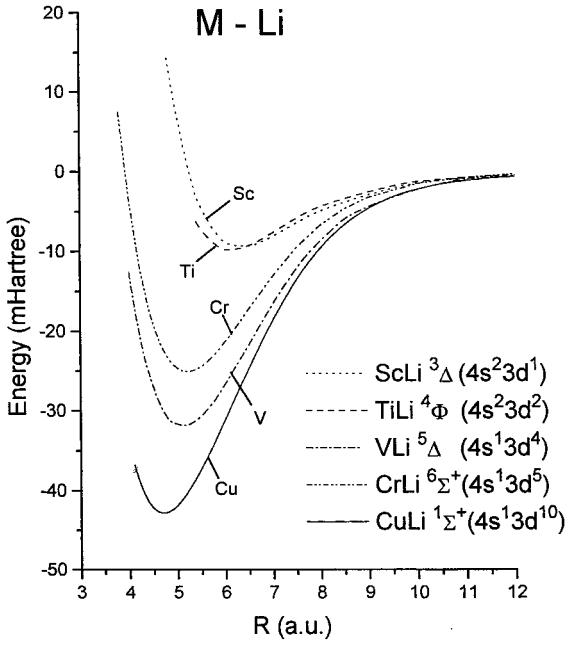

Figure 14. Potential energy curves for the transition-metal lithides.

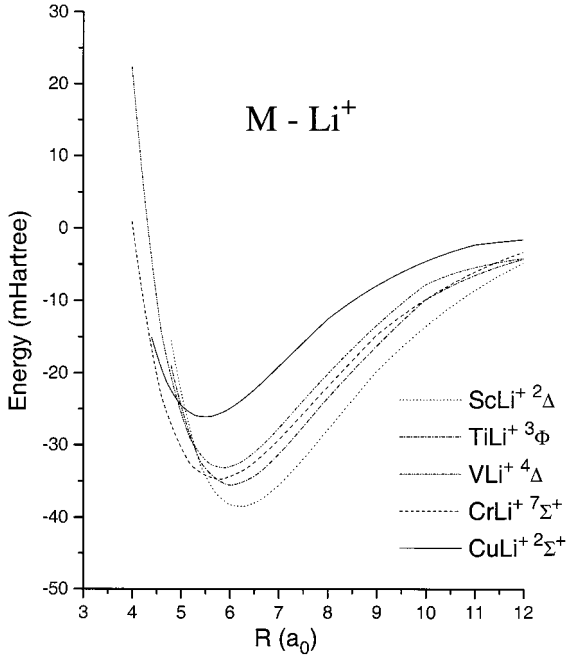

Figure 15. Potential energy curves for the monopositive transition-metal lithides.

Table 16. Calculated and Experimental Properties of CuLi ($X^1\Sigma^+$)

reference	R_e (Å)	ω_e (cm^{-1})	D_e (eV)	comment
Beckmann et al.[a]	2.65	-	1.30	
Bauschlicher et al.[b]	2.31	392	1.74	CPF
Lawson and Harrison[c]	2.43	356	1.62	ACPF
Brock et al.[d]	2.26	466	1.95	experiment

[a] Reference 178. [b] Reference 179. [c] Reference 180. [d] Reference 175.

Table 17. Calculated Spectroscopic Properties of MB^+ at the icMRCI+Q[a]

		State	R_e (Å)	ω_e (cm^{-1})	D_e (eV)	Electron Configuration
ScB^+	Sc–B:	$^4\Sigma^-$	2.16	500	1.95	$4s^{0.28}4p_\sigma^{0.10}d_\sigma^{0.42}d_\pi^{1.12}d_\delta^{0}2s^{1.52}2p_\sigma^{0.63}2p_\pi^{0.80}$
TiB^+	(δ)• Ti–B:	$^5\Delta$	2.104	507	2.12	$4s^{0.25}4p_\sigma^{0.08}d_\sigma^{0.44}d_\pi^{1.20}d_\delta^{1.0}2s^{1.57}2p_\sigma^{0.63}2p_\pi^{0.76}$
VB^+	(δ−)• (δ+)• V–B:	$^6\Sigma^+$	2.068	496	1.97	$4s^{0.21}4p_\sigma^{0.09}d_\sigma^{0.52}d_\pi^{1.22}d_\delta^{2.0}2s^{1.60}2p_\sigma^{0.59}2p_\pi^{0.76}$
CrB^+	4s→• Cr–B:	$^7\Sigma^+$	2.229	462	1.33	

[a] From Kalemos and Mavridis, refs 181−183.

calized one-electron bonds ($\sigma\pi^2$), with the boron 2s orbital forming a lone pair. Schematically, for ScB^+,

Sc–B: $^4\Sigma^-$

The calculated spectroscopic properties and the population analysis obtained from a CASSCF wave function are shown in Table 17.

IX. Transition-Metal Carbides

There are remarkably few calculations on the carbides, ScC,[184] TiC,[185,186] VC,[187] CrC,[188,189] NiC,[190,191] and their positive ions, ScC^+ [183c] and CrC^+.[277] The focus of the published studies has been the determination of the ground-state symmetry and an understanding of the bonding. When ground-state carbon interacts with a TM, the M = 0 component of the ^3P term has $^3\Sigma^-$ symmetry corresponding to C approaching the TM with both 2p electrons in π orbitals, while, in the $^3\Pi$ symmetry, one has a $2p_\sigma 2p_\pi$ occupation. Jeung and Koutecky[184] have studied ScC, using a MRCI approach for the valence electron with the core represented by the pseudopotential of Durand and Barthelat. They find many doublets and quartets of comparable energy with the lowest in the order $^4\Pi$ (0.0) < $^4\Delta$ (0.22 eV) < $^2\Pi$ (0.25 eV) < $^4\Sigma^-$ (0.27 eV). The bonding in the $^4\Pi$ is only slightly ionic ($Sc^{+0.24}C^{-0.24}$) and is described as being due to a delocalized one-electron σ bond (d_σ and p_σ), a conventional π bond (d_π and p_π), and an unpaired electron in a $\overline{sz}$ on Sc and a p_π on C. Symbolically

•Sc $\overline{-\bullet-}$ C $^4\Pi$

There have been two theoretical studies of TiC. Bauschlicher and Siegbahn[185] used a CASSCF/MRCI approach and found the ground state to be $^3\Sigma^+$ with a very low-lying (780 cm^{-1}) excited $^1\Sigma^+$ state. Hack et al.[186] found this same order, using MRCI (1250 cm^{-1}) and B3LYP (540 cm^{-1}) techniques, but found that the LSDA and BPW91 variants of DFT predicted the reverse order, making the $^1\Sigma^+$ the ground state. They also could not converge the CCSD method for the $^1\Sigma^+$ state, presumably due to its multiple-reference, open-shell character. Additionally, they found that the $^3\Sigma^+$ and $^1\Sigma^+$ states were not bound at the HF level. The population analysis of the $^3\Sigma^+$ state suggests that it is obtained from the $^5\Sigma^-$ component of the $^5F(sd^3)$ state of Ti interacting with the $^3\Sigma^-$ component of carbon. There are two π bonds, and a triplet coupled pair of σ electrons. One of the σ electrons is an sp hybrid (8σ or $\overline{sz}$) polarized to the rear of Ti, and the other is the remnant of a delocalized d_σ or 9σ electron that has acquired considerable $2p_\sigma$ character. Schematically,

• Ti $\overline{-\bullet-}$ C $^3\Sigma^+ (8\sigma\ 9\sigma\ 3\pi^4)$

The resulting electron distribution is

$$2s^{1.77}2p_\sigma^{0.61}2p_\pi^{1.90}4s^{0.84}4p^{0.21}3d_\sigma^{0.50}3d_\pi^{2.00}$$

The nature of the $^1\Sigma^+$ state is more complex. Both Bauschlicher and Siegbahn[185] and Hack et al.[186] note that its wave function is a strong mixture of the configuration $8\sigma^2 3\pi^4$ but with 8σ and 9σ orbitals that differ from the $^3\Sigma^+$ state. It does seem, however, that if one singlet couples the $\overline{sz}$ and $3d_\sigma + 2p_\sigma$, the $\overline{sz}$ would reoptimize to sz, so as to better overlap the now-modified $3d_\sigma + 2p_\sigma$, and the final charge distribution could be that calculated. Indeed, the $^1\Sigma^+$ state has a larger dipole moment (Ti^+C^-) than the $^3\Sigma^+$, and this is consistent with $\overline{sz}$ changing to sz.

Mattar[187] has used the LDF technique to study VC and concludes that it is a $^2\Delta$ corresponding to a triple bond and an unpaired d_δ electron. He also finds the $^2\Sigma^+$ and $^2\Pi$ states as the first and second excited states, respectively. A population analysis of the $^2\Delta$ wave function reveals the electron distribution,

$$2s^{1.83}2p_\sigma^{0.98}\ 2p_\pi^{1.83}4s^{0.28}3d_\sigma^{1.11}3d_\pi^{2.05}3d_\delta^{1.0}$$

This is consistent with V transferring a 4s electron to the empty $2p_\sigma$ in $^3\Sigma^-$ carbon and the resulting d^4 configuration on V forming a triple bond with the remaining electron in a $3d_\delta$ orbital. If the π bonds are more important than the σ, the first excited state would be the $^2\Sigma^+$ obtained by uncoupling the σ bonding pair and exciting the V d_σ electron to the empty $3d_\delta$ orbital, leaving the π system intact, preserving the number of d electrons, and forming a delocalized one-electron σ bond. To form a $^2\Pi$ state,

VC must break a π bond, making the $^2\Pi$ much higher in energy, as calculated. There have been three studies of CrC. The first two are by Shim and Gingerich,[188] who have used CASSCF calculations to predict the order,

$$^3\Sigma^- < {}^5\Sigma^- < {}^7\Sigma^- < {}^9\Sigma^-$$

with a gap of 0.55 eV separating the lowest and highest and considerable charge transfer from the Cr 4s to the C $2p_\sigma$. They suggest that one view these states as arising from the $Cr^+(^6S)$ and $C^-(^4S)$ states, recognizing that the $^5\Sigma^-$, $^7\Sigma^-$, and $^9\Sigma^-$ dissociate to neutral Cr ($4s3d^5$) in the ^7S state, while the $^3\Sigma^-$ is spin constrained to the ^5S state. Maclagan and Scuseria[189] have studied these same states, using DFT, CCSD, CASSCF, and MRCI techniques, and find the same order. Both sets of authors find that the HF method predicts the $^9\Sigma^-$ to be the ground state and, in fact, the only bound Σ^- state. This molecule illustrates an important relationship between multiplicity and the weights of configurations in a MRCI or CASSCF calculation. The wave function for the $^9\Sigma^-$ state can be thought of as having the eight valence orbitals high-spin coupled and being bound by the attraction between Cr^+ and C^-. Accordingly, it will have one dominant configuration,

$$3d_\sigma^1 3d_\pi^2 3d_\delta^2 2p_\sigma^1 2p_\pi^2$$

or

$$8\sigma^1 3\pi^2 1\delta^2 9\sigma^1 4\pi^2$$

where the Σ^- symmetry is maintained by the singly occupied δ_+ and δ_- orbitals.

The $^7\Sigma^-$ state is obtained by coupling a π-electron pair into a singlet

$$3d_\sigma^1 3d_{\pi_x}^1 3d_\delta^2 2p_\sigma^1 2p_{\pi_x}^1 (3d_{\pi_y} 2p_{\pi_y} + 2p_{\pi_y} 3d_{\pi_y})$$

and, since the $3d_{\pi_y}$ and $2p_{\pi_y}$ have a small overlap, they give rise to two orthogonal orbital configurations

$$8\sigma^1 9\sigma^1 3\pi_x^1 4\pi_x^1 1\delta^2 (3\pi_y^2 - \lambda 4\pi_y^2)$$

which, when symmetrized, are

$$8\sigma^1 9\sigma^1 1\delta^2 \{3\pi_x^1 4\pi_x^1 (3\pi_y^2 - \lambda 4\pi_y^2) + 3\pi_y^1 4\pi_y^1 (3\pi_x^2 - \lambda 4\pi_x^2)\}$$

and, so, going from $^9\Sigma^-$ to $^7\Sigma^-$ increases the multiconfigurational character substantially. Going to the $^5\Sigma^-$ results in

$$8\sigma^1 9\sigma^1 1\delta^2 (3\pi_x^2 - \gamma 4\pi_x^2)(3\pi_y^2 - \gamma 4\pi_y^2)$$

and to the $^3\Sigma^-$,

$$1\delta^2 (8\sigma^2 - \mu 9\sigma^2)(3\pi_x^2 - \gamma 4\pi_x^2)(3\pi_y^2 - \gamma 4\pi_y^2)$$

As one moves from Sc to Cu, the d orbitals contract and the d_π, p_π overlap less, and the simple Heitler London product

$$d_\pi\, p_\pi + p_\pi d_\pi$$

becomes increasingly less well represented by a doubly occupied π molecular orbital and forces a multiconfigurational character on the wave function. Maclagan and Scuseria note the need for caution when calculating these multireference states, using intrinsically single-reference methods such as HF, DFT, and single-reference CCSD. Kerkines and Mavridis[183c] have used the CASSCF+1+2 technique and studied 13 states of ScC^+, all within 2 eV of their predicted $^3\Pi$ ground state. Harrison[192] has studied CrC^+ and found the ground state to be $^4\Sigma^-$ characterized by two π bonds and a delocalized one-electron, σ bond high spin coupled to the two δ electrons. This illustrates, again (as in V ($^2\Delta$)), the weakness of the TM main group element σ bond when compared to two π bonds. The other ab initio molecular calculations we are aware of is the earliest found GVB study of NiC by Kitawia, Morokuma, and Csizmadia,[190] and the most recent study of Shim and Gingerich.[191] Kitawia et al. describe NiC as having a $^1\Sigma^+$ ground state with a triple bond and a charge of -0.56 electrons on C. They note the impossibility of converging the HF wave function and the critical importance of allowing for $\pi^2 \rightarrow \pi^{*2}$ excitations in the GVB wave function, which is consistent with the above discussion. The NiC bond is described as between the Ni sd^9 configuration and the carbon $^3\Pi$ ($p_\sigma p_\pi$) with a $4s + 2p_\sigma$ σ bond, a $3d_\pi + 2p_\pi$ bond and a formally dative π bond. Schematically,

$$d_\sigma^2\, d_\delta^4 (4s + p_\sigma)^2 (d_\pi + p_\pi)^4$$

Shim and Gingerich[191] have investigated 16 low-lying valence states, using CASSCF calculations and relativistic corrections. They calculate the ground state to be $^1\Sigma^+$, with R_e, ω_e equal to 1.621 Å and 874 cm^{-1}, which compare with the unpublished values of Brugh and Morse,[192] 1.631 Å (R_0) and 875 cm^{-1}. They calculate a considerably less ionic molecule than do Kitawia et al., assigning Ni a charge of +0.20 e. There is a growing body of spectroscopic data[193] on the carbides for which high-level calculations would be useful.

The available theoretical data for the carbides is collected in Table 18.

X. Transition-Metal Nitrides

A. The Early Nitrides: ScN, TiN, VN, and CrN

1. Ground States

There are several published calculations on the nitrides,[194−215] and most of these have focused on the early members and their positive ions, ScN,[194,199] TiN,[198,200−204] VN,[198,203,205,213] CrN,[198,203,205,206] MnN,[205] FeN,[206−208,212] NiN,[207] CuN,[209] ScN^+,[194,196,210,211] TiN^+,[194,210] VN^+,[194,210] CrN^+,[194,210,215] ScN^{2+},[194,214] and $TiN-CrN^{2+}$.[194] Calculations on the latter nitrides include MnN,[205] FeN,[206−208,212] FeN^+,[207] NiN,[207] CuN, and CuN^+.[209] The ground state of the early neutrals each has a triple bond with the remaining valence electrons localized on the TM. Accordingly, the

Table 18. Theoretical Data on Transition-Metal Carbides

molecule	state	R_e (Å)	ω_e (cm^{-1})	D_e (eV)	μ (D)	T_e (eV)	comments
ScC	$^4\Pi$	1.89	758	1.63 (^{2}D) 3.15 (^{4}F)	-	0.	*a*
	$^4\Delta$	2.25	487	-	-	0.22	
	$^2\Pi$	2.03	540	-	-	0.25	
	$^4\Sigma^-$	1.99	812	-	-	0.27	
	$^2\Sigma^+$	1.78	866	-	-	0.76	
TiC	$^3\Sigma^+$	1.77	830	3.08	1.53	0.0	*b*
	$^1\Sigma^+$	1.79	830	-	2.82	0.10	
	$^3\Delta$	1.80	860	-	7.78	0.87	
	$^3\Pi$	1.77	830	-	3.86	2.00	
	$^3\Sigma^+$	1.733	704	2.82	2.73	0.0	*c*
	$^1\Sigma^+$	1.790	592	2.66	2.16	0.155	
VC	$^2\Delta$	1.577	1054	6.77	5.94	0	*d*
	$^2\Sigma^+$	1.572	1065	-	3.14	0.32	
	$^2\Pi$	1.564	1065	-	4.21	2.15	
CrC	$^3\Sigma^-$	2.01	542	1.45	2.82	0.0	*e*
	$^5\Sigma^-$	2.04	523	-	3.06	0.15	
	$^7\Sigma^-$	2.06	605	-	3.64	0.26	
	$^9\Sigma^-$	2.13	499	-	4.38	0.28	
	$^5\Pi$	2.11	485	-	-	1.46	
	$^7\Pi$	2.19	495	-	-	1.61	
	$^3\Sigma^-$	1.676	675	3.00	6.84	0.	*f*
	$^5\Sigma^-$	1.756	515	2.00	2.85	1.00	D_e are all relative to ground-state products
	$^7\Sigma^-$	1.958	627	1.54	3.79	1.46	
	$^9\Sigma^-$	2.165	765	1.51	4.95	1.49	
CrC^+	$^4\Sigma^-$	1.735	726	1.41	-	0.0	*g*
	$^4\Pi$	2.059	-	0.58	-	0.83	
NiC	$^1\Sigma^+$	1.80	1219	1.0	-	0.0	*h*
	$^1\Sigma^+$	1.621	874	2.76	2.721	0.0	*i*
	$^1\Pi$	1.942	524	-	2.153	0.80	
	$^3\Sigma^+$	1.960	557	1.17	2.211	0.84	
	$^3\Pi$	1.957	564	-	2.644	0.92	
	$^1\Delta$	2.039	520	0.98	2.907	1.04	
	$^3\Delta$	2.029	525	0.96	2.849	1.07	
	$^1\Sigma^+$	1.631	875	-	-	-	experiment *j*

[a] Jung and Koutecky, ref 184. [b] Bauschlicher and Siegbahn, ref 185. [c] Hack et al., ref 186. [d] Mattar, ref 187. [e] Shim and Gingerich, ref 188. [f] Maclagan and Scuseria, ref 189. [g] Harrison, ref 215. [h] Kitawia et al., ref 190. [i] Shim and Gingerich, ref 191. [j] Reference 192.

valence electrons in Sc are all encumbered in the triple bond and the ground state is $^1\Sigma^+$. Note that, since the ground state of Sc is ^{2}D(s^{2}d) and the ground state of N is ^{4}S(p^3), a singlet ScN cannot dissociate to these limits, and the $^1\Sigma^+$ state correlates with the excited ^{4}F(sd^2) state of Sc. The ground state of TiN is $^2\Sigma^+$ with Ti's fourth valence electron going into a $\overline{\text{sz}}$ orbital localized on Ti. The ground state of VN is a $^3\Delta$ with the triplet coupled electrons in $\overline{\text{sz}}$ and d_δ orbitals. CrN has a $^4\Sigma^-$ ground state with the three unpaired electrons distributed as $\overline{\text{sz}}^1\ d^1_{\delta_+}\ d^1_{\delta_-}$.

The triple bond in TiN, VN, and CrN is very similar and results from the sd^{N+1} configuration of the TM. Both the σ bond, $3d_\sigma + 2p_\sigma$ and π bond $3d_\pi + 2p_\pi$ are polarized toward the N, resulting in a charge transfer of ~0.5 e. The situation in ScN is not so clear. Both Kunze and Harrison[195] and Daoudi et al.[199] have studied this molecule and agree on the ground-state symmetry but not its character. Kunze and Harrison suggest that the bonding is similar to the other early nitrides with a $3d_\sigma + 2p_\sigma$ bond. Daoudi et al. suggest that the π bond is, indeed, $3d_\pi + 2p_\pi$ but that the doubly occupied 2s forms a dative bond to Sc and the remaining two σ valence electrons have 4s and $2p_\sigma$ character and are coupled into an open-shell singlet.

$$(4s)\bullet \text{Sc}\overleftarrow{\text{N}}\bullet(p_\sigma) \qquad {}^1\Sigma^+$$

This is very similar to the bonding found by Kunze and Harrison[195] in Sc NH.

$$(4s)\bullet \text{Sc}\overleftarrow{\text{N}}-\text{H} \qquad {}^2\Sigma^+$$

While the character of the bonding at equilibrium in the ground states of TiN, VN, and CrN is easily characterized as being due to the sd^{N+1} configuration, considerable insight can be obtained by following the electron distribution as a function of internuclear distance. For example, to form $^2\Sigma^+$ TiN, one must go from the separated atoms containing five high-spin electrons in separate orbitals (Ti(s^{2}d^2) + N(p^3)) and one singlet-coupled electron pair (the metal 4s) to a molecule containing three singlet-coupled electron pairs (the triple bond) and one unpaired electron, a nontrivial transformation. We show, in Figure 16, the electron distribution as a function of bond length for $^2\Sigma^+$ TiN. As Ti and N approach one another, the earliest encounter is between a N $2p_\sigma$ electron and the spatially extended Ti 4s^2 pair. To reduce the Pauli repulsion between 4s^2 and the N $2p_\sigma$, Ti begins to excite some 4s to the $4p_\sigma$ while simultaneously transferring substantial electron density to the N $2p_\sigma$ orbital. This transfer begins at $R > 6\ a_0$ and is complete by $R = 4.50\ a_0$. As the nuclei come closer, the Ti $3d_\sigma$ begins to participate more fully and accepts some charge from the N $2p_\sigma$. Note that the declining

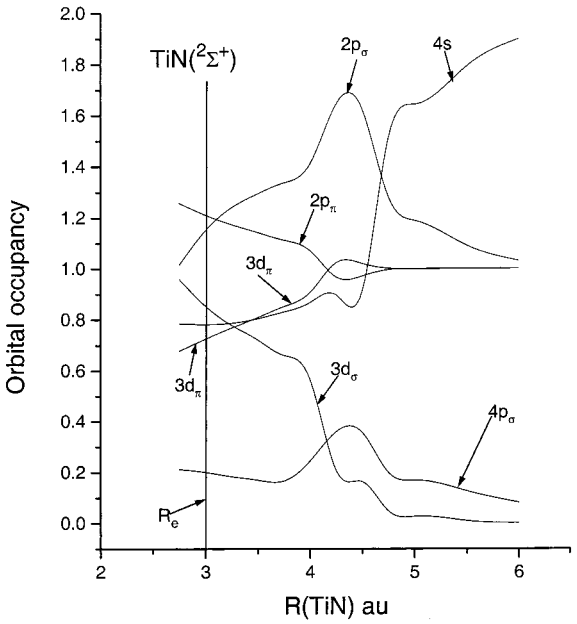

Figure 16. Electron population of valence orbitals of TiN as a function of internuclear separation.

Table 19. Equilibrium Populations of Valence Orbitals in Neutral Nitride Ground States[a]

		metal			nitrogen		
molecule	orbitals	4s	4p	3d	2s	2p	Total
ScN ($^1\Sigma^+$)	σ bond	0.17	0.18	0.50	0.02	1.13	2.00
	π bond	0.0	0.12	0.61	0.0	1.27	4.00
TiN ($^2\Sigma^+$)	σ bond	0.0	0.02	0.78	0.0	1.20	2.00
	π bond	0.0	0.05	0.75	0.0	1.20	4.00
	unpaired σ	0.79	0.17	0.04	0.0	0.00	1.00
VN ($^3\Delta$)	σ bond	0.0	0.02	0.80	0.01	1.17	2.00
	π bond	0.0	0.04	0.77	0.0	1.19	4.00
	unpaired σ	0.79	0.16	0.05	0.0	0.0	1.00
CrN ($^4\Sigma^-$)	σ bond	0.01	0.02	0.77	0.01	1.19	2.00
	π bond	0.0	0.02	0.80	0.0	1.18	4.00
	unpaired σ	0.78	0.15	0.07	0.0	0.0	1.00
	unpaired $\delta_\pm$	0.0	0.0	1.00	0.0	0.0	2.00

[a] Harrison, ref 203.

N $2p_\sigma$ occupation is mirrored by the increasing $3d_\sigma$ occupancy. It is clear that bond formation is driven by the charge transfer in the σ system and that the π bonds do not form until $R < 4.5\ a_0$. At equilibrium, the molecule has the polarity Ti^+N^- with approximately 0.5 electrons transferred from Ti to N. Interestingly, this is essentially the polarity at $R = 4.5\ a_0$, after the initial charge transfer and before the π bond formation. Representative equilibrium electron populations for the early nitrides are collected in Table 19, and the calculated ground-state properties are compared with experiment in Table 20.

2. Excited States

The excited states of the early transition-metal nitrides fall into two broad classes: those that maintain the metal-nitrogen triple bond and those that do not. Since all of the ScN valence electrons are involved in the bond, all of its excited states are obtained by breaking a bond. For example, breaking the σ bond results in the diradical

$$\bullet\,\mathrm{Sc}\equiv\mathrm{N}\,\bullet \qquad {}^{1,3}\Sigma^+$$

which may be either $^1\Sigma^+$ or $^3\Sigma^+$. Calculations place the $^3\Sigma^+$ 0.325 eV[195] or 0.281 eV[199] above the $X^1\Sigma^+$, suggesting that the ScN σ bond is rather weak, since the calculated D_e, relative to the spin-allowed products, is 4.56 eV. Examination of the high-spin σ electrons in $^3\Sigma^+$ shows that the metal localized one is predominately 4s, rather than $3d_\sigma$, while the one on N is $2p_\sigma$. When the electrons that form the singlet-coupled σ bond are triplet coupled, the metal orbital that had substantial $3d_\sigma$ character reverts to one with primarily 4s, and this relaxation accounts for the small $^3\Sigma^+ - X\ ^1\Sigma^+$ separation. Daoudi et al.[199] have calculated the $A\ ^1\Sigma^+$ state to be 0.707 eV above the $X\ ^1\Sigma^+$, in excellent agreement with the experimental value, 0.706 eV.

Breaking one of the π bonds in $X^1\Sigma^+$ and transferring the metal $3d_\pi$ to a $\overline{sz}$ or 4s, results in $^1\Pi$ and $^3\Pi$ states, both of which are low lying. Kunze and Harrison[195] have classified the lowest 14 electronic states of ScN according to its having a $\sigma\pi\pi$-triple, π-double, $\sigma\pi$-double, π-single, or σ-single bonds.

The lowest excited states of TiN are expected to arise[203] from exciting the unpaired $\overline{sz}$ electron on Ti to a $3d_\delta$ ($^2\Delta$) and $4p_\pi$ ($^2\Pi$). The lowest quartet state ($^4\Delta$) is obtained from triplet coupling the σ-bonding pair in the $^2\Delta$ state, resulting in

$$(\overline{sz})\bullet\ \overset{\bullet(\delta)}{\mathrm{Ti}}\equiv\mathrm{N}\bullet(p_\sigma) \qquad {}^2\Delta$$

Table 21 compares the experimental and calculated spectroscopic properties of several states of TiN. The T_e's are remarkably accurate, presumably because, in forming the excited states by moving a single electron from a metal-based $\overline{sz}$ to metal-based $3d_\delta$ and $4p_\pi$, we do not change the number of singlet-coupled electron pairs. In this context, it will be interesting to know how accurate the $^4\Delta$ state is. Harrison[203] has made detailed comparisons between theory and experiment for the excited states of TiN, VN, and CrN.

B. Latter Neutral Nitrides: MnN, FeN, CoN, NiN, and CuN

MnN. The ground $^6S(s^2d^5)$ state of Mn can form a triply bonded $^3\Sigma^-$ state with N

$$\overline{sz}^2 : \overset{\bullet\delta_+}{\underset{\bullet\delta_-}{\mathrm{Mn}\equiv\mathrm{N}}} \qquad {}^3\Sigma^-$$

and, given the stability of the s^2d^5 relative to the sd^6 configuration, this has a good chance to be the ground state. The $^6D(sd^6)$ configuration can also form triple bonds, so long as the doubly occupied d is not the $3d_\sigma$ or $3d_\pi$ orbitals. Accordingly, we may form

$$\overline{sz}\ d^2_{\delta_+} d_{\delta_-} (3d_\sigma + 2p_\sigma)^2 (3d_\pi + 2p_\pi)^4 \qquad {}^3\Delta_-$$

by doubly occupying either of the δ orbitals and singly occupying the other. Doubly ($\pi\pi$) bonded states can be formed from

$$\overline{sz}^1 d^2_\sigma\ d^1{}_{\delta_+}\ d^1_{\delta_-} 2p^1_\sigma (3d_\pi + 2p_\pi)^4 \qquad {}^{1,3,5}\Sigma^-$$

Table 20. Ground-State Properties of the Transition-Metal Nitrides

Molecule	State	R_e (Å)	ω_e (cm^{-1})	D_e (eV)	μ (D)	Q_{metal}	Reference
Sc ≡ N	$^1\Sigma^+$	1.768	726	2.75/4.56	6.04	+ 0.59	MRCI[195,203]
		1.714	766	2.27/3.91	—	+ 0.22	CIPSI[199]
		1.687[a]	795[a]	4.9[b]	—	—	Experiment
•Ti ≡ N	$^2\Sigma^+$	1.613	1024	4.18	3.25	+ 0.50	MRCI[203]
		1.630	1010	3.78	3.05	+ 0.37	MRCI[201]
		1.568	1139	8.05	3.65	+ 0.39	DFT[202]
		1.582[c]	1039[d]	4.9[b]	3.56[e]	—	Experiment
•V≡N	$^3\Delta$	1.608	974	3.74	2.83	+ 0.47	MRCI[203]
		1.5444*	1054*	—	3.212*/2.970$^+$	+ 0.36	*LDF and $^+$MRCI[213]
		1.561	1061	—	—	—	B3LYP[205]
		1.566[f]/	1033[g]	4.9[b]	3.07[j]	—	Experiment
		1.574[g]					
•CrN	$^4\Sigma^-$	1.619	854	2.75	2.00	+ 0.51	MRCI[203]
		1.62	—	3.18	2.08	+ 0.34	MRCI[206]
		1.535	846	—	—	—	B3LYP[205]
		1.563[i]	1050[h]	—	2.31[j]	—	Experiment
:MnN	$^5\Pi$ (?)	1.636	706	—	—	—	B3LYP[205]
	$^3\Sigma^-$ (?)	1.522	820	—	—	—	B3LYP[205] (0.03 eV (higher than quintet)
	$^5\Pi$ (?)	—	916[h]	—	—	—	Experiment
:FeN	$^2\Delta$	1.62	—	1.69	2.31	+ 0.34	T_e ($^4\Pi$) = 0.10 eV[206]
	$^2\Delta$	1.626	594	1.91	2.13	—	T_e ($^6\Sigma^+$) = 0.02 eV[208]
	$^2\Delta$	1.571	986	3.46	—	—	not B3LYP ground state[212]
•FeN	$^4\Pi$	1.569	1004	3.56	—	—	B3LYP ground state[212]
	Quartet	—	935[k]	—	—	—	Experiment
NiN	$^2\Pi$	1.82	—	1.36 (^{3}F)	—	+ 0.26	MRCI[207]
CuN	$^3\Sigma^-$	1.813	614	1.203	—	+ 0.27	MRCI[209]

[a] Ram and Bernath, ref 216. [b] Gingrich, ref 217. [c] Dunn, Hanson, and Rubinson, ref 218. [d] Douglas and Veilleti, ref 219. [e] Simard, Niki, and Hackett, ref 220. [f] Peter and Dunn, ref 221. [g] Simard, Masoni, and Hackett, ref 222. [h] Andrews, Bare, and Chertihin, ref 205. [i] Balfour, Qian, and Zhou, ref 223. [j] Steimle, Robinson, and Goodridge, ref 224. [k] Chertihin, Andrews, and Neurock, ref 212.

Note, this bonding permits an ionic component,

$$d_\sigma^2\, d^1{}_{\delta_+}\, d^1_{\delta_-}(2p_o)^2(3d_\pi + 2p_\pi)^4 \qquad {}^3\Sigma^-$$

Higher multiplicities can be generated from the $^3\Sigma^-$ by uncoupling the $\overline{sz}$ pair and exciting one to a $4p_\pi$, resulting in a $^5\Pi$. Other excited states can be formed

Table 21. Experimental and Calculated Spectroscopic Properties for Several States of TiN

	T_e (eV)				R_e (Å)				ω_e (cm^{-1})			
state	expt	JFH[d]	CB[e]	SM[f]	expt	JFH[d]	CB[e]	SM[f]	expt	JFH[d]	CB[e]	SM[f]
X $^2\Sigma^+$	0.0	0.0	0.0	0.0	1.582[b]	1.613	1.630	1.568	1039	1024	1010	1139
A′$^2\Delta$	0.934[a]	0.946	0.793	1.04	-	1.657	1.690	1.602	-	931	1020	990
$^4\Delta$	-	1.85	-	-	-	1.724	-	-	-	867	-	-
A$^2\Pi_r$	2.013[b]	2.01	2.01	1.95	1.596[b]	1.618	1.650	1.571	-	988	950	1081
B$^2\Sigma^+$	2.923[c]	-	-	-	(1.643)[c]	-	-	-	-	-	-	-

[a] Brabaharan, Coxon, Yamashita, ref 225. [b] Dunn et al., ref 218. [c] Bates, Ramieri, and Dunn, ref 226. [d] Harrison, ref 203. [e] Bauschlicher, ref 201. [f] Mattar, ref 202. [g] Douglas and Veilleti, ref 219.

Table 22. Calculated Properties of Low-Lying States of FeN

	R_e (Å)			T_e (eV)			D_e (eV)			μ (D)		ω_e (cm^{-1})	
	BS[a]	CAN[b]	FI[c]	BS[a]	CAN[b]	FI[c]	BS[a]	CAN[b]	FI[c]	BS[a]	FI[c]	CAN[b]	FI[c]
$^2\Delta$	1.62	1.571	1.626	0.	+0.10	0.	1.69	3.46	1.91	2.31	2.13	986	594
$^6\Sigma^+$	-	1.632	1.654	-	+0.48	0.02	-	3.08	1.89	-	3.08	863	715
$^4\Pi$	-	1.569	1.633	0.10	0.0	0.13	1.59	3.56	1.78	-	2.10	1004	768
$^4\Phi$	-	-	-	-	-	0.22	-	-	1.69	-	2.18	-	-

[a] Blomberg and Siegbahn, ref 206. [b] Chertihin, Andrews, and Neurock, ref 212. [c] Fiedler and Iwata, ref 208.

by breaking a σ or π bond and recoupling, etc. Andrews, Bare, and Chertihin[205] have identified MnN in solid argon (ω = 916 cm^{-1}) and have performed DFT calculations, using the B3LYP functional. They calculate the lowest triplet and quintet (spatial symmetry not given) and find ω (triplet) = 820 cm^{-1} and ω (quintet) = 706 cm^{-1}. Also, the optimized bond lengths are 1.522 Å (triplet) and 1.636 Å (quintet). The quintet is lower than the triplet by 0.8 kcal/mol. These results are consistent with a triply bonded triplet and a doubly bonded quintet. No other experiments or calculations have been reported.

FeN. The ^{5}D ground state of Fe(s^{2}d^6) can form a triple bond with N

$$\overline{sz}^2 d_{\delta_+}^2 \, d^1{}_{\delta-}(3d_\sigma + 2p_\sigma)^2(3d_\pi + 2p_\pi)^4 \qquad {}^2\Delta$$

as can the ^{5}F(sd^7) configuration

$$\overline{sz}^1 d_{\delta_+}^2 \, d^2{}_{\delta-}(3d_\sigma + 2p_\sigma)^2(3d_\pi + 2p_\pi)^4 \qquad {}^2\Sigma^+$$

We expect the $^2\Delta$ to be low lying but not the $^2\Sigma^+$. The reason can be seen in Table 12. The $d_{\delta_+}^2 d_{\delta_-}^2 d_\sigma d_{\pi_x} d_{\pi_y}$ configuration is the minor component of the $^4\Sigma^-$ (^{4}F) (only 20%) and the major component of the $^4\Sigma^-$ (^{4}P) (80%). Accordingly, the d couplings make the $^2\Sigma^+$ state derive its lineage from the ^{5}P (sd^7) rather than the ^{5}F, and the ^{5}P is over 2 eV above the ^{5}D. There have been four theoretical studies and one experimental study of FeN. Blomberg and Siegbahn[206,207] calculated several low-lying states, using the CASSCF technique and three of these using an ACPF method. They predict a $^2\Delta$ ground state (D_e = 1.69 eV) with a $^4\Pi$ 0.10 eV higher. The $^2\Delta$ has the structure discussed above, and the $^4\Delta$ is obtained from this by uncoupling the $\overline{sz}$ pair and exciting one electron to a 4p$_\pi$, resulting in

$$\overline{sz}^1 4p_\pi^1 3d_{\delta_+}^2 3d_{\delta_-}^1(3d_\sigma + 2p_\sigma)^2(3d_\pi + 2p_\pi)^4$$

Note that this gives rise to $^{2,4}\Phi$ and $^{2,4}\Pi$ states. Chertihin, Andrews, and Neurock[212] obtained the infrared spectrum of FeN in solid N_2 and Ar and performed DFT calculations on the lowest state of multiplicity 2, 4, and 6. No spatial symmetries were given. The calculated order is quartet < doublet (0.1 eV) < sextet (0.48 eV), with the following bond lengths and frequencies: quartet (1.569 Å, 1004 cm^{-1}), doublet (1.571 Å, 986 cm^{-1}), and sextet (1.632 Å, 863 cm^{-1}). Assuming the calculated doublet is $^2\Delta$ and the quartet is $^4\Pi$, the agreement with Blomberg and Siegbahn is reasonable. They[212] report a D_e of 3.56 eV for the quartet state, and their experimental value for ω is 938 cm^{-1}, almost midway between the computed values for $^2\Delta$ and $^4\Pi$. The most recent theoretical study is by Fiedler and Iwata,[208] who use the averaged quadratic coupled cluster (AQCC) technique to study the lowest 24 electronic states. These authors calculate the lowest four states as $^2\Delta$ (0.0) < $^6\Sigma^+$ (0.02 eV) < $^4\Pi$ (0.13 eV) < $^4\Phi$ (0.22 eV) with a D_e of 1.91 eV. In addition to the anticipated $^2\Delta$, $^4\Pi$, and $^4\phi$, these authors have identified the $^6\Sigma^+$ as a very low, possible ground state. This is an interesting state that we suspect traces its lineage to the $^5\Sigma^-$ component of the ^{5}F(sd^7) state and corresponds to a mixture of an ionic bond between Fe$^+$(d^7) and N$^-$(p^4) and a σ bond between Fe(sd^7) and N(p^3) with the configuration (see Table 14)

$$(\sqrt{4/5}d_{\pi_x}^2 d_{\pi_y}^2 d_{\delta_+}^1 d_{\delta_-}^2 + \sqrt{1/5}d_{\delta_+}^2 d_{\delta-}^2 d_{\pi_x}^1 d_{\pi_y}^1)\overline{sz}^1 2p_x^1 2p_y^1(3d_\sigma + 2p_\sigma)^2 \qquad {}^6\Sigma^+$$

and the ionic bond

$$(\sqrt{4/5}d_{\pi_x}^2 d_{\pi_y}^2 d_{\delta_+}^1 d_{\delta_-}^1 + \sqrt{1/5}d_{\delta_+}^2 d_{\delta_-}^2 d_{\pi_x}^1 d_{\pi_y}^1)2p_x^1 2p_y^1 2p_\sigma^2 \qquad {}^6\Sigma^+$$

The spectroscopic properties for these states are summarized in Table 22 and the energy levels in Figure 17.

CoN. There are no data (experimental or theoretical) for CoN. The ground configuration s^{2}d^7 can form a triple bond, $^1\Sigma^+(\overline{sz}^2\delta_+^2\,\delta_-^2)$; but, from Table 12, we

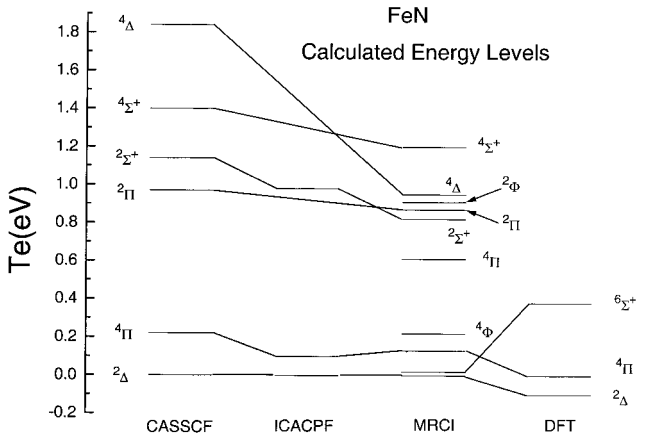

Figure 17. Calculated energy levels of FeN.

see that it is the excited ^{4}P, and not the ground ^{4}F, that will be dominant in the molecular wave function. Since the ^{4}P is 1.6 eV above the ^{4}F, the $^1\Sigma^+$ will have to have a bond energy greater than this excitation energy to compete for the ground state. The excited ^{4}F(sd^8) can form a $\pi-\pi$ double bond (via the $^4\Sigma^-$ component) that will result in a $^3\Sigma^+(\overline{sz}p_\sigma\delta_+^2\,\delta_-^2)$ or, perhaps, the ionic state $^1\Sigma^+(p_\sigma^2\,\delta_+^2\,\delta_-^2)$.

NiN. Siegbahn and Blomberg[207] have characterized a $^2\Pi$ state of NiN that results from the sd^9 configuration of Ni, with the d hole in the π symmetry. They calculate a bond length of 1.82 Å, which seems large, and a D_e of 1.36 eV. There are no experimental data with which to compare. The in situ Ni electron configuration is $4s^{0.96}\ 3d^{8.62}$, and the metal has a charge of +0.26. Presumably, the 3d occupancy is less than 9, because the one π bond is polarized toward N. Note that the unpaired π electron must be essentially localized on N.

$$(4s + p_\sigma)^2 d_\sigma^2 (d_{\pi_x} + p_x)^2 (d_{\pi_x} - p_x)^1 (d_{\pi_y} + p_y)^2 d_\delta^4 \quad {}^2\Pi$$

If one puts the d hole in the σ symmetry and forms a sd_σ and p_σ bond, one expects a $^4\Sigma^-$ state

$$\overline{sd}_\sigma^1 (sd_\sigma + p_\sigma)^2 (d_{\pi_x} + p_x)^2 (d_{\pi_y} + p_y)^2 (d_{\pi_x} - p_x)^1 (d_{\pi_y} - p_y)^1 d_\delta^4 \quad {}^4\Sigma^-$$

CuN. Daoudi et al.[209] have recently published a detailed study of CuN and CuN^+ (vide infra) in their ground and excited states. The ground state has a 4s + 2p σ bond, the Cu d^{10} configuration intact, a triplet coupled pair of π electrons on N, and therefore, $^3\Sigma^-$ symmetry. As with all of the TM nitrides, the metal is positively charged (+0.27 e). The lowest bound excited states are singlets and triplets of Σ^+, Π, and Δ symmetry that are obtained when ground-state Cu(sd^{10}) interacts with N(^{2}D). There are no experimental data on CuN.

C. Monopositive Nitrides

The early TM nitride cations have been studied by Kunze and Harrison[210] (ScN^+-CrN^+), Harrison[215] (CrN^+), and Elkhattabi[211] et al. (ScN^+). Additionally, Siegbahn and Blomberg[207] studied FeN^+, and Daoudi[209] et al. studied CuN^+. There are no experimental data on these systems.

The bonding in these ions is considerably less complex than in the neutral precursors. The asymptotic product is always the positive TM and neutral N, and, accordingly, it is the sd^N and d^{N+1} configuration of the metal that is important. Studies of ScN^+-CrN^+ suggest that the d^{N+1} configuration dominates the equilibrium electronic structure. Accordingly, the ground states are $Sc{=}N^{\bullet+}$ ($^2\Sigma^+$; $2p_\sigma^1$), $Ti{\equiv}N^+$($^1\Sigma^+$), $V{\equiv}N^+$($^2\Delta$; $d_{\delta_+}^1$), and $Cr{\equiv}N^+$($^3\Sigma^-$; $d_{\delta_+}^1 d_{\delta-}^1$). Siegbahn and Blomberg presumed the ground state of $Fe{\equiv}N^+$ to be $^1\Sigma^+$ ($d_{\delta_+}^2\,d_{\delta_-}^2$) and did not explore other options. Daoudi et al. determined that CuN^+ has a $^4\Sigma^-$ (p^3) ground state. The calculated properties of the ground states are collected in Table 23. The two results on ScN^+ are interesting, in that they predict similar D_e's and ω's but a large difference in R_e, d population, and Q, the Mulliken charge on the metal. Kunze and Harrison's calculated R_e for the neutral X $^1\Sigma^+$ ScN was larger than the experimental value by 0.08 Å, while Daoudi's was larger by 0.03 Å. Since Elkhattabi et al. used the same basis set and CIPSI method for ScN^+, we suspect their bond length is more reliable. The difference in d population and Q is in part due to Kunze and Harrison calculating these from the MCSCF wave function and D_e and R_e from the MCSCF+1+2 wave function. The similarity of the bond lengths in the sequence TiN^+-FeN^+ is consistent with each having a triple bond formed with increasingly contracted d orbitals. The slight jump in CrN^+ is characteristic of Cr^+ and reflects the stability of the d^5 shell. ScN^+ is not too different and suggests that the double bond determines the overall bond length and the delocalized σ electron is also contributing to the bonding. The large CuN^+ bond length reflects its dominant electrostatic origin. The calculated bond energies are all referred to the d^{N+1} configuration and decrease uniformly from TiN^+ to CuN^+, even though Ti^+ through Fe^+ use the d^{N+1} configuration to form a triple bond. It has been argued that the drop in D_e from TiN^+ to CrN^+ is due, in large measure, to the exchange-energy loss incurred in "flipping" the spins of the $3d_\sigma$ and $3d_\pi$ electrons in anticipation of forming a bond. Making this correction results in the curve labeled intrinsic in Figure 18. However, the large difference between TiN^+ ($^1\Sigma^+$) and FeN^+ ($^1\Sigma^+$) cannot be explained by this effect, as it is the same for both molecules. Siegbahn and Blomberg[207] have argued that the small D_e for FeN^+ is a consequence of a large repulsion energy between the d_δ orbitals. This factor, along with the much smaller size of the d orbitals in Fe, relative to Ti, and Fe's stronger in situ atomic coupling, all contribute to the large differential in D_e. It seems likely that the D_e of CoN^+ and NiN^+ will be less than FeN^+. The small D_e in CuN^+ is a consequence of the bond being electrostatic.

D. Dipositive Nitrides

The bonding in the dipositive nitrides of Sc, Ti, V, and Cr has been characterized as primarily electrostatic with small covalent character in the lower spin

Table 23. Calculated Properties of the Monopositive Transition-Metal Nitrides

Molecule	State	R_e (Å)	ω_e (cm^{-1})	D_e (eV)	d_{pop}	Q (metal)	Reference
Sc = N•$^+$	$^2\Sigma^+$	1.738	871	3.65	1.39	1.49	210
		1.649	829	3.44	1.79	0.99	211
Ti ≡ N$^+$	$^1\Sigma^+$	1.586	1045	4.80	2.46	1.43	210
V• ≡ N$^+$	$^2\Delta$	1.574	1005	3.79	3.54	1.38	210
Cr• ≡ N$^+$	$^3\Sigma^-$	1.596	864	2.15	4.60	1.33	210
:Fe: ≡ N$^+$	$^1\Sigma^+$	1.49	—	1.37	—	1.04	207
Cu N• $^+$	$^4\Sigma^-$	2.14	144	0.34	10.0	0.91	209

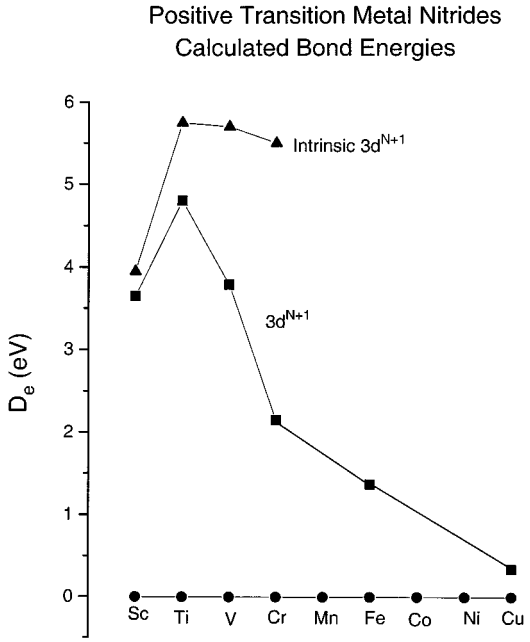

Figure 18. Calculated bond energies of the positive transition-metal nitrides.

states. The early members of this series are thermodynamically stable, while the latter are effectively so. The detailed electronic structure has been discussed by Harrison and Kunze,[194] who compared it to the neutral and monopositive nitrides. To date, there are no experimental data with which to compare.

XI. Transition-Metal Oxides

A. General Features

The emerging picture of the bonding in the low-lying states of the transition-metal oxides has an intimate mix of ionic and covalent components. The covalent component in the ground state typically involves ^{3}P oxygen with three π and one σ electron, $p_\sigma p_\pi^3$, bonding to the sd^{N+1} configuration of the neutral TM, and forming as many σ and π bonds as possible. The ionic component involves the sd^N or d^{N+1} configuration of M^+ bonding to the $p_\sigma p_\pi^4$ configuration of O^- (p^5). The σ bonds are usually between a singly occupied d_σ and p_σ in both the ionic and covalent pictures, while there are three classes of π bonds. One can form a traditional π bond by singlet coupling the singly occupied d_π and p_π orbitals resulting in a π bond that is polarized toward the oxygen. The presence of double occupied p_π orbitals on O opens the possibility for two additional types of π bonds. One can have a dative bond in which a doubly occupied p_π orbital delocalizes into an empty $3d_\pi$ and is polarized toward the metal, and one can also have an effective one-electron π bond from the interaction $p_\pi^1 + p_\pi^2$, which produces a doubly occupied π and a singly occupied π^* orbital. There have been many calculations on individual TM oxides and a few on the entire sequence. In this latter category are the CISD pseudopotential studies of Dolg, Wedig, Stoll, and Preuss,[227] the CCSD(T) and CASSCF/ICACPF studies of Bauschlicher and Maitre,[228] and the semiemperical studies of Bakalbassis, Stiakaki, Tsipis, and Tsipis.[229] In the former category, one has ScO,[230–233] TiO,[234–241] VO,[231,242] CrO,[243–248] MnO,[249] FeO,[238,250–253] CoO,[254,255] NiO,[256,257] and CuO.[258–266] In what follows, we will discuss the salient features of the electronic structure of the individual oxide and refer to specific calculations as warranted. We shall then look at the overall trends in the series.

B. Individual Oxides

ScO. The ground state of ScO has $^2\Sigma^+$ symmetry and may be thought of as resulting from the covalent interaction between Sc($4s\ 3d_\sigma\ 3d_{\pi_x}$) and O($2p_\sigma 2p_x\ 2p_y^2$) forming

$$\overline{sz}\,(3d_\sigma + 2p_\sigma)^2\,(3d_{\pi_x} + 2p_x)^2\,2p_y^2 \qquad ^2\Sigma^+$$

where the 4s on Sc polarizes away from the bond and is represented as $\overline{sz}$. This results in a molecule that has somewhat more than two bonds and may be represented as •Sc ⇋ O. The ionic interaction be-

Table 24. Comparison of Calculated Properties of ScO with Experiment[a]

	R_e (Å)	ω_e (cm^{-1})	D_e (eV)	T_e (eV)	μ (D)	d_{pop}	Q (metal)	comment
$X^2\Sigma^+$	1.646	1042	-	0.	3.59	1.16	0.74	SDCI[d]
	1.675	930	6.38	0.	3.21	1.43	0.54	CPF[d]
	1.63	1120	-	0.	2.96	1.45	0.44	MRCI (pseudopotential)[e]
	1.666	994	9.09	0.	3.83	1.36	0.42	LDF[f]
	1.680	971	6.96	0.	3.91	1.41	0.40	UCCSD(T)[g]
	1.685	974	5.84	0.	3.54	-	-	SEFIT[h]
	1.668	965	7.01[b]	0.	4.55[c]	-	-	experiment
$A^2\Delta_r$	1.709	902	-	1.834	9.08	1.94	0.93	SDCI[d]
	1.741	772	-	1.845	6.71	2.08	0.70	CPF[d]
	1.74	748	-	2.04	-	2.30	0.47	MRCI (pseudopotential)[e]
	1.703	895	-	1.773	7.11	-	-	LDF[f]
	1.726	846	-	1.863	-	-	-	experiment
$A^2\Pi_r$	1.661	914	-	2.08	4.453	1.47	0.81	SDCI[d]
	1.691	853	-	2.08	3.696	1.70	0.63	CPF[d]
	1.67	887	-	2.17	-	1.65	0.49	MRCI (pseudopotential)[e]
	1.685	897	-	1.912	3.96	-	-	LDF[f]
	1.6858	876	-	2.044	4.2 ± 0.2[c]	-	-	experiment

[a] Experimental data from Merer, ref 267, unless otherwise noted. [b] D_0. [c] Shirley, Scurlock, and Steimle, ref 268. [d] Reference 231. [e] Reference 232. [f] Reference 233. [g] Reference 228. [h] Reference 227.

tween $Sc^+(4s3d_\sigma)$ and $O^-(2p_\sigma 2p_\pi^4)$ contributes the Coulombic stabilization as well as a covalent $3d_\sigma + 2p_\sigma$ bond and two dative bonds in the π system while the 4s again polarizes into $\overline{sz}$. Low-lying excited states are obtained by preserving the triple bond and exciting the $\overline{sz}$ into a $3d_\delta$ ($^2\Delta_r$), $3d_\pi$ ($^2\Pi_r$), or a $4p_\pi$ ($^2\Pi_r$). The $^2\Delta_r$ state preserves the bonding of the ground state but requires that Sc acquire considerable in situ d^3 character. The $^2\Delta_r$ state is a compromise between the lower-energy $\overline{sz} \rightarrow 3d_\pi$ excitation that decreases the dative bond in the π system but adds more d^3 character and the higher-energy $\overline{sz} \rightarrow 4p_\pi$ excitation that preserves the dative π bond. These states have been studied by Carlson, Ludena, and Moser[230] (HF calculations); Bauschlicher and Langhoff[231] (SDCI and CPF); Jeung and Koutecky[231] (MRCI [pseudopotential]); Mattar[233] (LDF); Bauschlicher and Maitre;[228] and Dolg, Wedig, Stoll, and Preuss;[227] and their results are compared with experiment in Table 24. There are several interesting features to these data. First, while the SDCI and CPF methods give similar and accurate T_e's, they agree less well for all other listed properties. Interestingly, these two methods provide bounds for R_e and ω_e. The calculated dipole moment in the ground state is in poor agreement with experiment, with the LDF and UCCSD(T) coming closest. The LDF is close to the bond length in the ground state and also reproduces the bond length and comes within the experimental uncertainty for the dipole moment in the $^2\Pi_r$ state. The dipole moment in the $^2\Delta_r$ state is predicted to be very large, due, essentially, to the loss of the $\overline{sz}$ mitigating influence. Note that while the $^2\Pi_r$ also loses $\overline{sz}$, it acquires a π orbital ($3d_\pi$ and $4p_\pi$) polarized away from the π bonds.

TiO. The ground state ($^3\Delta$) of TiO results from the covalent interaction of ($sd_\sigma\, d_{\pi_x}\, d_\delta$) with O ($p_\sigma\, p_x\, p_y^2$) forming $d_\sigma + p_\sigma$, and $d_{\pi_x} + p_x$ bonds, with some delocalization of p_y^2 into the empty d_{π_y}. The 4s orbital polarizes away from the bond

$$\overline{sz}^1 d_{\pm}^1 (d_\sigma + p_\sigma)^2 (d_{\pi_x} + p_x)^2 p_y^2 \qquad ^3\Delta_r$$

Low-lying excited states obtained from the $\overline{sz} \rightarrow d_{\delta_\pm}$ ($^3\Sigma^-$) or $\overline{sz} \rightarrow (4p_\pi + 3d_\pi)$ excitations ($^{1,3}\Pi$ and $^{1,3}\Phi$). A $^1\Delta_r$ state results from singlet coupling the $\overline{sz}$ and $d_{\delta_\pm}$ orbitals. One can also excite the $d_{\delta_\pm}$ electron to a $4p_\pi + 3d_\pi$ orbital and form $^{1,3}\Pi$ and $^{1,3}\Phi$ states. The excitation $d_{\delta_\pm} \rightarrow \overline{sz}$ results in the low-lying $^1\Sigma^+$.

Several of these states can also be formed from the ionic asymptote $Ti^+(sd^2) + O^-(p_\sigma p_\pi^4)$ by forming a $d_\sigma + p_\sigma$ bond and keeping the d_π orbitals formally empty, permitting p_π^4 delocalization from O^-. This results in

$$\overline{sz}^1 d_{\pm}^1 (d_\sigma + p_\sigma)^2 p_\pi^4 \qquad ^{1,3}\Delta$$

as well as $^3\Sigma^-$, $^{1,3}\Pi$, $^{1,3}\Phi$, and $^1\Sigma^+$, as with the covalent picture. These asymptotes interact and provide additional stabilization.

There have been several studies of TiO, starting with the SCF calculation of Carlson and Moser,[234] in which they identified $^3\Delta$ as the ground state. Carlson and Nesbit[235] studied the $^1\Sigma^+$ state (HF); Bauschlicher, Bagus, and Nelin[236] carried out CASSCF calculations on various low-lying states and characterized the bonding as primarily covalent with highly polarized double bonds. Sennesal and Schamps[237] calculated spectroscopic properties for five triplet and five singlet states, using an STO basis and SDCI. Bauschlicher, Langhoff, and Komornicki[238] have explored the problems with calculating the dipole moment, using MRCI and ACPF techniques. These authors detail the remarkable sensitivity of the dipole moment to the level of electron correlation recovered in the calculation. They estimate that including all valence correlation will result in a dipole of 3.4 D, considerably larger than the experimental value of 2.96 ± 0.05 D. Bergstrom, Lunell, and Eriksson[239] have studied the ability of a large number of DFT functionals to account for the properties of the $^3\Delta$ and $^1\Sigma^+$ states. Langhoff[269] has published a thorough study of the spectroscopy of TiO, using MRCI and MCPF techniques. We compare the results of selected calculations with experiment in Table 25. Most calculations predict R_e and ω_e in reasonable agreement with experiment, while the UCCSD(T)[228] and

Table 25. Comparison of Theory and Experiment: TiO, VO, CrO

molecule	R_e (Å)	ω_e (cm^{-1})	μ (D)	D_e (eV)	comment
TiO ($X^3\Delta$)	1.628	1014	3.52	6.84	UCCSD(T)[a](D is D_0)
	1.624	1097	3.07	5.69	MEFIT (CISD)[b]
	1.630	1045	-	-	SCF/CI[c]
	1.632	963	2.665	-	MCPF (3s3p)[d]
	1.622	1042	3.91	6.96	B3LYP[e]
	1.620	1026	-	8.14	BP86[f]
	1.620[g]	1009[g]	2.96[h]	6.87[i]	experiment
VO ($X^4\Sigma^-$)	1.578	890	3.09	5.32	MEFIT (CISD)[b]
	1.602	1028	3.60	6.32	UCCSD(T)[a]
	1.604	959	2.50	5.74	CPF[j]
	1.574	1483	3.61	4.81	SCF[l]
	1.589[g]	1011[g]	3.355[k]	6.44[g]	experiment
CrO($^5\Pi$)	1.622	864	-	4.79	B3LYP[m]
	1.634	853	3.988	-	MRCI+Q[n]
	1.647	850	3.2	4.00	MRCI(ECP)[o]
	1.660	820	-	3.09	SDCI[p]
	1.634	888	3.89	4.30	RCCSD(T)[a]
	1.604	1265	5.08	3.31	MEFIT(CISD+Q)[b]
	1.6213[g]	885[g]	3.88[n]	4.41[g]	experiment

[a] Reference 228. [b] Reference 227. [c] Reference 237. [d] Reference 238. [e] Reference 239. [f] Reference 240. [g] Reference 267. [h] Reference 270. [i] Reference 241. [j] Reference 231. [k] Reference 271. [l] Reference 242. [m] Reference 247. [n] Reference 246. [o] Reference 245.

B3LYP[240] results also agree with the experimental D_e.

VO. The $^4\Sigma^-$ ground state of VO results from V(s $d_\sigma d_{\delta_+} d_{\delta_-} d_{\pi_x}$) interacting with O($p_\sigma p_x^1 p_y^2$), forming

$$\overline{sz}\, d_{\delta_+} d_{\delta_-} (d_\sigma + p_\sigma)^2 (d_{\pi_x} + p_x)^2 p_y^2 \qquad {}^4\Sigma^-$$

Low-lying states were obtained from $d_{\delta_+} \rightarrow \overline{sz}$ ($^2\Delta$), $\overline{sz} \rightarrow (4p_\pi + 3d_\pi)$ $^{2,4}\Pi$, $d_{\delta_+} \rightarrow (4p_\pi + 3d_\pi)$ $^{2,4}\Pi$, and $^{2,4}\Phi$, and $\overline{sz} \rightarrow d_{\delta_+}$ ($^2\Delta_i$).

The earliest calculation (HF) on VO was by Carlson and Moser,[242] who identified $^4\Sigma^-$ as the probable ground state. Subsequent (SDCI and CPF) studies by Bauschlicher and Langhoff[231] characterized the $X^4\Sigma^-$, $A'^4\Phi$, $A^4\Pi$, and $^2\Delta_i$ (d_δ^3) states. These and other calculations are compared with experiment in Table 25.

CrO. Although the $^5\Pi$ ground state of CrO dissociates to ground-state neutral products, Jasien and Stevens[245] suggest that it may be thought of as resulting from both covalent and ionic interaction between Cr^+ in the sd^4 or d^5 configuration and O^- ($p_\sigma^2 p_\pi^3$), resulting in

$$(\overline{sz} + d_\sigma)^1 d_{\delta_-}^1 d_{\delta_+}^1 d_{\pi_y}^1 (d_{\pi_x} + p_x)^2 p_\sigma^2 p_y^2 \qquad {}^5\Pi$$

In this picture, CrO has a covalent π bond, a dative σ bond due to p_σ^2, and the stabilization that is obtained from the ionic interaction and the polarization of the $\overline{sz}$ orbital. This is consistent with the population analysis of Bauschlicher and Maitre,[228]

$$4s^{0.74}\, 4p_\sigma^{0.08} 3d_\sigma^{0.78} 4p_\pi^{0.17} 3d_\pi^{1.72} 3d_\delta^{1.99}$$

Bauschlicher, Nelin, and Bagus[243] calculate a $^7\Pi$ as the second excited state (0.92 eV higher), and its population analysis, $3d^{4.35}$, suggests it is also a mixture of the above configurations, with the sd^4 dominant. This interesting result says that breaking the π bond in the $^5\Pi$ state requires only 0.92 eV, presumably as a result of the exchange energy gained when the liberated d_{π_x} rejoins the high-spin d shell. $O^-(p_\sigma p_\pi^4)$ can form Σ^+ states with Cr^+ (d^5 or sd^4). The $d^{4.98}$ population of $^5\Sigma^+$ shows that it is dominated by $Cr^+(d^5)$

$$d_\delta^2\, d_\pi^2 (d_\sigma + p_\sigma)^2 p_\pi^4 \qquad {}^5\Sigma^+$$

On the other hand, the $^7\Sigma^+$ has a population $d^{4.23}$ and is a mixture of both Cr^+ sd^4 and d^5 configurations with no two-electron bonds.

The sd^4 configuration can form Π and Δ states with $O^-(p_\sigma p_\pi^4)$,

$$\overline{sz}\, d_\delta^2 d_\pi (d_\sigma + p_\sigma)^2 p_\pi^4 \qquad {}^5\Pi_r$$

and

$$\overline{sz}\, d_\delta d_\pi^2 (d_\sigma + p_\sigma)^2 p_\pi^4 \qquad {}^5\Delta_r$$

Nelin and Bauschlicher[244] have compared CrO, MoO, and WO and found a common $^5\Pi$ ground state. Jasien and Stevens[245] have compared CrO and CrO^+, using MRCI techniques. Steimle et al.[246] have measured the dipole moments in the $X^5\Pi$ and $B^5\Pi$ states and calculated μ in the $X^5\Pi$ state, using a finite field MRCI+Q calculation and found excellent agreement (calculated, 3.9880 D; experimental, 3.88 ± 0.13 D).

These authors also computed μ as an expectation value from the MRCI function and found 3.170 D. After seven natural orbital iterations, the energy decreased by 0.131 mh, while μ increased to 3.663 D. Clearly, μ is extremely sensitive to the quality of the wave function, and the finite-field approach seems preferable. Finally, Espelid and Borve[247] have calculated D_e for $X^5\Pi$, using a variety of high-level, correlated techniques, including UCCSD(T) and MCPF.

There are five states of CrO that have been characterized experimentally,[267] $X^5\Pi < A^5\Sigma^+ < A'^5\Delta_r < B^5\Pi < C(?)$, and only the first two have been studied theoretically. The theoretically characterized $^7\Sigma^+$ and $^7\Pi$ states have not been seen experimentally. The results of selected calculations on the $X^5\Pi$ state are compared with experiment, in Table 25. The RCCSD(T)[228] calculations are in excellent agreement with experiment.

MnO. The ground $^6\Sigma^+$ state of MnO is best viewed as $Mn^+(sd^5)$, forming a $d_\sigma + p_\sigma$ bond with $O^-(p_\sigma p_\pi^4)$, with some partial π bonding due to the $3d_\pi^1$, $2p_\pi^2$ interaction.

$$\overline{sz}\, d_\delta^2\, d_\pi^2 (d_\sigma + p_\sigma)^2 p_\pi^4 \qquad {}^6\Sigma^+$$

This is consistent with the population analysis of Bauschlicher and Maitre,[228]

$$4s^{0.68} 4p_\sigma^{0.06} 3d_\sigma^{0.98} 4p_\pi^{0.30} 3d_\pi^{2.35} 3d_\delta^2$$

Excited states can be formed from $\overline{sz} \rightarrow 4p_\sigma$ or $4p_\pi$

Table 26. Comparison of Theory and Experiment: MnO, FeO, CoO

molecule	R_e (Å)	ω_e (cm^{-1})	μ (D)	D_e (eV)	comment
MnO ($X^6\Sigma^+$)	1.660	713	7.32	2.44	MEFIT (CISD)[a]
	1.665	794	3.44	-	ICACPF[b]
	1.964	632	-	-	HF/limited CI[c]
	1.6477	832	-	3.83	experiment[d]
FeO ($X^5\Delta$)	1.68	681	3.30	-	MCSCF(RECP)[e]
	1.632	832	7.42	2.70	MEFIT(CISD+Q)[a]
	1.609	885	4.17	3.65	ICACPF[b]
	1.614	887	-	4.04	B3LYP[f]
	1.635	819	4.523	-	MRCI[g]
	1.616	907	-	-	DFT[h]
	1.616	880	4.7 ± 0.2	4.17 ± 0.08	experiment[d]
CoO ($X^4\Delta$)	1.621	909	3.46	3.64	RCCSD(T)[b]
	1.623	896	6.41	2.22	MEFIT(CISD)[a]
	1.630	969	4.25	6.26	DFT (LSD)[i]
	1.60	854	-	3.94 ± 0.14	experiment[d]

[a] Reference 227. [b] Reference 228. [c] Reference 249. [d] Reference 267. [e] Reference 251. [f] Reference 252. [g] Reference 238. [h] Reference 253. [i] Reference 254.

excitations, resulting in $^6\Sigma^+$ and $^6\Pi$ states or coupling the $\overline{sz}$ into a quartet with $d_\delta^2\, d_\pi^2$, resulting in $^4\Sigma^+$.

The earliest calculation on MnO was by Pinchemel and Schamps,[254] who used HF wave functions to characterize the first few states as resulting from $Mn^+(sd^5) + O^-(p^5)$. Dolg[227] et al. used a CISD (pseudopotential) wave function to characterize the $X^6\Sigma^+$ state. The results of the available theoretical calculations are compared with experiment, in Table 26.

FeO. The ground $X^5\Delta$ state of FeO is obtained from the $Fe^+(sd^6) + O^-(p_\sigma\, p_\pi^4)$ configuration with a $d_\sigma + p_\sigma$ bond, a polarized 4s orbital, and some partial π bonding (as in MnO) from the d_π, p_π^2 interaction resulting in

$$4sd_\delta^3\, d_\pi^2(d_\sigma + p_\sigma)^2 p_\pi^4 \qquad {}^5\Delta_i$$

There is a very-low-lying (~150 cm^{-1}) $^7\Sigma^+$ that can result from $d_\delta \rightarrow 4p_\sigma$

$$4p_\sigma^1\, 4s^1\, d_\delta^2\, d_\pi^2(d_\sigma + p_\sigma)^2 p_\pi^4 \qquad {}^7\Sigma^+$$

or perhaps from the purely electrostatic $Fe^{++}(sd^5) + O^{=}(p^6)$ asymptote

$$d_\pi^2\, d_\delta^2 \overline{sd}^1\, sd^1\, d_\sigma^1\, p_\sigma^2\, p_\pi^4 \qquad {}^7\Sigma^+$$

where $\overline{sd}_\sigma$ and sd_σ are 4s, $3d_\sigma$ hybrids. This $^7\Sigma^+$ has been calculated by Krauss and Stevens[251] and Dolg[227] et al. to be the ground state by 0.25−0.10 eV. Unfortunately, neither group has published a detailed population analysis, so the physical makeup of the $^7\Sigma^+$ is obscure. As of this writing, theory has not succeeded in conclusively demonstrating that the $^5\Delta_i$ is $< {}^7\Sigma^+$, as found experimentally. Other low-lying states may be generated from the $^5\Delta_i$ by $d_\delta \rightarrow 4s$ ($^5\Sigma^+$) or $d_\delta \rightarrow d_\pi$ ($^5\Pi_i$). The dipole moment of FeO has been studied by Bauschlicher[238] et al. using a variety of correlation methods and the iterative natural orbital method and, as with CrO and TiO, have demonstrated the remarkable sensitivity of the one-electron property to the level of correlation. In this instance, the iterative natural-orbital approach starts with a MRCI energy of −1337.640637 au and a μ of 4.562 D and, after eight iterations, has an energy of −1337.641511 au and a μ of 5.201 D. The calculated μ changes by 15%, while the total energy changes by 0.9 mh. Indeed, the MCPF wave function with an energy of −1337.665507 predicts a μ of 4.271 D. We collect, in Table 26, the calculated properties of $X^5\Delta$ and compare with experiment.

CoO. The ground state of CoO has been experimentally determined to have $^4\Delta$ symmetry. Dolg[227] et al. have calculated a $^4\Delta$ ground state with a $^4\Sigma^- \sim$ 0.5 eV higher. Piechota and Suffczynski's[254] DFT study predicts a $^4\Sigma^-$ ground state, with the $^4\Delta$ 0.49 eV higher. Langhoff and Bauschlicher[158] note that the $^6\Delta$ is the CASSCF ground state, while the $^4\Delta$ is the MRCI ground state. The $^4\Delta$ results from the interaction of the $^5\Delta$ component of the Co^+ (sd^7; ^5F) with the $^2\Sigma^+$ component of $O^-(p_\sigma p_\pi^4)$ with a σ bond between the d_σ and the p_σ and two electrons in a sd_σ hybrid.

$$\overline{sd}^2{}_\sigma d_{\delta_+}^2\, d_{\delta_-}^1\, d_\pi^2(d_\sigma + p_\sigma)^2 p_\pi^4 \qquad {}^4\Delta$$

Note that this permits some partial π bonding between d_π and p_π^2. The $^4\Sigma^-$ resulting from the $^5\Sigma^-$ component of $Co^+(sd^7; {}^5F)$ is competitive for the ground state, because this interaction predicts the same σ and π bonding as the $^4\Delta$,

$$\overline{sd}_\sigma d_\delta^4\, d_\pi^2(d_\sigma + d_\sigma)2p_\pi^4 \qquad {}^4\Sigma^-$$

However, since the $^5\Sigma^-$ state of ^5F has two components

$$(\sqrt{4/5}d_\pi^4\, d_\delta^2 + \sqrt{1/5}d_\delta^4\, d_\pi^2)d_\sigma 4s \qquad {}^5\Sigma^-$$

and only the second term or 20% of this function is involved in the bonding, and the atomic $^5\Delta$ is "pure"

$$d_{\delta_+}^2\, d_{\delta_-}^1\, d_\pi^2\, d_\sigma^2 4s^1 \qquad {}^5\Delta$$

the $^4\Delta$ emerges as the ground state. Additional low-lying states are obtained from the $^4\Delta$ by $\overline{sd}^2{}_\sigma \rightarrow \overline{sz}^1\overline{sd}_\sigma^1$ resulting in a $^6\Delta$, and from the $^4\Sigma^-$ by coupling the $\overline{sd}_\sigma$ with the d_π^2 into a doublet, resulting in $^2\Sigma^-$.

Table 27. Comparison of Theory and Experiment: NiO and CuO

molecule	R_e (Å)	ω_e (cm^{-1})	μ (D)	D_e (eV)	comment
NiO($X^3\Sigma^-$)	1.60	841	-	3.95	GVB/CI[a]
	1.67	690	6.00	-	MRCI+Q[b]
	1.591	848	6.72	2.63	CISD[c]
	1.626	850	3.91	3.75	RCCSD(T)[d]
	1.631	828	-	3.91 ± 0.17	experiment[e]
CuO($X^2\Pi$)	1.90	-	-	0.8	MCSCF[f]
	1.768	653	-	1.91	MRCI[g]
	1.875	527	-	1.40	SDCI[h]
	1.82	-	-	2.57	SDCI[j]
	1.749	626	4.28	2.73	CPF[k]
	1.72	601	-	-	MRD-CI(relativistic)[l]
	1.752	618	-	2.60	MP2(ECP)[m]
	1.766	588	-	-	DFT/B3LYP[n]
	1.771	572	5.00	2.70	CCSD(T)[d]
	1.894	595	6.66	1.98	MEFIT(CISD)[c]
	1.724	640	4.45[o]	2.89[i]	experiment[e]

[a] Reference 256. [b] Reference 243. [c] Reference 227. [d] Reference 228. [e] Reference 267. [f] Reference 258. [g] Reference 259. [h] Reference 260. [i] Reference 157. [j] Reference 262. [k] Reference 263. [l] Reference 264. [m] Reference 265. [n] Reference 266. [o] Reference 283.

There are also RCCSD(T) calculations of Bauschlicher and Maitre[228] on the $^4\Delta$ state alone. We compare the calculated and experimental spectroscopic properties in Table 26. The calculated bond lengths are remarkably consistent and all larger than experiment. The D_e's vary widely, with the RCCSD(T) result being closest to experiment and the DFT characteristically overestimating the experimental value.

NiO. Little is known about NiO, other than its ground state seems to have $^3\Sigma^-$ symmetry. Calculations by Walch and Goddard,[256] Bauschlicher, Nelin, and Bagus,[243] Dolg[227] et al., and Bauschlicher[257] give this result and characterize many other low-lying states. These calculations suggest one view NiO as Ni^+ in the sd^8 or d^9 configuration interacting with $O^-(p^5)$, and the various states arise from the location of the d hole in Ni^+ and the p hole in O^-. The bonding is dominated by ionic considerations, and the order of the low-lying states is determined by differential stabilization due to various one-electron bonds. $X^3\Sigma^-$ results from a π hole on both Ni^+ and O^-

$$d_\delta^4(d_\sigma^2 + \overline{sd}_\sigma^2)(d_{\pi_x}^2\, d_{\pi_y}^1\, p_x^1\, p_y^2)p_\sigma^2 \quad \text{or}$$
$$d_\delta^4(d_\sigma^2 + \overline{sd}_\sigma^2)(d_\pi + p_\pi)^4(d_\pi - p_\pi)^2p_\pi^2 \qquad ^3\Sigma^-$$

which permits two one-electron π bonds, in a manner similar to those in $^3\Sigma^-$ (O_2). Also, the attraction of p_σ^2 for the nuclear charge on Ni^+ is found to be important in stabilizing this state. The first excited state is a $^3\Pi$, which is obtained from a σ hole on Ni^+ and a π hole on O^-

$$d_\delta^4(\overline{sd}_\sigma^1\, p_\sigma^2)(d_\pi^4\, p_\pi^3) \quad \text{or}$$
$$d_\delta^4(sd_\sigma + p_\sigma)^2(sd_\sigma - p_\sigma)^1(d_\pi + p_\pi)^4(d_\pi - p_\pi)^3 \quad ^3\Pi$$

which permits a one-electron bond in both the σ and π symmetries. The $^1\Pi$ should be considerably higher because of the large exchange-energy loss the molecule would suffer because of the spin recoupling. The next state is the $^1\Sigma^+$, which results from singlet coupling the two singly occupied σ orbitals,

$$d_\delta^4\, d_\pi^4(sd_\sigma + p_\sigma)^2p_\pi^4 \quad \text{or}$$
$$d_\delta^4(sd_\sigma + p_\sigma)^2(d_\pi + p_\pi)^4(d_\pi - p_\pi)^4 \qquad ^1\Sigma^+$$

The calculated properties (Table 27) of $X^3\Sigma^-$ are in reasonable agreement with experiment.

CuO. The ground $X^2\Pi$ and first excited $^2\Sigma^+$ are separated by 0.96 eV and result from the interaction of Cu^+ (d^{10} and sd^9) with $O^-(p_\sigma^2\, p_\pi^3$ and $p_\sigma^1\, p_\pi^4)$. The $^2\Pi$ configuration looks like

$$(s + d_\sigma)^2d_\delta^4\, d_{\pi_x}^2(d_{\pi_y} + p_y)^3p_x^2\, p_\sigma^2 \quad \text{or}$$
$$\overline{sd}_\sigma^{\,2}\, d_\delta^4(d_{\pi_x} + p_x)^2(d_{\pi_x} - p_x)^2(d_{\pi_y} + p_y)^2(d_{\pi_y} - p_y)^1p_\sigma^2$$

with the Cu electron population

$$4s^{0.60}4p_\sigma^{0.06}3d_\sigma^{1.80}\, d_\delta^4\, d_\pi^{3.91}4p_\pi^{0.11}$$

while the $^2\Sigma^+$ is a mixture of

$$d_\delta^4\, d_\pi^4(d_\sigma + p_\sigma)^3p_\pi^4$$

and

$$d_\delta^4\, d_{\pi_x}^2\, p_x^2(4s + 3d_\sigma)^3(d_{\pi_y} + p_y)^2p_\sigma^2$$

with the resulting Cu population

$$3d^{9.61}4s^{0.31}4p_\pi^{0.34}4p_\sigma^{0.07}$$

Clearly, both states are dominated by ionic bonding with subtle differential effects due to covalent interactions between the ions. There are several detailed analyses available[258−266] for the bonding in these two states. A large number of excited states have been studied by Madhavan and Newton[262] and Hippe and Peyerimhoff,[264] and these have helped clarify the experimental assignments. The results of the calculation on the $X^2\Pi$ state are collected in Table 27.

Overview. The electronic structure of the ground states of TM oxides is mirrored in the experimental properties collected in Table 28. We also tabulate the population analysis results of Bauschlicher and Mai-

Table 28. Experimental Spectroscopic Properties for Transition-Metal Oxides[a]

		R_e (Å)	ω_e (cm^{-1})	D_0 (eV)	μ (D)	4s	4p$_?$	3d$_\sigma$	3d$_\sigma$	3d$_?$	d$_{pop}$
ScO	$^2\Sigma^+$	1.668	965	7.01 ± 0.12	4.55[b]	0.81	0.12	0.58	0.79	0.04	1.41
TiO	$^3\Delta$	1.620	1009	6.87[c] ± 0.10	2.96 ± 0.05[d]	0.75	0.10	0.65	0.88	1.02	2.55
VO	$^4\Sigma^-$	1.589	1011	6.44 ± 0.20	3.355 ± 0.014[e]	0.73	0.09	0.70	0.92	1.96	3.57
CrO	$^5\Pi$	1.615	898	4.77[f]	3.88 ± 0.13[g]	0.74	0.08	0.78	1.72	1.99	4.49
MnO	$^6\Sigma^+$	1.646	840	3.83 ± 0.08	-	0.68	0.06	0.98	2.35	2.00	5.32
FeO	$^5\Delta$	1.616	880	4.17 ± 0.08	4.7 ± 0.2[h]	0.56	0.05	1.09	2.48	2.99	6.55
CoO	$^4\Delta$	1.629	853	3.94 ± 0.14	?	1.05	0.08	1.48	2.74	2.98	7.19
NiO	$^3\Sigma^-$	1.627	838	3.87 ± 0.03	?	0.88	0.05	1.62	2.81	3.97	8.40
CuO	$^2\Pi$	1.724	640	2.85 ± 0.15	4.45 ± 0.3[i]	0.60	0.06	1.80	3.91	3.98	9.69

[a] R_e, ω_e, and D_0 from Merer,[267] unless otherwise noted. Electron populations from Bauschlicher and Maitre[228] [b] Reference 268. [c] Reference 241. [d] Reference 270. [e] Reference 271. [f] Reference 282. [g] Reference 246. [h] Reference 272. [i] Reference 283.

tre.[228] The significant 4s occupation in each of the oxides, regardless of the relative energies of the sd^N and d^{N+1} states of the ions, is presumably due to the enhancement of the ionic attraction by the large 4s polarizability. Sc, Ti, and V can all form $2^1/_2$ electron bonds without suffering a large exchange-energy loss or by using an excited state of the ion, and their large D_o's and decreasing R_e's are consistent with this. At Cr, one must use the $^6\Delta$ (sd^4) state of Cr$^+$, and the abrupt drop in D_o and slight increase in R_e are obtained. At MnO, the π bond order continues to drop because electronic structure is dominated by Mn$^+$ (sd^5), which puts two d$_\pi$ electrons in the path of the oxygen p$_\pi^4$, and D_0 drops and R_e increases, relative to CrO. Fe, Co, and Ni have very similar bond lengths, dissociation energies, and vibrational frequencies, reflecting the presence of a d$_\sigma$ bond and two one-electron π bonds across the series. The bonding changes again at CuO, becoming much more ionic, and R_e increases while D_0 drops significantly, relative to NiO. Steimle[224] et al. have discussed the variation of μ/R_e for the early transition-metal oxides and nitrides. For the oxides, the ratio decreases in going from ScO to TiO and then increases monotonically from TiO to CrO. For the nitrides, however, the ratio decreases monotonically from TiN to CrN. The dipole moment of ScN is not known experimentally, but Harrison[215] predicts that this ratio will decrease in going from ScN to CrN.

C. Monopositive Oxides

There is great interest in the reactions of gas-phase TM oxides, and a reliable database of bond energies has been established.[172] There are, however, few calculations on the electronic structure. Tilson and Harrison[273] studied the products of the reaction of Sc$^+$ with H_2O, using MCSCF and MRCI techniques, and identified the ground state of ScO$^+$ as $^1\Sigma^+$ resulting from the ^{3}D (d$_\pi^2$) configuration of Sc$^+$ interacting with O$^-$(p$_\sigma^2$ p$_\pi^2$). They describe the molecule as having two π bonds, polarized toward O, and a σ dative bond resulting from the O p$_\sigma^2$ and Sc having a charge of +1.28. The first two excited states are $^3\Delta$ < $^3\Sigma^+$. There are no reported calculations on TiO$^+$, although one expects it to be triply bonded, with an unpaired electron in the 3d$_\delta$ orbital. VO$^+$ has been studied by Carter and Goddard[274] using GVB/CI techniques, by Broclawik[275] using DFT methods, and by Dyke[276] et al. using the HF method. These authors find a $^3\Sigma^-$ ground state corresponding to a triple bond with a high-spin d$_\delta^2$ pair. There have been several calculations on CrO$^+$. Dyke[280] et al. used a limited CI calculation to interpret their photoelectron spectroscopy experiments and to assign the $^4\Sigma^-$ as the ground state. Harrison[277] used POL/CI techniques to predict a $^4\Pi$ ground state with the $^4\Sigma^-$ 0.25 eV higher. This agrees with the subsequent MP study of Takahara, Yamaguchi, and Fueno,[278] who predicted a $^4\Pi$ ground state with the $^4\Sigma^-$ only 0.03 eV higher. However, a MRCI study by Jasien and Stevens[245] predicts the $^4\Sigma^-$ below the $^4\Pi$ by 0.10 eV. As can be seen in Table 29, the bond lengths calculated for these two states are in reasonable agreement with one another but not with that derived from the photoelectron spectrum. Both of these states require that the bond order be less than that in VO$^+$, because one puts the extra electron into a σ* or π* orbital, resulting in a significant drop in D_0 from 5.98 eV (VO$^+$) to 3.25 eV (CrO$^+$). MnO$^+$ has also been studied by Takahara[278] et al., and they predict a $^5\Pi$ ground state. The ground state of FeO$^+$ has been calculated to be $^6\Sigma^+$ by Fiedler[279] et al., using high-level techniques including CCSD(T) and CASPT2. They calculate D_e to be 3.59 eV, which compares well with the 3.28 eV DFT (B3LYP) results of Glukhovtser, Bach, and Nagel[252] and the experiment result of 3.52 eV by Armentrout[281] et al. There do not seem to be

Table 29. Calculated and Experimental Properties of the Transition-Metal Oxide Positive Ions

molecule	state	R_e (Å)	ω_e (cm^{-1})	D_0 (eV)	comment
ScO$^+$	$^1\Sigma^+$	1.651	1134	6.40	MRCyI[a]
VO$^+$	$^3\Sigma^-$	1.54	1146	6.89	DFT[b]
	-	1.56	-	5.63	GVB/CI[c]
	-	1.536	1150	-	HFS[d]
	-	1.54[d]	1060[d]	5.85[e]	experiment
CrO$^+$	$^4\Pi$	1.623	915	2.85	MRCI[f]
	-	1.622	895	2.90	MRCI[g]
	-	1.685	-	1.76	APUMP[h]
	$^4\Sigma^-$	1.650	-	2.59	MRCI[f]
	-	1.638	801	2.99	MRCI[g]
	-	1.623	-	1.71	APUMP[h]
	$^4\Sigma^-$	1.79 ± 0.01[i]	640 ± 30[i]	3.72[e]	experiment
MnO$^+$	$^5\Pi$	1.811	-	1.91	APUMP[h]
	-	-	-	2.95[e]	experiment
FeO$^+$	$^6\Sigma^+$	1.643	915	3.65	Schwaz[j]
	-	1.640	-	3.34	DFT (B3LYP)[k]
	-	-	-	3.457[e]	experiment
CuO$^+$	$^3\Sigma^-$	1.79	600	1.36	MRCI[l]
				1.67[e]	experiment

[a] Reference 273. [b] Reference 275. [c] Reference 274. [d] Reference 276. [e] Reference 172. [f] Reference 277. [g] Reference 245. [h] Reference 278. [I] Reference 280. [j] Reference 279. [k] Reference 252. [l] Reference 264.

Table 30. Experimental Ground-State Properties (eV) of the Transition-Metal Oxides and Their Positive Ions

		D_0[a] (MO)	IP[a] (MO)	ion	D_0[b] (MO^+)	IP[c] (M)	Δ[d]
ScO	$^2\Sigma^+$	7.01 ± 0.12	-	$^1\Sigma^+$	7.14	6.562	-
TiO	$^3\Delta$	6.87(7)[e]	6.8198(7)[e]	$^2\Delta$	6.88(7)	6.82812(4)	−0.002
VO	$^4\Sigma^-$	6.44 ± 0.20	7.25 ± 0.01	$^3\Sigma^-$	5.85	6.74	+0.08
CrO	$^5\Pi$	4.77[f]	7.85 ± 0.02[g]	$^4\Pi$ or $^4\Sigma^-$	3.72	6.763	−0.04
MnO	$^6\Sigma^+$	3.83 ± 0.08	8.65 ± 0.2	$^5\Pi$	2.95	7.432	−0.34
FeO	$^5\Delta$	4.17 ± 0.08	8.9 ± 0.16	$^6\Sigma^+$[h]	3.47	7.90	−0.3
CoO	$^4\Delta$	3.94 ± 0.14	8.9 ± 0.2	$^3\Sigma^-$	3.25	7.86	−0.4
NiO	$^3\Sigma^-$	3.91 ± 0.17	9.5 ± 0.2	$^2\Pi$	2.74	7.633	−0.7
CuO	$^2\Pi$	2.75 ± 0.2	9.15[i]	$^3\Sigma^-$[i]	1.62	7.724	-

[a] Reference 267 unless otherwise noted. [b] Reference 172. [c] Reference 10. [d] $\Delta = D_0(MO) + IP(M) - (D_0(MO^+) + IP(MO))$. [e] Reference 241. [f] Reference 282. [g] Reference 280. [h] Reference 279. [i] Computed value from reference 264.

any calculations on CoO^+ and NiO^+, although Carter and Goddard[274] predicted their ground states to be $^3\Sigma^-$ and $^2\Pi$, respectively. Hippe and Peyerimhoff[264] have predicted the ground state of CuO^+ to be $^3\Sigma^-$ followed by $^3\Pi$ and $^1\Pi$ states. Their calculated IP of CuO implies a D_e of 1.32 eV, somewhat lower than the experimental value of 1.67 eV. The bonding in $^3\Sigma^-$ (CuO) is an intimate mixture of $Cu^+(^1S)$ + $O(p_\sigma^2 p_\pi^2)$ (two weak π bonds) and $Cu^+(sd^9)$ + O (p_σ p_π^3) (a 4s + p_σ σ bond). We compare the experimental D_0^0's for the oxides and their positive ion, in Table 30.

XII. Transition-Metal Fluorides

A. Introduction

Very few high-level calculations have been reported for many of the transition-metal fluorides, ScF,[284−288] TiF,[289] VF,[299] CrF,[290,291] FeF,[292−294] CuF;[295−298,320,321,339] but, from these, one concludes that the bonding in the low-lying states is very ionic and that the relative order of these states should track those of the positive ion in the field of a negative charge. This interpretation was put forth early by Carlson and Moser[284] (ScF), Scott and Richards[285] (ScF), and Pouilly[292] et al. (FeF) and has been reinforced by Harrison[286] (ScF) and Langhoff[287,288] et al. (ScF). It has also been used by Field[300] and others[301] to develop a ligand field model for the electronic states of MF. While the low-lying states are easily predicted from the lowest term of sd^N and d^{N+1} of M^+, it is not always possible to predict which is the ground state. Indeed, calculations and experiment have shown that many of the fluorides have very closely spaced states.

The similarity between the low-lying states of the fluorides and hydrides has also been noted, and this seems to be a consequence of the (formal) single bond in both and the strength of the atomic coupling in the residual positive ion. For example, if H bonds to a s^2d^N atom, we can imagine the wave function as

$$\overline{sz}\, d^N(sz + 1s)^2$$

whereas, if F does the same, one has

$$\overline{sz}\, d^N(sz + p_\sigma)^2 p_\pi^4$$

The bond may be covalent in the hydride case and essentially ionic (p_σ^2) in the fluoride case, and this will affect the magnitudes of the splittings in the $\overline{sz}$ d^N configuration but not their symmetries and relative order. Occasionally the larger negative charge on F will alter the order from H, as in FeH ($^4\Delta$) and FeF ($^6\Delta$), and these details may be rationalized. This modification of the hydride order is more likely to occur on the right-hand side of the TM block, where the sd^N and d^{N+1} configurations result in terms of different multiplicity, and the F will favor the high-spin option with the s orbital occupied. A similar rationalization is obtained when considering the sd^{N+1} configuration interacting with H or F.

B. Individual Fluorides

ScF. The electronic spectrum of ScF has been widely studied, both theoretically[284−288] and experimentally.[303−315] The pioneering theoretical study was by Carlson and Moser,[284] who studied the lowest $^1\Sigma^+$ and $^3\Delta_r$ states, using the HF model. Although they calculated the $^3\Delta_r$ as lower than $^1\Sigma^+$, they realized that electron correlation would most likely differentially lower the $^1\Sigma^+$, which they predicted to be the ground state. This was confirmed experimentally by McLeod and Weltner.[304] Scott and Richard[285] used a limited CI to study the orbital composition of the $^3\Delta_r$, $^1\Pi$, and $^3\Phi$ states. Harrison[286] determined the geometry, vibrational frequencies, charge distributions, and nature of the bonding in the first 30 states, using GVB and CI techniques. He determined the $^3\Delta_r - X^1\Sigma^+$ splitting to be 0.33−0.59 eV, according to the level of CI used. Langhoff[287,288] et al. performed a MRCI study of the spectroscopic constants and radiative lifetime for most of the singlet and triplet states below 28000 cm^{-1}. They calculate the a $^3\Delta_r - X^1\Sigma^+$ splitting to be 0.35 eV, correlating 18 electrons at the CPF plus relativistic correction level. Shenyavskaya[310] et al. have determined the splitting to be 0.25 eV. We compare, in Table 31, the calculated and experimental results for these two lowest states. The low-lying singlet and triplet states of ScF, $^{1,3}\Sigma^+$, $^{1,3}\Pi$, and $^{1,3}\Delta$, result from the interactions of $Sc^+(sd)$ with $F^-(p^6)$. All things being equal, one expects the order $\Delta < \Pi < \Sigma^+$ for each multiplicity with the triplet being lower. However, the $Sc^+(4s^2)$ state is 1.45 eV above the $^3D(sd)$ and differentially lowers the $^1\Sigma^+$ by polarizing away from the bond and reducing the repulsion of the F^- and Sc^+ electrons. This reduced repulsion permits the two ions to come closer, further stabilizing the molecule and resulting in the significantly shorter bond in the $X^1\Sigma^+$ (1.787 vs 1.856 Å). While this stabilization will be possible for the remaining fluorides, it will be reduced in importance,

Table 31. Calculated and Experimental Data on the $^1\Sigma^+$ and $^3\Delta$ States of ScF

state	R_e (Å)	ω_e (cm^{-1})	μ (D)	D_0 (eV)	T_e (eV)	comment
$^1\Sigma^+$	1.807	725	1.410	5.91	0.	CPF(8e)[a]
$^1\Sigma^+$	1.794	713	1.721	5.85	0.	CPF(18e)[a]
$^1\Sigma^+$	1.811	724	-	4.34	0.	GVB/POLCI[b]
$^1\Sigma^+$	1.787[c]	736[c]	1.72[d]	6.1[e]	0.	experiment
$^3\Delta$	1.886	612	2.733	-	0.26	CPF(8e)[a]
$^3\Delta$	1.868	640	2.939	-	0.35	CPF(18e)[a]
$^3\Delta$	1.922	596	-	-	0.59	GVB/POLCI[b]
$^3\Delta$	1.856[c]	649[c]	-	-	0.25[f]	experiment

[a] References 287, 288. [b] Reference 286. [c] Reference 164. [d] Reference 305. [e] Reference 313. [f] Reference 310.

as the $4s^23d^{N-1}$ state of the other TM ions is significantly higher (see Figure 3). This differential stabilization retains the triplet order

$$^3\Delta < {}^3\Pi < {}^3\Sigma^+$$

but alters the singlet order

$$^1\Sigma^+ \ll {}^1\Delta < {}^1\Pi$$

resulting in a $^1\Sigma^+$ ground state.

TiF. The ground state of TiF has been a matter of controversy for many years. Dieber and Kay assigned the ground state as $^4\Sigma^-$ ($\sigma\delta^2$) and interpreted the spectroscopic feature at 3.04 eV as due to the $^4\Pi-X^4\Sigma^-$ transition. This was questioned by Shenyavskaya and Dubov,[317] who performed a rotational analysis on the 0−0 and 1−0 bands and reassigned the ground state as $^2\Delta$ ($\sigma^2\delta$). Recently, Ram et al. observed a $^4\Phi-{}^4\Phi$ transition, using Fourier transform emission and laser excitation spectroscopy, and assigned the ground state as $X^4\Phi$ ($\sigma\pi\delta$). The earliest theoretical work was by Gambi,[319] who suggested that the ground state was either $^4\Sigma^-$ or $^2\Delta$. Gurvich[306] et al. used HF and CI techniques and modified several of the assignments of Shenyavskaya and Dubov and suggested $^4\Sigma^-$ as the ground state with the $^4\Phi$ 0.58 eV above. Dement'ev and Simkin[321] used HF/CI calculations and found the order $^4\Sigma^- \sim {}^4\Phi \ll {}^2\Delta$. Herrera and Harrison[322] used MCSCF calculations and predicted a $^4\Phi$ ground state with $^4\Sigma^-$ 0.1 eV higher. Most recently, Boldyrev and Simons[289] studied this system, using large basis sets and highly correlated wave functions, and, at the CCSD(T) level, predicted the order $X^4\Phi < {}^4\Sigma^-$ (0.080 eV) $< {}^2\Delta$ (0.266 eV).

The qualitative features of the bonding may be interpreted in terms of Ti^+ ($^4F(sd^2)$) interacting with $F^-(p^6)$, giving rise to doublets and quartets of Φ, Δ, Π, and Σ^- symmetry. At large internuclear separation, where the atomic coupling is important, we expect the ^4F term of Ti^+ to separate into $\Phi \lesssim \Sigma^- < \Pi_r < \Delta_r$ for each multiplicity with the quintets lower and the doublets offset by ~0.5 eV (based on the $^4F-{}^2F$ separation). The companion $^4F(d^3)$ would also result in these symmetries but in the atomic-coupling driven order

$$\Delta < \Pi < \Phi \sim \Sigma^-$$

minimizing the number of d_σ electrons. When these terms interact, they stabilize the $^4\Phi$ and $^4\Sigma^-$ relative to the Π and Δ and would support a $^4\Phi$ ground state,

$$(4s + 3d_\sigma)\, d_\pi\, d_\delta\, p^6$$

The $^2\Delta$ state calculated by Boldyrev and Simons[289] must come from the $^2\Delta$ ($sd_\sigma\, d_\delta$) interacting with the s^2d_δ configuration of Ti^+ (as in $^1\Sigma^+$ Sc^+) and forming a sd^2_σ hybrid. This $^2\Delta$ state should have a shorter bond (1.777 Å) than the $^4\Phi$ (1.869 Å) and $^4\Sigma^-$ (1.832 Å), as these authors calculate.

VF. Jones and Krishnamurty[323] interpreted the emission spectrum of VF in the 3440−3660 Å region, in terms of a $X^5\Pi$ ground state ($\omega_e = 571.4$ cm^{-1}) by analogy with CrO. Averyanov and Khait[299] have calculated the vertical excitation energies, using a modest basis and a small CI, and determined the order, $X^5\Delta$ (0.0) < $^5\Pi$ (1700 cm^{-1}) < $^5\Sigma^-$ (3400 cm^{-1}) < $^5\Phi$ (6400 cm^{-1}). No geometry optimization was attempted.

One expects the low-lying states to result from V^+ (sd^3 and d^4) and F^-. The sd^3 configuration will give rise to quintets and triplets in the order

$$\Delta < \Pi < \Phi < \Sigma^-$$

with the Δ and Π states obtaining additional stability by interacting with the corresponding states from the d^4 term. This interaction will be manifested as sd_σ hybrids

$$sd^1_\sigma\, d^2_\pi\, d^1_d\, p^6 \qquad {}^5\Delta$$

and

$$sd^1_\sigma\, d^1_\pi\, d^2_d\, p^6 \qquad {}^5\Pi$$

Close by, one expects $^5\Sigma^+$, $^5\Phi$, and $^5\Sigma^-$, with the seven associated triplets offset as in the free ion.

CrF. The ground state of CrF is $X^6\Sigma^+$ and the $A^6\Sigma^+-X^6\Sigma^+$ transition has been studied by Launila[324] and Koivisto and Wallin and Launila,[325] while the $B^6\Pi-X^6\Sigma^+$ has been studied by Wallin, Koivisto, and Launila.[326] Additionally, Okabayashi and Tanimoto[327] have analyzed the rotational spectrum of CrF in the $X^6\Sigma^+$ state. There have been three computational studies. An MCSCF study by Herrera and Harrison[322] suggested that the low-lying states are obtained from Cr^+ in the ^6S (d^5) and $^6D(sd^4)$, with the $X^6\Sigma^+$ being primarily from the sd^4. A similar conclusion was reached by Bencheikh[290] et al. on the basis of ligand field theory and DFT calculations. Recently, Harrison and Hutchison[291] have studied the sextets and quartets that are obtained from the d^5 and sd^4 configurations, using large atomic natural orbital basis sets and a variety of ab initio methods, including MRCI and RCCSD(T). They also include scalar relativistic effects perturbatively and explore the consequence of correlating the 3s and 3p electrons on the transition metal. Their results are compared with experiment and those of Bencheikh et al. in Table 32 and in Figure 19. Harrison and Hutchison calculate that the $X^6\Sigma^+$ state has the in situ Cr population $4s^{0.79}3d^{4.37}$, while that of the $A^6\Sigma^+$ is $4s^{0.23}$-$3d^{4.70}$, confirming that considerable mixing of d^5 and sd^4 has occurred and that $X^6\Sigma^+$ traces its lineage to

Table 32. Comparison of CrF Calculations with Experiment

	T_e (cm^{-1})			R_e (Å)			ω_e (cm^{-1})		
state	Harrison[a] et al.	exp	Bencheikh[b] et al.	Harrison[a] et al.	exp	Bencheikh[b] et al.	Harrison[a] et al.	exp	Bencheikh[b] et al.
$X^6\Sigma^+$	0	0	0	1.783	1.784	1.788	679	664	720
$A^6\Sigma^+$	9818	9953	-	1.908	1.892	-	571	581	-
$B^6\Pi$	7551	8134	11007 (10136)	1.831	1.828	1.818	632	629	699
$^4\Sigma^+$	9102	-	11370 (8160)	1.785	-	1.761	691	-	755
$^6\Delta$	11916		17506 (16635)	1.879		1.875	594		662
$^4\Pi$	11978	-	15167 (11957)	1.783		1.744	644		782
$^4\Delta$	15750		20393 (17187)	1.813		1.781	611		723

[a] $X^6\Sigma^+$, $B^6\Pi$, and $^6\Delta$ states are calculated using RCCSD(T) (3s3p/relativistic); $A^6\Sigma^+$ is a MRCI result using the Davidson correction at the 3s3p/relativistic level. T_e values for quartets are referred to the $X^6\Sigma^+$ calculated at the same CID level. Reference 291. [b] Reference 290. The transition energies in parentheses result from semiempirical corrections to calculated DFT results.

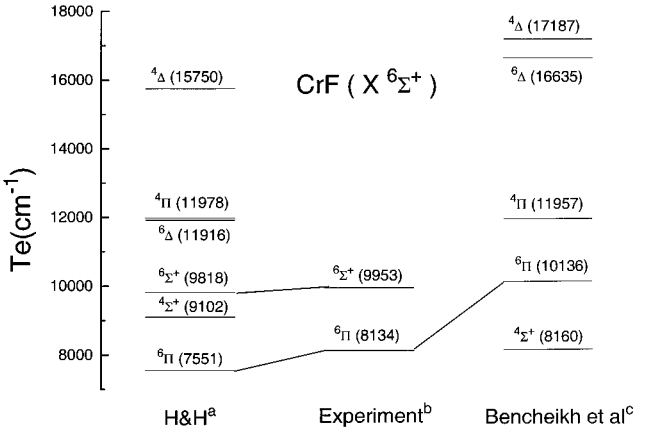

Figure 19. Comparison of the calculated energy levels of CrF with experiment. a: ref 291. b: ref 324−326. c: ref 290.

the excited ^{6}D state of Cr^+. A similar result was found by Bencheikh et al. Since the $^6D-^6S$ separation is 1.5 eV, this is a striking example of the importance of the role the 4s electron plays in differentially lowering the in situ energy of the sd^N relative to the d^{N+1} configuration.

MnF. The ground state of this molecule is $X^7\Sigma^+$ from $Mn^+(sd^5) + F^-(p^6)$, but there are no reported theoretical studies. Experimental studies have been published by Launila and Simard[328,329] and Launila, Simard, and James,[335] who discussed the similarity of the spectra of Mn^+, MnH, and MnF. We expect the bonding to be primarily ionic with some partial π bonds resulting from $(d_\pi + p_\pi)^2(d_\pi - p_\pi)^1$ interactions.

FeF. Pouilly[330] et al. determined the ground state to be $^6\Delta_i$ through a combination of emission and absorption experiments as well as HF/CI calculations. Additionally, they found the quartets arising from the d^7 configuration to be higher than the sextet states from the sd^6 configuration. Ram[331] et al. have observed the near-infrared emission spectrum and have determined the molecular constants for the $g^4\Delta$ state. They have also discussed the similarity of the spectra of FeF, FeH, and Fe^+. Allen and Ziurys[332] have analyzed the pure rotational spectrum and conclusively demonstrated that the ground state is $^6\Delta_i$. They also analyze the bond lengths in several metal fluorides as well as in FeH (1.787 Å), FeC (1.593 Å), FeO (1.619 Å), and FeF (1.784 Å). From these analyses, they conclude that there is considerable covalent character in FeF.

Bauschlicher[293] calculated the spectroscopic properties of the $X^6\Delta$ and the quartets $^4\Delta$, $^4\Phi$, and $^4\Sigma^-$ at the CCSD(T) level and the $^6\Delta$ and $^4\Delta$ at the MCPF and the $^6\Delta$ at the B3LYP level. The theoretical results for R_e and ω_e in the $^6\Delta$ state are as follows: CCSD-(T) (1.794 Å, 651 cm^{-1}), MCPF (1.794 Å, 650 cm^{-1}), and B3LYP (1.797 Å, 648 cm^{-1}) and are in reasonable agreement with the experimental values[330] 1.780 Å and 663 cm^{-1}.

The low-lying states result from Fe^+ in the ^{4,6}D-(sd^6) and ^{4}F(d^7) states. The sd^6 configuration will generate $^{4,6}\Delta < {}^{4,6}\Pi < {}^{4,6}\Sigma^+$, with the $^6\Delta$ lowest and the quartets offset by less than 1 eV, the atomic $^6D-^4D$ separation. The $^4\Delta$ and $^4\Pi$ from d^7 will lower their companions from the sd^6 configuration, resulting in a differential lowering of the lowest $^4\Delta$ and $^4\Pi$, and this reduces the 1 eV quartet-sextet offset, but not by enough to overtake the $X^6\Delta$.

CoF. There are very few data on CoF. Adam[333] et al. have recorded the laser-induced fluorescence and determined $\omega_e = 662.6$ cm^{-1} and suggested that the ground state is $^3\Phi$. Ram[334] et al. have confirmed the assignment and characterized several other excited states. They have also discussed the correlations between the energy levels of CoF, CoH, and Co^+. There are no theoretical calculations on this system, and one expects the ground terms to be obtained from the interaction between Co^+ sd^7 and d^8. Even though the d^8 is lower than the sd^7 in the free ion, we expect the in situ character of the wave function to have substantial s character, as in CrF, and anticipate a series of low-lying quintets and triplets in the "d^7 order", $\Phi < \Sigma^- < \Pi < \Delta$, with the triplets stabilized by interacting with their companions in the d^8 configuration. Another view is that the d^8 gives rise to the triplets in the "d^8 order", $^3\Delta < {}^3\Sigma^- < {}^3\Pi < {}^3\Phi$, and these are differentially stabilized by their companions in the sd^7 configuration. Detailed calculations are needed to resolve these ambiguities and determine the number of d electrons in the various states. For example, is the proposed $^3\Phi$ ground state the low-spin coupled sd^7 or is it from the d^8?

NiF. The experimental energy levels of NiF have recently been summarized by Dufour[336] et al. and Dufour and Pinchemel.[337] The ground state is a $^2\Pi$ with a very low-lying $^2\Sigma$ (252 cm^{-1}) and a $^2\Delta$ and another $^2\Sigma$ nearby. One expects the bonding to involve the sd^8 and d^9 configurations of Ni^+. The d^9 will give rise to doublets in the order $^2\Sigma^+ < {}^2\Pi < {}^2\Delta$ (minimize d_σ occupancy, maximize d_δ), while the sd^8 results in doublets and quartets in the order $\Delta < \Sigma^- < \Pi < \Phi$. As the internuclear separation decreases from infinity, the d^9 states split in the order shown, with an increasingly larger separation. The sd^8 states also decrease in energy as the nuclei approach, with the quartets below the doublets. One expects these states to drop more rapidly than the d^9, because of the polarizability of the 4s, the enhanced attraction of the Ni^{2+} core for F^-, and the reduced electron−electron repulsion between Ni^+ and F^-. The $^2\Delta$ and $^2\Pi$ states in the sd^8 sheaf will differentially stabilize their counterparts from the d^9 configuration. The experiments of Dufour and Pinchemel[337] suggest that the $^2\Pi$ is sufficiently stabilized to drop below its companion $^2\Sigma^+$, and we expect the next state to be the $^2\Delta(d^9)$. There should be a group of quartets $^4\Delta < {}^4\Sigma^- < {}^4\Pi < {}^4\Phi$ in the d^8 order and close by the remaining doublets. To date, no quartets have been seen. Dafour, Caretti, and Pinchemel[338] have interpreted the spectrum, using ligand-field studies.

CuF. The ground and low-lying excited states have been characterized in several studies. The ground state is a $^1\Sigma^+$, almost certainly from the $Cu^+(^1S)$ state, while the low-lying states are obtain from $Cu^+(^3D\text{-}(sd^9))$. The singlets and triplets from the sd^9 configuration are ordered $\Sigma^+ < \Pi < \Delta$ (minimize d_σ, maximize d_σ) and interleave such that the experimental order is

$$X^1\Sigma^+ < {}^3\Sigma^+ (1.81\ eV) < {}^3\Pi(2.18\ eV) < {}^1\Sigma^+(2.39\ eV) < {}^1\Pi(2.51\ eV) < {}^3\Delta(2.83\ eV)$$

Calculations by Dufour, Schamps, and Barrow[295] have been instrumental in unraveling the spin−orbit complicated experimental spectrum. Nguyen, McGinn, and Fitzpatrick[296] have used MP4 with a modest basis to study the ground and low-lying states and find good agreement with experiment, as do Ramirez-Soles and Daudey[297] in a MRCI study. Calculations have also been reported by Lee and Potts[321] to explain the photoelectron spectrum, by Seys et al. at the minimal basis HF level, and by Jeung et al. who obtained excellent agreement with experiment using a flexible GTO basis and CI. Hrusak[298] et al. examined the importance of orbital relaxation in the QCID method. Relativistic effects have been studied at the MP2 level by Laerdahl, Saue, and Faegri[320] and in the context of DFT by van Wullen.[339]

C. Monopositive Fluorides

There have been two experimental studies of TiF^+. The first was the velocity modulation laser spectroscopic study of Focsa[340] et al., who determined the molecular constants for the $X^3\Phi$ ($R_e = 1.780$ Å, $\omega_e = 781\ cm^{-1}$) and $^3\Delta$ ($R_e = 1.7509$ Å, $\omega_e = 880\ cm^{-1}$, $T_e \sim 17660\ cm^{-1}$). The second was the mass spectrometric study of Schröder, Harvey, and Schwarz,[341] who measured the ionization energy of TiF^+ (15.2 ± 0.3 eV). Schröder et al. also performed CCSD(T) calculations that predicted $R_e = 1.81$ Å for $X^3\Phi$, somewhat larger than the experimental value of 1.780 Å. Harrison[215] has studied CrF^+, using POLCI techniques, and finds $X^5\Sigma^+$ ($R_e = 1.753$ Å, $\omega_e = 770\ cm^{-1}$, $D_e = 87$ kcal/mol) and $^5\Pi$ ($R_e = 1.773$ Å, $T_e = 0.62$ eV). The calculated D_e is significantly larger than the two experimental values[342,343] for D_0, 69 and 71 kcal/mol. Bauschlicher[293] has used CCSD(T) and DFT (B3LYP) techniques to study FeF^+ and finds $X^5\Delta$ (CCSD(T)) ($R_e = 1.713$ Å, $\omega_e = 790\ cm^{-1}$, and $D_0 = 4.371$ eV). Bencheikh[294] has used DFT and ligand-field theory to estimate the relative energies of the electronic states of FeF^+.

D. Dipositive Fluorides

Schröder et al. have measured the vertical ionization energy of TiF^{+2} as 28 ± 3 eV, which compares favorably with their calculated CCSDCT value of 26.9 eV. They characterize the ground state of TiF^{+2} as $^2\Delta$ with a bond length of 1.66 Å and a bond energy relative to $Ti^+(^4F)$ and $F^+(^3P)$ as 7.6 eV. TiF^{+2} ($^2\Delta$) is, therefore, thermodynamically stable. One expects the equilibrium character to be $Ti^{++}F$ and the $^2\Delta$ state to result from (Table 10) $d_\delta^1\ (d_\sigma + p_\sigma)^2\ p_\pi^4\ {}^2\Delta$.

XIII. Concluding Remarks

The reliability of calculations on transition-metal containing diatomics has improved markedly over the past few years. The basis set and extent of electron correlation required for an accurate representation of the bond length and energies of the ground and low-lying electronic states is reasonably well understood. The molecular dipole moment has been shown to be exquisitely sensitive to the quality of the wave function and the method of calculation (expectation value or energy derivative), and additional experimental values will be valuable in further understanding this sensitivity. Noticeably absent in the reported calculations are the hyperfine properties that are so valuable in the experimental assignment of electronic configurations. These one-electron operators are easily calculated and provide another very direct probe of the electron distribution. Scalar relativistic effects are important for quantitative accuracy, and there have been few attempts to include spin−orbit effects ab initio. More interpretive studies of the electron density would be useful, perhaps using the Bader[344] analysis or the electron localization function of Becke and Edgecombe[345] and Savin[346] et al. or perhaps simply from density differences. Most of the theoretical analysis of the bonding is on the orbital or nonobservable level, and it would be useful to move toward bonding concepts based on the observable electron density. Finally, one cannot help but be struck by the remarkable symbiosis between theory and experiment in unraveling the structure of these complicated but fascinating molecules.

XIV. References

(1) Veillard, A. *Chem. Rev.* **1991**, *91*, 743.
(2) Koga, N.; Morokuma, K. *Chem. Rev.* **1991**, *91*, 823.

(3) Wojciechowska, M.; Haber, J.; Lomnicki, S.; Stoch, J. *J. Mol. Catal. A* **1999**, *141*, 155.
(4) Rao, C. N. R. *Annu. Rev. Phys. Chem.* **1989**, *40*, 291.
(5) Carlson, K. D.; Claydon C. R. *Adv. High Temp. Chem.* **1967**, *1*, 43 and other articles in this series.
(6) *High-Temperature Science: Future Needs and Anticipated Developments*; National Academy of Science: Washington, DC, 1979.
(7) Weltner, W., Jr. *Science* **1967**, *155*, 155.
(8) White, N. M.; Wing, R. F. *Astrophys. J.* **1978**, *222*, 209.
(9) Brown, W. A.; Kose, R.; King, D. A. *J. Mol. Catal. A* **1999**, *141*, 21.
(10) Moore, C. E. *Atomic Energy Levels*; National Bureau of Standards: Washington DC, 1949; Circ., No. 467, Vol. 1 and 2.
(11) The 1998 Nobel Prize in Chemistry was awarded to J. A. Pople and W. Kohn for their role in this remarkable development.
(12) See also: Waber, J. T.; Cromer, D. T. *J. Chem. Phys.* **1965**, *12*, 4116.
(13) See, for example, the representative studies: Bauschlicher, C. W.; Maitre, P. *Theor. Chem. Acta.* **1995**, *90*, 189. Harrison, J. F. *J. Phys. Chem.* **1996**, *100*, 3513. Dai, D.; Balasubramanian, *J. Mol. Spectrosc.* **1993**, *161*, 455. Boldyrev, A. I.; Simons, J. *J. Mol. Spectrosc.* **1998**, *188*, 138.
(14) Carter, E. A.; Goddard, W. A., III *J. Phys. Chem.* **1984**, *88*, 1485.
(15) Froese Fischer, C. *J. Phys. B* **1977**, *10*, 1241.
(16) Hay, P. J. *J. Chem. Phys.* **1977**, *66*, 4377.
(17) Guse, M.; Ostlund, N. S.; Blyholder, G. D. *Chem. Phys. Lett.* **1979**, *61*, 526.
(18) Botch, B. H.; Dunning, T. H., Jr.; Harrison, J. F. *J. Chem. Phys.* **1981**, *75*, 3466.
(19) Bauschlicher, C. W., Jr.; Walch, S. P.; Partridge, H. *J. Chem. Phys.* **1982**, *76*, 1033.
(20) Martin, R. L. *Chem. Phys. Lett.* **1980**, *75*, 290.
(21) Raghavachari, K.; Trucks, G. W. *J. Chem. Phys.* **1989**, *91*, 1062.
(22) Martin, R. L.; Hay, P. J. *J. Chem. Phys.* **1981**, *75*, 4539.
(23) Dunning, T. H., Jr. Private correspondence.
(24) *Modern Electronic Structure Theory*; Yarkony, R., Ed.; World Scientific: New York, 1995.
(25) *Quantum Mechanical Electronic Structure Calculations with Chemical Accuracy*; Langhoff, S. R., Ed.; Kluwer: Dordrecht, The Netherlands, 1995.
(26) *Advances in Chemical Physics; Ab Initio Methods in Quantum Chemistry* II; Lawley, K. P., Ed.; Wiley-Interscience: New York, 1987.
(27) *Advances in Quantum Chemistry*; Löwdin, P. O., Ed.; Academic Press: New York, 1999; Vol. 34.
(28) Cowan, R. D.; Griffin, D. C. *J. Opt. Soc. Am.* **1976**, *66*, 1010.
(29) Martin, R. L. *J. Phys. Chem.* **1983**, *87*, 750.
(30) Hess, B. A. *Phys. Rev. A.* **1986**, *33*, 3742.
(31) Hehre, W. J.; Radom, L.; Schleyer, P. v. R.; Pople, J. A. *Ab Initio Molecular Orbital Theory*; Wiley: New York, 1986.
(32) Langhoff, S. R.; Davidson, E. R. *Int. J. Quantum Chem.* **1974**, *8*, 61.
(33) Ahlrichs, R.; Schart, P.; Ehrhardt, C. *J. Chem. Phys.* **1985**, *82*, 890.
(34) Chong, D. P.; Langhoff, S. R. *J. Chem. Phys.* **1986**, *84*, 5606.
(35) Cizek. *Adv. Chem. Phys.* **1969**, *14*, 35.
(36) Purvis, G. D.; Bartlett, R. J. *J. Chem. Phys.* **1982**, *76*, 1910.
(37) Bartlett, R. J. *Annu. Rev. Phys. Chem.* **1981**, *32*, 359.
(38) Raghavachari, K.; Trucks, G. W.; Pople, J. A.; Head-Gordon, M. *Chem. Phys. Lett.* **1989**, *157*, 479.
(39) Pople, J. A.; Head-Gordon, M.; Raghavachari, K. *J. Chem. Phys.* **1987**, *87*, 5968.
(40) Møller, C.; Plesset, M. S. *Phys. Rev.* **1934**, *46*, 618.
(41) Handy, N. C.; Knowles, P. J.; Somasundram, K. *Theor. Chim. Acta* **1985**, *68*, 87.
(42) Gill, P. M. W.; Pople, J. A.; Radom, L.; Nobes, R. H. *J. Chem. Phys.***1988**, *89*, 7307.
(43) Shepard, R. *Adv. Chem. Phys.* **1987**, *69*, 63.
(44) Olsen, J.; Yeager, D. L.; Jorgensen, P. *Adv. Chem. Phys.* **1983**, *54*, 1.
(45) McWeeny, R.; Sutcliffe, B. T. *Comput. Phys. Rep.* **1985**, *2*, 217.
(46) Roos, B. O. In *Methods in Computational Molecular Physics*; Diercksen, G. H. F., Wilson, S., Eds.; Reidel: Dordrecht, 1983.
(47) Siegbahn, P. E. M. *Faraday Symp. Chem. Soc.* **1984**, *19*, 97.
(48) Roos, B. O. In *Advances in Chemical Physics; Ab Initio Methods in Quantum Chemistry II*; Lawley, K. P., Ed.; Wiley: New York, 1987.
(49) Hay, P. J.; Hunt, W. J.; Goddard, W. A., III *J. Am. Chem. Soc.* **1972**, *94*, 8293.
(50) Werner, H. J.; Knowles, P. J. *J. Chem. Phys.* **1988**, *89*, 5803.
(51) Knowles, P. J.; Werner, H. J. *Chem. Phys. Lett.* **1988**, *145*, 514.
(52) Murray, C. W.; Davidson, E. R. *Chem. Phys. Lett.* **1991**, *187*, 451.
(53) Anderson, K.; Malmqvist, P. A.; Roos, B. O.; Sadlej, A. J.; Wolinski, K. *J. Phys. Chem.* **1990**, *94*, 5483.
(54) Hirao, K. *Chem. Phys. Lett.* **1992**, *190*, 374.
(55) Roos, B. O. *Adv. Chem. Phys.* **1996**, *93*, 219.
(56) Docken, K.; Hinze, J. *J. Chem. Phys.* **1972**, *57*, 4928.
(57) Werner, H. J.; Meyer, W. *J. Chem. Phys.* **1981**, *74*, 5794.
(58) Hay, P. J.; Wadt, W. R. *J. Chem. Phys.* **1985**, *82*, 299.
(59) Krauss, M.; Stevens, W. J. S. *Annu. Rev. Phys. Chem.* **1984**, *35*, 357.
(60) Kendall, R. A.; Dunning, T. H., Jr. *J. Chem. Phys.* ***1992***, *96*, 6796.
(61) Woon, D. E.; Dunning, T. H., Jr. *J. Chem. Phys.* **1993**, *98*, 1358.
(62) Woon, D. E.; Dunning, T. H., Jr. *J. Chem. Phys.* **1993**, *99*, 3730.
(63) Wachters, A. J. H. *J. Chem. Phys.* **1970**, *52*, 1033.
(64) Partridge, H. J. *J. Chem. Phys.* **1989**, *90*, 1043.
(65) Widmark, P. O.; Malmqvist, P. A.; Roos, B. O. *Theor. Chim. Acta* **1990**, *77*, 291.
(66) Widmark, P. O.; Persson, B. J.; Roos, B. O. *Theor. Chim. Acta* **1991**, *79*, 419.
(67) Pierloot, K.; Dumez, B.; Widmark, P. O.; Roos, B. O. *Theor. Chim. Acta* **1995**, *90*, 87.
(68) Bauschlicher, C. W., Jr. *Theor. Chim. Acta* **1995**, *92*, 183.
(69) Almlöf, J.; Taylor, P. R. *J. Chem. Phys.* **1987**, *86*, 4070.
(70) Raffenetti, R. C. *J. Chem. Phys.* **1973**, *58*, 4452.
(71) Dunning, T. H., Jr. *J. Chem. Phys.* **1970** *53*, 2823.
(72) Hohenberg, P.; Kohn, W. *Phys. Rev. B* **1964**, *136*, 864.
(73) Kohn, W.; Sham, L. J. *Phys. Rev. A* **1965**, *140*, 1133.
(74) Zeigler, T. *Chem. Rev.* **1991**, *91*, 651.
(75) *Density Functional Theory, Advances in Quantum Chemistry;* Academic Press: New York, 1998; Vol. 33.
(76) Slater, J. C. The Self-Consistent Field for Molecules and Solids. *Quantum Theory of Molecules and Solids, Vol. 4*; McGraw-Hill: New York, 1974.
(77) Becke, A. D. *J. Chem. Phys.* **1993**, *98*, 1372.
(78) Becke, A. D. *J. Chem. Phys.* **1993**, *98*, 5648.
(79) Munch, D.; Davidson, E. R. *J. Chem. Phys.* **1975**, *63*, 980.
(80) Pittel, B.; Schwarz, W. H. E. *J. Phys. B: At. Mol. Phys.* **1978**, *11*, 769.
(81) Dunning, T. H., Jr.; Botch, B. H.; Harrison, J. F. *J. Chem. Phys.* **1980**, *72*, 3419.
(82) Bauschlicher, C. W., Jr. *J. Chem. Phys.* **1980**, *73*, 2510.
(83) Wilson, R. G.; Sharma, C. S. *J. Phys. B: At. Mol. Phys.* **1980**, *13*, 3285.
(84) Martin, R. L. *Chem. Phys. Lett.* **1980**, *75*, 290.
(85) Bauschlicher, C. W., Jr.; Walch, S. P. *J. Chem. Phys.* **1981**, *74*, 5922.
(86) Fischer, C. F. *J. Chem. Phys.* **1982**, *76*, 1934.
(87) Bauschlicher, C. W., Jr.; Walch, S. P.; Partridge, H. *Chem. Phys. Lett.* **1984**, *103*, 291.
(88) Pélissier, M.; Davidson, E. R. *Int. J. Quantum Chem.* **1984**, *25*, 483.
(89) Salter, E. A.; Adamowicz, L.; Bartlett, R. J. *Chem. Phys. Lett.* **1985**, *122*, 23.
(90) Sunil, K. K.; Jordan, K. D. *J. Chem. Phys.* **1985**, *82*, 873.
(91) Jankowski, K.; Polasik, M. *J. Phys. B: At. Mol. Phys.* **1985**, *18*, 2133.
(92) Jankowski, K.; Polasik, M. *J. Phys. B: At. Mol. Phys.* **1985**, *18*, 4383.
(93) Rohlfing, C. M.; Martin, R. L. *Chem. Phys. Lett.* **1985**, *115*, 104.
(94) Sunil, K. K.; Jordan, K. D. *Chem. Phys. Lett.* **1986**, *128*, 363.
(95) Salter, E. A.; Adamowicz, L.; Bartlett, R. J. *Chem. Phys. Lett.* **1986**, *130*, 152.
(96) Langhoff, S. R.; Bauschlicher, C. W., Jr. *J. Chem. Phys.* **1986**, *84*, 4485.
(97) Bauschlicher, C. W., Jr. *J. Chem. Phys.* **1987**, *86*, 5591.
(98) Bauschlicher, C. W., Jr.; Siegbahn, P.; Pettersson, L. G. M. *Theor. Chim. Acta* **1988**, *74*, 479.
(99) Bauschlicher, C. W., Jr.; Langhoff, S. R.; Taylor, P. R. *Chem. Phys. Lett.* **1989**, *158*, 245.
(100) Raghavachari, K.; Trucks, G. W. *J. Chem. Phys.* **1989**, *91*, 2457.
(101) Andersson, K.; Roos, B. O. *Chem. Phys. Lett.* **1992**, *191*, 507.
(102) Murphy, R. B.; Messmer, R. P. *J. Chem. Phys.* **1992**, *97*, 4974.
(103) Pierloot, K.; Tsokos, E.; Roos, B. O. *Chem. Phys. Lett.* **1993**, *214*, 583.
(104) Russo, T. V.; Martin, R. L.; Hay, P. J. *J. Chem. Phys.* **1994**, *101*, 7729.
(105) (a) Ricca, A.; Bauschlicher, C. W., Jr. *Theor. Chim. Acta* **1995**, *92*, 123. (b) Bauschlicher, W. A., Jr.; Langhoff, S. R.; Barnes, L. A. *J. Chem. Phys.* **1989**, *91*, 2399.
(106) Das, G. *J. Chem. Phys.* **1981**, *74*, 5766.
(107) Walch, S. P.; Bauschlicher, C. W., Jr. *J. Chem. Phys.* **1983**, *78*, 4597.
(108) Bauschlicher, C. W.; Walch, S. P.; Langhoff, S. R. In *Quantum Chemistry: The Challenge of Transition Metals and Coordination Chemistry*; Veillard, A., Ed.; Reidel: Dordrecht, 1986; p 15.
(109) Pélissier, M.; Daudey, J. P.; Malrieu, J. P.; Jeung, G. H. In *Quantum Chemistry: The Challenge of Transition Metals and Coordination Chemistry*; Veillard, A., Ed.; Reidel: Dordrecht, 1986; p 37.
(110) Wedig, U.; Dolg, M.; Stoll, H.; Pneuss, H. In *Quantum Chemistry: The Challenge of Transition Metals and Coordination Chemistry*; Veillard, A., Ed.; Reidel: Dordrecht, 1986; p 79.
(111) Tranquille, M. In *Quantum Chemistry: The Challenge of Transition Metals and Coordination Chemistry*; Veillard, A., Ed.; Reidel: Dordrecht, 1986; p 53.

(112) Chong, D. P.; Langhoff, S. R.; Bauschlicher, C. W., Jr.; Walch, S. P.; Partridge, H. *J. Chem. Phys.* **1986**, *85*, 2850.
(113) Ziegler, T.; Li, J. *Can. J. Chem.* **1994**, *72*, 783.
(114) Barone, V.; Adamo, C. *Int. J. Quantum Chem.* **1997**, *61*, 443.
(115) Scott, P. R.; Richards, W. G. *J. Phys. B: At. Mol. Phys.* **1974**, *7*, 1679.
(116) Kunz, A. B.; Guse, M. P.; Blint, R. J. *J. Phys. B: At. Mol. Phys.* **1975**, *8*, L358.
(117) Bauschlicher, C. W., Jr.; Walch, S. P. *J. Chem. Phys.* **1982**, *76*, 4560.
(118) Alvarado-Swaisgood, A. E.; Harrison, J. F. *J. Phys. Chem.* **1985**, *89*, 5198.
(119) Bruna, P. J.; Anglada, J. In *Quantum Chemistry: The Challenge of Transition Metals and Coordination Chemistry*; Veillard, A., Ed.; Reidel: Dordrecht, 1986; p 67.
(120) Anglada, J.; Bruna, P. J.; Peyerimhoff, S. D. *Mol. Phys.* **1989**, *66*, 541.
(121) Scott, P. R.; Richards, W. G. *J. Phys. B: At. Mol. Phys.* **1974**, *7*, L347.
(122) Scott, P. R.; Richards, W. G. *J. Phys. B: At. Mol. Phys.* **1974**, *7*, 500.
(123) Bauschlicher, C. W., Jr. *J. Phys. Chem.* **1988**, *92*, 3020.
(124) Anglada, J.; Bruna, P. J.; Peyerimhoff, S. D. *Mol. Phys.* **1990**, *69*, 281.
(125) Henderson, G. A.; Das, G.; Wahl, A. C. *J. Chem. Phys.* **1975**, *63*, 2805.
(126) Dai, D.; Balasubramanian, K. *J. Mol. Spectrosc.* **1993**, *161*, 455.
(127) Bagus, P. S.; Schaefer, H. F., III *J. Chem. Phys.***1973**, *58*, 1844.
(128) Blint, R. J.; Kunz, A. B.; Guse, M. P. *Chem. Phys. Lett.* **1975**, *36*, 191.
(129) Langhoff, S. R.; Bauschlicher, C. W., Jr.; Rendell, A. P. *J. Mol. Spectrosc.* **1989**, *138*, 108.
(130) Walker, J. H.; Walker, T. E. H.; Kelly, H. P. *J. Chem. Phys.* **1972**, *57*, 2094.
(131) Scott, P. R.; Richards, W. G. *J. Chem. Phys.* **1975**, *63*, 1690.
(132) Walch, S. P. *Chem. Phys. Lett.* **1984**, *105*, 54.
(133) Bauschlicher, C. W., Jr.; Langhoff, S. R. *Chem. Phys. Lett.* **1988**, *145*, 205.
(134) Sodupe, M.; Lluch, J. M.; Oliva, A.; Illas, F.; Rubio, J. *J. Chem. Phys.* **1990**, *92*, 2478.
(135) Langhoff, S. R.; Bauschlicher, C. W., Jr. *J. Mol. Spectrosc.* **1990**, *141*, 243.
(136) Freindorf, M.; Marian, C. M.; Hess, B. A. *J. Chem. Phys.* **1993**, *99*, 1215.
(137) Bagus, P. S.; Björkman, C. *Phys. Rev. A.* **1981**, *23*, 461.
(138) Walch, S. P.; Bauschlicher, C. W., Jr. *Chem. Phys. Lett.* **1982**, *86*, 66.
(139) Blomberg, M. R. A.; Siegbahn, P. E. M.; Roos, B. O. *Mol. Phys.* **1982**, *47*, 127.
(140) Rohlfing, C. M.; Hay, P. J.; Martin, R. L. *J. Chem. Phys.* **1986**, *85*, 1447.
(141) Marian, C. M.; Blomberg, M. R. A.; Siegbahn, P. E. M. *J. Chem. Phys.* **1989**, *91*, 3589.
(142) Bauschlicher, C. W., Jr.; Langhoff, S. R.; Komornicki, A. *Theor. Chim. Acta* **1990**, *77*, 263.
(143) Pou-Amérigo, R.; Merchán, M.; Nebot-Gil, I.; Malmqvist, P. A.; Roos, B. O. *J. Chem. Phys.* **1994**, *101*, 4893.
(144) Raghavachari, K.; Sunil, K. K.; Jordan, K. D. *J. Chem. Phys.* **1985**, *83*, 4633.
(145) Hluva, M.; Barthelat, J. C.; Pélissier, M.; Spiegelmann, F. *Chem. Phys. Lett.* **1986**, *132*, 205.
(146) Merchan, M.; Daudey, J. P.; Gonzalez-Luque, R.; Nebot-Gil, I. *Chem. Phys.* **1990**, *148*, 69.
(147) Marian, C. *J. Chem. Phys.* **1990**, *94*, 5574.
(148) Schilling, J. B.; Goddard, W., III; Beauchamp, J. L. *J. Am. Chem. Soc.* **1986**, *108*, 582.
(149) Pettersson, L. G. M.; Bauschlicher, C. W., Jr.; Langhoff, S. R.; Partridge, H. *J. Chem. Phys.* **1987**, *87*, 481.
(150) Ohanessian, G.; Goddard, W. A., III *Acc. Chem. Res.* **1990**, *23*, 386.
(151) Mavrides, A.; Harrison, J. F. *J. Chem. Soc., Faraday Trans.* **1989**, *85*, 1391.
(152) Alvarado-Swaisgood, A. E.; Allison, J.; Harrison, J. F. *J. Phys. Chem.* **1985**, *89*, 2517.
(153) Sodupe, M.; Lluch, J. M.; Oliva, A.; Illas, F.; Rubio, J. *J. Chem. Phys.* **1989**, *90*, 6436.
(154) Langhoff, S. R.; Bauschlicher, C. W., Jr. *J. Astrophys.* **1991**, *375*, 843.
(155) Anglada, J.; Bruna, P. J.; Grein, F. *J. Chem. Phys.* **1990**, *92*, 6732.
(156) Harrison, J. F.; Christopher, P. S. *Mol. Phys.* **1999**, *96*, 31.
(157) Armentrout, P. B.; Sunderlin, L. S. *Transition Metal Hydrides*; Dedréu, A., Ed.; VCH Publishers: New York, 1992; pp 1−64.
(158) Langhoff, S. R.; Bauschlicher, C. W., Jr. *Annu. Rev. Phys. Chem.* **1988**, *39*, 181.
(159) Bauschlicher, C. W., Jr.; Langhoff, S. R. *Transition Metal Hydrides*; Dedréu, A., Ed.; VCH Publishers: New York, 1992; pp 103−126. (b) Bauschlicher, C. W., Jr.; Langhoff, S. R. *Int. Rev. Phys. Chem.* **1990**, *9*, 149.
(160) Steimile, T. C.; Shirley, J. E. *J. Chem. Phys.* **1991**, *95*, 7179.
(161) Chen, Y.; Clemmer, D. E.; Armentrout, P. B. *J. Chem. Phys.* **1991**, *95*, 1228.
(162) Chen, Y.; Clemmer, D. E.; Armentrout, P. B. *J. Chem. Phys.* **1992**, *98*, 4929.
(163) Chen, Y.; Clemmer, D. E.; Armentrout, P. B. *J. Chem. Phys.* **1993**, *98*, 4929.
(164) Huber, K. P.; Herzberg, G. *Constants of Diatomic Molecules*; Van Nostrand Reinhold: New York, 1979.
(165) Sunderlin, L. S.; Armentrout, P. B. *J. Phys. Chem.* **1990**, *94*, 3589.
(166) Schultz, R. H.; Armentrout, P. B. *J. Chem. Phys.* **1991**, *94*, 2262.
(167) Fisher, E. R.; Armentrout, P. B. *J. Phys. Chem.* **1990**, *94*, 1674.
(168) Goddard, W. A., III; Walch, S. P.; Rappe, A. K.; Upton, T. H. *J. Vacuum Sci. Technol.* **1997**, *14*, 416.
(169) Gray, J. A.; Rice, S. F.; Field, R. W. *J. Chem. Phys.* **1985**, *82*, 4717.
(170) Balfour, W. J.; Lindgren, B.; O'Connor, S. *Phys. Scr.* **1983**, *28*, 551.
(171) Alvarado-Swaisgood, A. E.; Harrison, J. F. *Theochem.* **1988**, *46*, 155.
(172) Armentrout, P. B.; Kickel, B. L. *Organometallic Ion Chemistry*; Freiser, B., Ed.; Kluwer Academic Publishers: Dordrecht, 1996; pp 1−45.
(173) Neubert, A.; Zmbov, K. F. *Trans. Faraday Soc.* **1984**, *70*, 2219.
(174) Van Zee, R. J.; Baumann, C. A.; Weltner, W., Jr. *Chem. Phys.* **1985**, *113*, 524.
(175) Brock, L. R.; Knight, A. M.; Reddic, J. E.; Pilgrim, J. S.; Duncan, M. A. *J. Chem. Phys.* **1997**, *106*, 6268.
(176) Russon, L. M.; Rothschoph, G. K.; Morse, M. D. *J. Chem. Phys.* **1997**, *107*, 1079.
(177) Harrison, J. F. *J. Phys. Chem.* **1983**, *87*, 1323.
(178) Beckmann, H.-O.; Pacchione, G.; Jeung, G. H. *Chem. Phys. Lett.* **1985**, *116*, 423.
(179) Bauschlicher, C. W., Jr.; Langhoff, S. R.; Partridge, H.; Walch, S. P. *J. Chem. Phys.* **1987**, *86*, 5603.
(180) Lawson, D. B.; Harrison J. F. *J. Phys. Chem.* **1996**, *100*, 6081.
(181) Kalemos, A.; Mavridis, A. *Adv. Quantum Chem.* **1999**, *32*, 69.
(182) Kalemos, A.; Mavridis, A. *J. Phys. Chem. A.* **1998**, *102*, 5982.
(183) Kalemos, A.; Mavridis, A. *J. Phys. Chem. A.* **1999**, *103*, 3336. (b) Kalemos, A.; Mavridis, A. *J. Phys. Chem. A* **1999**, *103*, 3336. (c) Kerkines, I. S. K.; Mavridis, A. Private communication.
(184) Jeung, G. H.; Koutecky, J. *J. Chem. Phys.* **1988**, *88*, 3747.
(185) Bauschlicher, C. W., Jr.; Siegbahn, P. E. M. *Chem. Phys. Lett.* **1984**, *104*, 331.
(186) Hack, M. D.; Maclagan, R. G. A. R.; Scuseria, G. E.; Gordon, M. S. *J. Chem. Phys.* **1996**, *104*, 6628.
(187) Mattar, S. M. *J. Phys. Chem.* **1993**, *97*, 3171.
(188) Shim, I.; Gingerich, K. A. *Int. J. Quantum Chem.* **1992**, *42*, 349.
(189) Maclagan, R. G. A. R.; Scuseria, G. E. *J. Chem. Phys.* **1997**, *106*, 1491.
(190) Kitaura, K.; Morokuma, K.; Csizmadia, I. G. *J. Mol. Struct.* **1982**, *88*, 119.
(191) Shim, I.; Gingerich, K. A. *Chem. Phys. Lett.* **1999**, *303*, 87.
(192) Reported in 191.
(193) Adam, A. G.; Peers, J. R. D. *J. Mol. Spectrosc.* **1997**, *181*, 24 and references therein.
(194) Harrison, J. F.; Kunze, K. L. *Organometallic Ion Chemistry*; Freiser, B., Ed.; Kluwer Academic Publishers: Dordrecht, 1996.
(195) Kunze, K. L.; Harrison, J. F. *J. Am. Chem. Soc.* **1990**, *112*, 3812.
(196) Mavrides, A.; Kunze, K.; Harrison, J. F.; Allison, J. *ACS Symposium Series 428*; Marks, T. J., Ed.; American Chemical Society: Washington, DC, 1990.
(197) Tientega, F.; Harrison, J. F. *Chem. Phys. Lett.* **1994**, *223*, 202.
(198) Jeung, G. H.; Koutecky, J. *J. Chem. Phys.* **1988**, *88*, 3747.
(199) Daoudi, A.; Elkhattabi, S.; Berthier, G.; Flament, J. P. *Chem. Phys.* **1998**, *230*, 31.
(200) Carlson, K. D.; Claydon, C. R.; Moser, C. *J. Chem. Phys.* **1967**, *46*, 4963.
(201) Bauschlicher, C. W., Jr. *Chem. Phys. Lett.* **1983**, *100*, 515.
(202) Mattar, S. M. *J. Phys. Chem.* **1993**, *97*, 3171.
(203) Harrison, J. F. *J. Phys. Chem.* **1996**, *100*, 3513.
(204) Mattar, S. M.; Hamilton, W. D.; Kingston, C. T. *Chem. Phys. Lett.* **1997**, *271*, 125.
(205) Andrews, L.; Bare, W. D.; Chertihin, G. V. *J. Phys. Chem. A* **1997**, *101*, 8417.
(206) Blomberg, M. R. A.; Siegbahn, P. E. M. *Theor. Chim. Acta* **1992**, *81*, 365.
(207) Siegbahn, P. E. M.; Blomberg, M. R. A. *Chem. Phys.* **1984**, *87*, 189.
(208) Fiedler, A.; Iwata, S. *Chem. Phys. Lett.* **1997**, *271*, 143.
(209) Daoudi, A.; Benjelloun, A. T.; Flament, J. P.; Berthier, G. *J. Mol. Spectrosc.* **1999**, *194*, 8.
(210) Kunze, K. L.; Harrison, J. F. *J. Phys. Chem.* **1989**, *93*, 2983.
(211) Elkhattabi, S.; Daoudi, A.; Flament, J. P.; Berthier, G. *Chem. Phys.* **1999**, *241*, 257.
(212) Chertihin, G. V.; Andrews, L.; Neurock, M. *J. Phys. Chem.* **1996**, *100*, 14609.
(213) Mattar, S. M.; Doleman, B. J. *Chem. Phys. Lett.* **1993**, *216*, 369.

(214) Kunze, K. L.; Harrison, J. F. *J. Phys. Chem.* **1991**, *95*, 6418.
(215) Harrison, J. F. *J. Phys. Chem.* **1986**, *90*, 3313.
(216) Ram, R. S.; Bernath, P. F. *J. Chem. Phys.* **1992**, *96*, 6344.
(217) Gingrich, R. A. *J. Chem. Phys.* **1968**, *49*, 19.
(218) Dunn, T. M.; Hanson, L. K.; Rubinson, R. A. *Can. J. Phys.* **1970**, *48*, 1657.
(219) Douglas, A. E.; Veillete, P. M. *J. Chem. Phys.* **1980**, *72*, 5378.
(220) Simard, B.; Niki, H.; Hackett, P. A. *J. Chem. Phys.* **1990**, *92*, 7012.
(221) Peter, S. L.; Dunn, T. M. *J. Chem. Phys.* **1989**, *90*, 5333.
(222) Simard, B.; Masoni, C.; Hackett, P. A. *J. Mol. Spectrosc.* **1989**, *136*, 44.
(223) Balfour, W. J.; Qian, C. X. W.; Zhou, C. *J. Chem. Phys.* **1997**, *106*, 4383.
(224) Steimle, T. C.; Robinson, J. S.; Goodridge, D. *J. Chem. Phys.* **1999**, *110*, 881.
(225) Brabaharan, K.; Coxon, J. A.; Yamashita, A. B. *Specrochim. Acta A* **1985**, *41*, 847.
(226) Bates, J. K.; Ramieri, N. L.; Dunn, T. M. *Can. J. Phys.* **1976**, *54*, 915.
(227) Dolg, M.; Wedig, U.; Stoll, H.; Preuss, H. *J. Chem. Phys.* **1987**, *86*, 2123.
(228) Bauschlicher, C. W., Jr.; Maitre, P. *Theor. Chim. Acta* **1995**, *90*, 189.
(229) Bakalbassis, E. G.; Stiakaki, M. D.; Tsipis, A. C.; Tsipis, C. A. *Chem. Phys.* **1996**, *205*, 389.
(230) Carlson, K. D.; Ludena, E.; Moser, C. *J. Chem. Phys.* **1965**, *43*, 2408.
(231) Bauschlicher, C. W., Jr.; Langhoff, S. R. *J. Chem. Phys.* **1986**, *85*, 5936.
(232) Jeung, G. H.; Koutecky, J. *J. Chem. Phys.* **1988**, *88*, 3747.
(233) Mattar, S. M. *J. Phys. Chem.* **1993**, *97*, 3171.
(234) Carlson, K. D.; Moser, C. *J. Phys. Chem.* **1963**, *67*, 2644.
(235) Carlson, K. D.; Nesbit, R. K. *J. Chem. Phys.* **1964**, *41*, 1051.
(236) Bauschlicher, C. W., Jr.; Bagus, P. S.; Nelin, C. J. *Chem. Phys. Lett.* **1983**, *101*, 229.
(237) Sennesal, J. M.; Schamps, J. *Chem. Phys.* **1987**, *114*, 37.
(238) Bauschlicher, C. W., Jr.; Langhoff, S. R.; Komornicki, A. *Theor. Chim. Acta* **1990**, *77*, 263.
(239) Bergström, P.; Lunell, S.; Eriksson, L. A. *Int. J. Quantum Chem.* **1996**, *59*, 427.
(240) Walsh, M. B.; King, R. A.; Schaefer, H. F., III *J. Chem. Phys.* **1999**, *110*, 5224.
(241) Loock, H.; Simard, B.; Wallen, S.; Linton, C. *J. Chem. Phys.* **1998**, *109*, 8980.
(242) Carlson, K. D.; Moser, C. *J. Chem. Phys.* **1966**, *44*, 3259.
(243) Bauschlicher, C. W., Jr.; Nelin, C. J.; Bagus, P. S. *J. Chem. Phys.* **1985**, *82*, 3265.
(244) Nelin, C. J.; Bauschlicher, C. W., Jr. *Chem. Phys. Lett.* **1985**, *118*, 221.
(245) Jasien, P. G.; Stevens, W. J. *Chem. Phys. Lett.* **1988**, *147*, 72.
(246) Steimle, T. C.; Nachman, D. F.; Shirley, J. E.; Bauschlicher, C. W., Jr.; Langhoff, S. R. *J. Chem. Phys.* **1989**, *91*, 2049.
(247) Espelid, O.; Borve, K. J. *J. Phys. Chem. A* **1997**, *101*, 9449.
(248) Espelid, O.; Borve, K. J.; Jensen, V. R. *J. Phys. Chem. A* **1998**, *102*, 10414.
(249) Pinchemel, B.; Schamps, J. *Chem. Phys.* **1976**, *18*, 481.
(250) Bagus, P. S.; Preston, H. J. T. P. *J. Chem. Phys.* **1973**, *59*, 2986.
(251) Krauss, M.; Stevens, W. J. *J. Chem. Phys.* **1985**, *82*, 5584.
(252) Glukhovtser, M. N.; Bach, R. D.; Nagel, C. J. *J. Phys. Chem. A* **1997**, *101*, 316.
(253) Chertihin, G. V.; Saffel, W.; Yustein, J. T.; Andrews, L. Neurock, M.; Ricca, A.; Bauschlicher, C. W., Jr. *J. Phys. Chem. A.* **1996**, *100*, 5261.
(254) Piechota, J.; Suffczynski, M. *Phys. Rev. A* **1993**, *48*, 2679.
(255) Chertihin, G. V.; Citra, A.; Andrews, L.; Bauschlicher, C. W., Jr. *J. Phys. Chem. A.* **1997**, *101*, 8793.
(256) Walch, S. P.; Goddard, W. A., III *J. Am. Chem. Soc.* **1978**, *100*, 1338.
(257) Bauschlicher, C. W., Jr. *Chem. Phys.* **1985**, *93*, 399.
(258) den Boer, D. H. W.; Kaleveld, E. W. *Chem. Phys. Lett.* **1980**, *69*, 389.
(259) Basch, H.; Osman, R. *Chem. Phys. Lett.* **1982**, *93*, 51.
(260) Bagus, P.; Nelin, C. J.; Bauschlicher, C. W., Jr. *J. Chem. Phys.* **1983**, *79*, 2975.
(261) Langhoff, S. R.; Bauschlicher, C. W., Jr. *Chem. Phys. Lett.* **1986**, *124*, 241.
(262) Madhavan, P. V.; Newton, M. D. *J. Chem. Phys.* **1985**, *83*, 2337.
(263) Langhoff, S. R.; Bauschlicher, C. W., Jr. *Chem. Phys. Lett.* **1986**, *124*, 241.
(264) Hippe, D.; Peyerimhoff, S. D. *Mol. Phys.* **1992**, *76*, 293.
(265) Maki, L.; Boughdiri, S. F.; Barthelat, J. C. *J. Phys. Chem. A* **1997**, *101*, 4224.
(266) Chertihin, G. V.; Andrews, L.; Bauschlicher, C. W., Jr. *J. Phys. Chem. A* **1997**, *101*, 4026.
(267) Merer, A. J. *Annu. Rev. Phys. Chem.* **1989**, *40*, 407.
(268) Shirley, J.; Scurlock, C.; Steimle, T. *J. Chem. Phys.* **1990**, *93*, 1568.
(269) Langhoff, S. R. *Astrophys. J.* **1997**, *481*, 1007.
(270) Steimle, T. C.; Shirley, J. E. *J. Chem. Phys.* **1989**, *91*, 8000.
(271) Suenram, R. D.; Fraser, G. T.; Lovas, F. J.; Gillies, C. W. *J. Mol. Spectrosc.* **1991**, *148*, 114.
(272) Steimle, T. C.; Nachman, D. F.; Shirley, J. E.; Merer, A. J. *J. Chem. Phys.* **1989**, *90*, 5360.
(273) Tilson, J. L.; Harrison, J. F. *J. Phys. Chem.* **1991**, *95*, 5097.
(274) Carter, E. A.; Goddard, W. A., III *J. Phys. Chem.* **1988**, *92*, 2109.
(275) Broclawik, E. *Int. J. Quantum Chem.* **1995**, *56*, 779.
(276) Dyke, J. M.; Gravenor, B. W. J.; Hastings, M. P.; Morris, A. *J. Phys. Chem.* **1985**, *89*, 4613.
(277) Harrison, J. F. *J. Phys. Chem.* **1986**, *90*, 3313.
(278) Takahara, Y.; Yamaguchi, K.; Fueno, T. *Chem. Phys. Lett.* **1989**, *158*, 95.
(279) Fiedler, A.; Hrusak, J.; Koch, W.; Schwarz, H. *Chem. Phys. Lett.* **1993**, *211*, 242.
(280) Dyke, J. M.; Gravenor, B. W. J.; Lewis, R. A.; Morris, A. *J. Chem. Soc., Faraday Trans. 1* **1983**, *79*, 1083.
(281) Fisher, E. R.; Elkind, J. L.; Clemmer, D. E.; Georgrades, R.; Lok, S. K.; Aristov, N.; Sunderlin, L. S.; Armentrout, P. B. *J. Phys. Chem.* **1990**, *93*, 2676.
(282) Kang, H.; Beauchamp, J. L. *J. Am. Chem. Soc.* **1986**, *108*, 5663.
(283) Steimle, T. C.; Nachman, D. F.; Fletcher, D. A. *J. Chem. Phys.* **1987**, *87*, 5670.
(284) Carlson, K. D.; Moser, C. *J. Chem. Phys.* **1967**, *46*, 35.
(285) Scott, P. R.; Richards, W. G. *Chem. Phys. Lett.* **1974**, *28*, 101.
(286) Harrison, J. F. *J. Phys. Chem.* **1983**, *87*, 1312.
(287) Langhoff, S. R.; Bauschlicher, C. W., Jr.; Partridge, H. *J. Chem. Phys.* **1988**, *89*, 396.
(288) Langhoff, S. R.; Bauschlicher, C. W., Jr.; Partridge, H. *J. Chem. Phys.* **1988**, *89*, 7649.
(289) Boldyrev, A. I.; Simons, J. *J. Mol. Spectrosc.* **1998**, *188*, 138.
(290) Bencheikh, M.; Kowisto, R.; Launila, O.; Flament, J. P. *J. Chem. Phys.* **1997**, *106*, 6231.
(291) Harrison, J. F.; Hutchison, *Mol. Phys.* **1999**, *97*, 1009.
(292) Pouilly, B.; Schamps, J.; Lumley, D. J. W.; Barrow, R. F. *J. Phys. B: Atom Mol. Phys.* **1978**, *11*, 2289.
(293) Bauschlicher, C. W., Jr. *Chem. Phys.* **1996**, *211*, 163.
(294) Bencheikh, M. *J. Mol. Spectrosc.* **1997**, *183*, 419.
(295) Dufour, C.; Schamps, J.; Barrow, R. F. *J. Phys. B* **1982**, *15*, 3819.
(296) Nguyen, M. T.; McGinn, M. A.; Fitzpatrick, N. J. *J. Chem. Soc., Faraday Trans.* **1986**, *82*, 1427.
(297) Ramirez-Solis, A.; Daudey, J. P. *Chem. Phys.* **1989**, *134*, 111.
(298) Hrusak, J.; Ten-no, S.; Iwata, S. *J. Chem. Phys.* **1997**, *106*, 7185.
(299) Averyanov, A. S.; Khait, Y. G. *Opt. Spektrosk.* **1989**, *67*, 1408.
(300) Field, R. W. *Ber Bunsen-Ges. Phys. Chem.* **1982**, *86*, 771.
(301) Carette, P.; Dufour, C.; Pinchemel, B. *J. Mol. Spectrosc.* **1993**, *161*, 323.
(302) Ram, R. S.; Bernath, P. F.; Davis, S. *J. Chem. Phys.* **1996**, *104*, 6949.
(303) Zmbov, K. F.; Margrave, J. L. *J. Chem. Phys.* **1967**, *47*, 3122.
(304) McLeod, D., Jr.; Weltner, W., Jr. *J. Phys. Chem.* **1966**, *70*, 3293.
(305) Simard, B.; Vasseur, M.; Hackett, P. A. *Chem. Phys. Lett.* **1991**, *176*, 303.
(306) Gurvich, L. V.; Shenyavskaya, E. A. *Opt. Spectrosc.* (English Translation) **1963**, *14*, 161.
(307) Zmbov, K. F.; Margrave, J. L. *J. Chem. Phys.* **1967**, *46*, 35.
(308) Brewer, L.; Green, D. W. *High Temp. Sci.* **1969**, *1*, 26.
(309) Barrow, R. F.; Bastin, M. W.; Moore, D. L. G.; Pott, C. J. *Nature* **1967**, *215*, 1072.
(310) Shenyavskaya, E. A.; Ross, A. J.; Topouzkhanian, A.; Wannous, G. *J. Mol. Spectrosc.* **1993**, *162*, 327.
(311) Lebeault-Dorget, M.-A.; Effantin, C.; Bernard, A.; D'Incan, J.; Chevaleyre, J.; Shenyavskaya, E. A. *J. Mol. Spectrosc.* **1994**, *163*, 276.
(312) Shenyavskaya, E. A.; Vergeœ, J.; Topouzkhanian, A.; Lebeault-Dorget, M.-A.; D'Incan, J.; Effantin, C.; Bernard, A. *J. Mol. Spectrosc.* **1994**, *164*, 129.
(313) Hildenbrand, D. L.; Lau, K. H. *J. Chem. Phys.* **1995**, *102*, 3769.
(314) Shenyavskaya, E. A.; Lebeault-Dorget, M.-A.; Effantin, C.; D'Incan, J.; Bernard, A.; Vergeœ, J. *J. Mol. Spectrosc.* **1995**, *171*, 309.
(315) Kaledin, L. A.; McCord, J. E.; Heaven, M. C. *J. Mol. Spectrosc.* **1995**, *171*, 569.
(316) Dieber, R. L.; Kay, J. G. *J. Chem. Phys.* **1969**, *51*, 3547.
(317) Shenyavskaya, E. A.; Dabov, V. M. *J. Mol. Spectrosc.* **1985**, *113*, 85.
(318) Ram, R. S.; Peers, J. R. D.; Teng, Y.; Adam, A. G.; Muntianu, A.; Bernath, P. F.; Davis, S. P. *J. Mol. Spectrosc.* **1997**, *184*, 186.
(319) Gambi, R. *Gazz. Chem. Ital.* **1975**, *105*, 27.
(320) Laerdahl, J. K.; Saue, T.; Faegri, K. *Theor. Chem. Acc.* **1997**, *97*, 177.
(321) Lee, E. P. F.; Potts, A. W. *Chem. Phys. Lett.* **1980**, *76*, 532.
(322) Herrera, F. L., Harrison, J. F., 50th Molecular Spectroscopy Symposium, Columbus, Ohio, 1995.
(323) Jones, W. E.; Krishnamurty, G. *J. Phys. B* **1980**, *13*, 3375.
(324) Launila, O. *J. Mol. Spectrosc.* **1995**, *169*, 373.
(325) Koivisto, R.; Wallen, S.; Launila, O. *J. Mol. Spectrosc.* **1995**, *172*, 464.

(326) Wallen, S.; Koivisto, R.; Launila, O. *J. Chem. Phys.* **1996**, *105*, 388.
(327) Okabayashi, T.; Tanimoto, M. *J. Chem. Phys.* **1996**, *105*, 7421.
(328) Launila, O.; Simard, B. *J. Mol. Spectrosc.* **1992**, *154*, 407.
(329) Launila, O.; Simard, B. *J. Mol. Spectrosc.* **1992**, *154*, 93.
(330) Pouilly, B.; Schamps, J.; Lumley, D. J. W.; Barrow, R. F. *J. Phys. B: Atom. Mol. Phys.* **1978**, *11*, 2281.
(331) Ram, R. S.; Bernath, P. F.; Davis, S. P. *J. Mol. Spectrosc.* **1996**, *179*, 282.
(332) Allen, M. D.; Ziurys, L. M. *J. Chem. Phys.* **1997**, *106*, 3494.
(333) Adam, A. G.; Fraser, L. P.; Hamilton, W. D.; Steeves, M. C. *Chem. Phys. Lett.* **1994**, *230*, 82.
(334) Ram, R. S.; Bernath, P. F.; Davis, S. P. *J. Mol. Spectrosc.* **1995**, *173*, 158.
(335) Launila, O.; Simard, B.; James, A. M. *J. Mol. Spectrosc.* **1993**, *159*, 161.
(336) Dufour, C.; Hikmet, I.; Pinchemel, B. *J. Mol. Spectrosc.* **1994**, *165*, 398.
(337) Dufour, C.; Pinchemel, B. *J. Mol. Spectrosc.* **1995**, *173*, 70.
(338) Dufour, C.; Carette, P.; Pinchemel, B. *J. Mol. Spectrosc.* **1991**, *148*, 303.
(339) van Wullen, C. *J. Chem. Phys.* **1998**, *109*, 392.
(340) Focsa, C.; Pinchemel, B.; Collet, D.; Huet, T. R. *J. Mol. Spectrosc.* **1998**, *189*, 254.
(341) Schröder, D.; Harvey, J. N.; Schwarz, H. *J. Phys. Chem.* **1998**, *102*, 3639.
(342) Kent, R. A.; Margrave, J. L. *J. Am. Chem. Soc.* **1996**, *87*, 3582.
(343) Flesch, G. D.; White, R. M.; Svec, H. J. *Int. J. Mass Spectrom. Ion Phys.* **1969**, *3*, 339.
(344) Bader, R. F. W. *Chem. Rev.* **1991**, *91*, 893.
(345) Becke, A. D.; Edgecombe, K. E. *J. Chem. Phys.* **1990**, *92*, 5397.
(346) Savin, A.; Reinhard, Nesper, R.; Wengert, S.; Fässler, T. F. *Angew. Chem., Int. Ed. Engl.* **1997**, *36*, 1808.

CR980411M